SANDIA REPORT
SAND2009-3115
Unlimited Release
Printed June 2009

Implementation of Equilibrium Aqueous Speciation and Solubility (EQ3 type) Calculations into Cantera for Electrolyte Solutions

Harry K. Moffat, Carlos F. Jové Colón

Prepared by
Sandia National Laboratories
Albuquerque, New Mexico 87185-0836

Sandia is a multiprogram laboratory operated by Sandia Corporation,
a Lockheed Martin Company, for the United States Department of Energy's
National Nuclear Security Administration under Contract DE-AC04-94AL85000.

Issued by Sandia National Laboratories, operated for the United States Department of Energy by Sandia Corporation.

Available to DOE and DOE contractors from

U.S. Department of Energy
Office of Scientific and Technical Information
P.O. Box 62
Oak Ridge, TN 37831

Telephone: (865) 576-8401
Facsimile: (865) 576-5728
E-Mail: reports@adonis.osti.gov
Online ordering: http://www.osti.gov/bridge

Available to the public from

U.S. Department of Commerce
National Technical Information Service
5285 Port Royal Rd.
Springfield, VA 22161

Telephone: (800) 553-6847
Facsimile: (703) 605-6900
E-Mail: orders@ntis.fedworld.gov
Online order: http://www.ntis.gov/help/ordermethods.asp?loc=7-4-0#online

SAND2009-3115
Unlimited Release
Printed June 2009

Implementation of Equilibrium Aqueous Speciation and Solubility (EQ3 type) Calculations into Cantera for Electrolyte Solutions

Harry K. Moffat
Nanoscale and Reactive Processes

Carlos F Jové Colón
Yucca Mountain Project (YMP) Technical Support (Upper Barrier System)

Sandia National Laboratories
P. O. Box 5800
Albquerque, NM 87185-0888

Abstract

In this report, we summarize our work on developing a production level capability for modeling brine thermodynamic properties using the open-source code Cantera. This implementation into Cantera allows for the application of chemical thermodynamics to describe the interactions between a solid and an electrolyte solution at chemical equilibrium. The formulations to evaluate the thermodynamic properties of electrolytes are based on Pitzer's model to calculate molality-based activity coefficients using a real equation-of-state (EoS) for water. In addition, the thermodynamic properties of solutes at elevated temperature and pressures are computed using the revised Helgeson-Kirkham-Flowers (HKF) EoS for ionic and neutral aqueous species. The thermodynamic data parameters for the Pitzer formulation and HKF EoS are from the thermodynamic database compilation developed for the Yucca Mountain Project (YMP) used with the computer code EQ3/6. We describe the adopted equations and their implementation within Cantera and also provide several validated examples relevant to the calculations of extensive properties of electrolyte solutions.

Acknowledgments

We are grateful for the funding provided by ASC to develop this model, implement it in Cantera, and write this SAND report. We also would like to voice our appreciation for the vision and extremely agile platform that Prof. D. G. Goodwin has created in Cantera that allows for the logical implementation of complex thermodynamics models into an object-oriented constitutive-modeling framework. The thermodynamic models implemented in this work would be nothing without the experimental discoveries with subsequent model development involving the analysis, retrieval, and prediction of the thermodynamic properties of electrolyte solutions.

Table of Contents

1 Introduction

This report describes the implementation of the standard form of Pitzer equations and the revised Helgeson-Kirhham-Flowers (HKF) Equation of State (EoS) within Cantera to calculate thermodynamic properties of electrolyte solutions and to conduct equilibrium speciation and solubility calculations as a function of solute concentration, pressure, and temperature. This effort is a subtask of a larger effort to generate the numerical software necessary to model water layers, relevant to atmospheric corrosion. In these water layers, in contrast to imbibed conditions, there is almost always a strong electrolyte present. At equilibrium, the strong electrolyte serves to stabilize the water-electrolyte phase, causing the activity of water to decrease substantially relative to the pure water phase. That is, the equilibrium relative humidity (RH) in the system can exert changes in the activity of water in these aqueous layers therefore imposing variations in the activity coefficients of all solute species in solution. These variations in activity coefficients (i.e., deviation from unity) in electrolytes can have strong effects on the solubility of solids and gases, and in the formation of aqueous complexes in the aqueous film. For this reason, accurate quantification of the effects of ionic strength on the activity of water is essential in the modeling of solubility and aqueous speciation in electrolyte solutions.

Cantera is a general purpose object-oriented constitutive modeling package with interfaces to C++, FORTRAN, Python, and Matlab. Its origins lie in modeling combustion systems and allied chemical vapor deposition processes [41]. However, it's been used extended to solid oxide fuel cell (SOFC) modeling [53], and it has been extended to model soot formation [8] using a sectional bin formulation. Currently, extensions for electrode reactions relevant to corrosion systems, where modeling the conditions for desiccation of brine systems are a prerequisite, and battery modeling are being sought after. The equilibrium speciation and solubility calculations referred to here as "EQ3-type" are related to the EQ3NR component of the code package EQ3/6 [7]. The software package EQ3/6, developed by Dr. Thomas J. Wolery of Lawrence Livermore National Laboratory (LLNL), is used to conduct calculations relevant to geochemical modeling of fluid-mineral interactions involving dilute aqueous solutions and strong electrolytes. The EQ6 component is used for reaction path modeling involving titration of a solid, gas, or aqueous species into solution in both time-independent (reaction progress) or time-dependent (kinetic) modes. There is no equivalent of EQ6 in this Cantera implementation. There are other computer codes that could perform "EQ3-type" of calculations, for example, WATEQ [9], PHREEQC [13], and Geochemist's Workbench [10, 11]. These codes compute the equilibrium concentrations of aqueous and gas species for a given input of solution composition as constrained by pressure, temperature, and ionic strength. Other input constraints used when calculating the concentration of aqueous species are charge balancing with respect to some charged aqueous species or that defined by saturation with respect to mineral solid or a gas (e.g., solubility). In comparison to software package EQ3/6, this Cantera implementation has the capability to compute multiphase chemical equilibrium between solids, aqueous species, and gases. The basic output generated by Cantera for this type of equilibrium calculations is similar to that of EQ3NR where it provides the equilibrium molal concentrations of aqueous species and molar abundances of gases, activities of aqueous constituents, and thermodynamic properties of the solution. It should be noted, however, that

some important differences exist between the this Cantera implementation and EQ3NR (or other codes such as PHREEQC and Geochemist's Workbench) as to the capability of explicitly constraining run inputs such as fixed pH or any other species concentration, or constraints on charge balancing. These features will be expanded into the Cantera EQ3 implementation and is work in progress.

In this report, we lay out the formulations of the standard Pitzer equations in terms of the expression for the excess Gibbs free energy and its derivatives with respect to solutes and solvents. The complete equations, as implemented within Cantera, are described. The implemented Pitzer formulations are referred herein as 'standard' and correspond to the original form of the equations given by Pitzer (1973, 1991) [12, 18]. There are variants of the Pitzer equations developed over the last two decades that involves, for example, extensions of the ion interaction terms to accommodate ionic strength dependencies or the use of ion pairing reactions that essentially act as an additional parameter [77,79]. The motivation of extending the standard form of Pitzer equations is mainly to accurately represent the thermodynamic properties of electrolytes at elevated ionic strengths where deviations from experiments were significantly reduced by practically adding another parameter to the Pitzer formulation [79]. The Pitzer thermodynamic database developed for the Yucca Mountain Project (YMP) and used here with Cantera is parameterized to be consistent with the standard form of the Pitzer formulations. In the literature, it is usually stated that the standard form of the Pitzer equations are limited to solutions not exceeding an ionic strength of about six molal. This is probably due to the overall maximum ionic strength for the large set of electrolytes considered by Pitzer and coworkers in their parameterizations. However, the work by Rard and Wijesinghe [19] and Wijesinghe and Rard [68] demonstrated that a standard Pitzer model can accurately reproduce osmotic coefficient data for very soluble electrolytes such as $Ca(NO_3)_2$(aq) and $NaNO_3$(aq) over the range of ionic strengths and temperatures considered in experimental studies. Their results show a very strong agreement with those obtained using extended Pitzer formulations developed to model strong electrolytes. The methods of Wijesinghe (2003) [19] and Wijesinghe and Rard (2005) [68] were adopted in the development of the YMP Pitzer thermodynamic database for cases of strong electrolytes. Details on the development of the YMP Pitzer thermodynamic database are given elsewhere (see Appendix I of [43].

Next, the details of the implementation within Cantera will be addressed. Verification of the implementation within Cantera is carried out by a comparison of the mixture activity coefficient, osmotic coefficient, and Debye-Hückel parameter against published data for some binary salts like NaCl, as a function of temperature and molality. An example thermodynamic equilibrium calculation involving between NaCl solid, NaCl electrolyte solution, and air is carried out and reported as a verification exercise.

In subsequent sections, a description of the formulations for the mixture enthalpy, mixture heat capacity, and mixture solution volumes, in terms of derivatives of the previously derived activity coefficients and osmotic coefficient to complete the implementation of the Pitzer equations. Verification of computed results is conducted in the form of comparisons against selected values reported for the NaCl, $MgSO_4$, and Na_2SO_4 salt systems for excess enthalpy, heat capacity, and osmotic coefficient calculations. The solubility of halite (NaCl solid) and sylvite (KCl solid) in mixed

NaCl-KCl electrolyte solutions was evaluated and compared to solubility data. Finally, the solubility of calcite ($CaCO_3$) in NaCl at a fixed P_{CO2} was also evaluated and compared to experimental data.

We don't go into detail about the derivation or motivation for the equations chosen. That would require an extensive discussion and these formulations have been described in detail elsewhere. It would also be a mute point, considering that a vast amount of experimental data for liquid brines has been fit to be used with the implementations in the code EQ3/6. We note, however, the Pitzer formulation is effective at describing binary interaction with a minimum number of parameters and has been shown to be effective at capturing the interactions of multi-component brines also with a minimum number of additional ternary interaction parameters.

Cantera is an open source application developed by Prof. David G. Goodwin from the applied physics department at Caltech and is hosted on sourcefource.net. The electrochemistry modules described here have been copywrited by Sandia/DOE for open source distribution and will be added to the sourceforge.net Cantera distribution.

2 Gibbs Excess Free Energy Formulation

Pitzer (1973, 1991) expresses his equations in terms of a formulation for the excess Gibbs free energy. The Pitzer model is an extension of the Debye-Hückel model for ionic solutions, employing an ionic strength-dependent and temperature-dependent virial coefficient expansion to account for short-range interactions not handled by the Debye-Hückel term. The excess Gibbs free energy formulation is based on the ideal molal solution model (which is anything but ideal, since there is a singularity when the solvent concentration goes to zero), introduced in ref. [4]. Let's show this below.

Pitzer's basic presentation starts on p. 85 of ref. [18]. In that presentation, the chemical potential for solutes, *i*, μ_i , and water, *o*, μ_o , is defined as:

$$\mu_i = \mu_i^{\triangle}(T,P) + RT\ln\left(\frac{m_i\,\gamma_i^{\triangle}}{m^{\triangle}}\right), \text{ where } m_i = \frac{n_i}{\tilde{M}_o n_o} \text{ and } \tilde{M}_o = \frac{M_o}{1000} \tag{1}$$

$$\mu_o = \mu_o^o(T,P) + RT\ln\left(a_o\right)$$

$\mu_i^{\triangle}(T,P)$ is the standard state of solute *i* on a one molal ideal solution basis. m_i is the molality of solute *i*, M_o represents the number of moles of water present in one kilogram of water (1 kg/0.018015 kg·mol^{-1} = 55.508 mol·kg^{-1}), and $\gamma_i^{\triangle}$ corresponds to the molality-based activity coefficient for solute *i*. $\mu_o^o(T,P)$ stands for the standard state for water, i.e., pure water at the temperature and pressure of the solution, and a_o designates the water activity at the temperature, pressure, and composition of the solution. The $m^{\triangle}$ term in the denominator with units of 1 molal (1 gmol kg^{-1}) represents consistency with the standard state adopted in this formulation which is that unit of activity for a hypothetical one molal solution referenced to infinite dilution at any given *T* and *P*. The total Gibbs Energy, $G = n\tilde{G}$, an extensive quantity, is equal to

$$\left(n\tilde{G}\right) = n_o\mu_o + \sum_i n_i\,\mu_i \tag{2}$$

where n is the total moles of solution, n_o corresponds to the number of moles of water, and n_i designates the number of moles of solute *i*. Then, the Gibbs free energy of mixing, $\Delta G_{mix,\triangle}$, an extensive quantity is equal to:

$$\Delta G_{mix,\triangle} = \left(n\tilde{G}\right) - \left(n_o\mu_o^o + \sum_{i\neq 0} n_i\,\mu_i^{\triangle}\right) = RT\left(\ln\left(a_o\right) + \sum_{i\neq 0} n_i\,\ln\left(\frac{m_i\,\gamma_i^{\triangle}}{m^{\triangle}}\right)\right) \tag{3}$$

Pitzer (1973, 1991) introduces the osmotic coefficient in order to replace the water activity term using the following definition for the osmotic coefficient (ϕ):

$$\phi = \frac{-1}{\tilde{M}_o \sum_{i\neq 0} m_i} \ln\left(a_o\right) = \frac{-n_o}{\sum_{i\neq 0} n_i} \ln\left(a_o\right) \tag{4}$$

Plugging this expression in yields:

$$\Delta G_{mix,\vartriangle} = RT\left(-\phi\left(\sum_{i\neq 0} n_i\right) + \sum_i n_i \ln\left(\frac{m_i \gamma_i^{\vartriangle}}{m^{\vartriangle}}\right)\right) = RT\left(\sum_{i\neq 0} n_i \left(\ln\left(\frac{m_i \gamma_i^{\vartriangle}}{m^{\vartriangle}}\right) - \phi\right)\right) \tag{5}$$

$\Delta G_{mix,\vartriangle}$ is broken up into 2 parts. The first part assumes that the osmotic coefficient is equal to 1, and the molality-based activity coefficients are equal to one; this is called the ideal Gibbs free energy of mixing, $\Delta G_{mix,\vartriangle}^{id,\vartriangle}$.

$$\Delta G_{mix,\vartriangle}^{id,\vartriangle} = RT\left(\sum_{i\neq 0} n_i \left(\ln\left(\frac{m_i}{m^{\vartriangle}}\right) - 1\right)\right) \tag{6}$$

Eqn.) is the same result obtained by Eqn. (15) of ref. [4], for the ideal molal solution model. The second part of the Gibbs energy of mixing, Pitzer labels as the excess Gibbs free energy, $G_{ex,\vartriangle}$, it includes everything else that is not part of the ideal molal solution model.

$$G_{ex,\vartriangle} = \Delta G_{mix,\vartriangle} - \Delta G_{mix,\vartriangle}^{id,\vartriangle} = \Delta G_{mix,\vartriangle} - RT\left(\sum_{i\neq 0} n_i \left(\ln\left(\frac{m_i}{m^{\vartriangle}}\right) - 1\right)\right) \tag{7}$$

Note, we have included the symbol $\vartriangle$ as a subscript to differentiate from the real G_{ex} expression which is based on differences from the true molar-based ideal solution behavior. By dividing by $\tilde{M}_o n_o$, the excess Gibbs free energy may be put on a per kg of water basis:

$$\frac{G_{ex,\vartriangle}}{\tilde{M}_o n_o} = \frac{\Delta G_{mix,\vartriangle}}{\tilde{M}_o n_o} - RT\left(\sum_{i\neq 0} m_i \left(\ln\left(\frac{m_i}{m^{\vartriangle}}\right) - 1\right)\right) . \tag{8}$$

Plugging Eqn.) into the general equation, Eqn.), yields the expression for $G_{ex,\vartriangle}$

$$G_{ex,\vartriangle} = RT\left(\sum_{i\neq 0} n_i \left(\ln\left(\gamma_i^{\vartriangle}\right) + 1 - \phi\right)\right) \tag{9}$$

$$\frac{G_{ex,\vartriangle}}{\tilde{M}_o n_o} = RT\left(\sum_{i\neq 0} m_i \left(\ln\left(\gamma_i^{\vartriangle}\right) + 1 - \phi\right)\right) \tag{10}$$

Eqn.), which is on a per kg solvent basis, is the starting place for the rest of Pitzer's work. All formulas start with virial coefficient expansions involving expressions for $G_{ex,\vartriangle}$. Further details on the Pitzer equations and related parameters are discussed in Section 4.

2.1 Partial Derivatives of the Excess Gibbs Free Energy

Let's derive the relationship of the partial derivatives of Eqn. (2) with respect to the species mole numbers to the molality based activity coefficients and osmotic coefficient. The definition of the chemical potential is given by Eqn. (11). All other partial molar properties follow the same form.

$$\left(\frac{dG}{dn_i}\right)_{T,p,n_j} = \bar{\mu}_i\left(T,P,\boldsymbol{x}\right) \tag{11}$$

n_i is the number of moles of species *i* in the solution. This may be combined with the expression for the extrinsic Gibbs free energy in terms of the chemical potentials, Eqn. (11), to yield Eqn. (12):

$$G = \sum_{k=0}^{n} n_k\ \bar{\mu}_k \tag{12}$$

Then, taking the total derivative of Eqn. (12) and substituting into Eqn. (11) yields:

$$dG\ = \sum_{k=0}^{n}\ \bar{\mu}_k dn_k + \sum_{k=0}^{n}\ n_k d\bar{\mu}_k \tag{13}$$

But, it's also true that the general functional total derivative of the Gibbs free energy $G = G\left(T,P,n_k\right)$ is given by the following expression

$$\begin{aligned} dG\ &= \left(\left.\frac{dG}{dT}\right|_{P,n_k}\right)dT + \left(\left.\frac{dG}{dP}\right|_{T,n_k}\right)dP + \sum_{k=0}^{n}\left(\left.\frac{dG}{dn_k}\right|_{T,P}\right)dn_k \\ &= \left(\left.\frac{dG}{dT}\right|_{P,n_k}\right)dT + \left(\left.\frac{dG}{dP}\right|_{T,n_k}\right)dP + \sum_{k=0}^{n}\ \bar{\mu}_k dn_k \end{aligned} \tag{14}$$

Substituting Eqn. (13) into Eqn. (14) yields the Gibbs-Duhem equation, Eqn. (15).

$$\begin{aligned} \left(\left.\frac{dG}{dT}\right|_{P,n_k}\right)dT + \left(\left.\frac{dG}{dP}\right|_{T,n_k}\right)dP - \sum_{k=0}^{n}\ n_k d\bar{\mu}_k\ &= 0 \\ S\ dT - V\ dP + \sum_{k=0}^{n}\ n_k d\bar{\mu}_k &= 0 \end{aligned} \tag{15}$$

Note, often this equation is applied at constant *T* and *P* which reduces to:

$$\sum_{k=0}^{n}\ n_k d\bar{\mu}_k\ = 0 \tag{16}$$

However, note that Eqn. (15) still contains the temperature and pressure dependence. Eqn. (16) is very useful in the sense that for a solution containing water and a dissolved salt, it takes the form:

$$n_w d\bar{\mu}_w + n_{sc_i} d\bar{\mu}_{sc_i} = 0$$
$$n_w d\bar{\mu}_w = -n_{sc_i} d\bar{\mu}_{sc_i} \tag{17}$$

where n_w and $\bar{\mu}_w$ refers to the number of moles and the chemical potential of water, respectively. Likewise, n_{sc_i} and $\bar{\mu}_{sc_i}$ designate the number of moles and the chemical potential of the salt component i, respectively. For this case of a multicomponent solution, this equation allows for the determination of the thermodynamic properties of the salt components from those of water (see [83]; Chapter 34.)

This analysis may be carried over to the excess Gibbs free energies by applying the following separation to the analysis above:

$$G = G^{id,\triangle} + G_{ex,\triangle} \tag{18}$$

$G^{id,\triangle}$ is the "ideal" component of the total Gibbs free energy expression, which is not an ideal solution. In the analysis above,

$$G^{id,\triangle} = n_o \mu_o^o + \sum_{k\neq 0} n_k \mu_k^{\triangle} + \tilde{M}_o n_o \left(RT \sum_{k\neq 0} m_k \left(\ln\left(m_k\right) - 1 \right) \right) \tag{19}$$

where $\mu_k^{\triangle} = \mu_k^o - RT \ln \tilde{M}_o m^{\triangle}$ and

$$\frac{dG_{id,\triangle}^{id,\triangle}}{dn_o} = \mu_o^o - RT\tilde{M}_o \sum_{k\neq 0} m_k \quad \text{and} \quad \frac{dG_{id,\triangle}^{id,\triangle}}{dn_k} = \mu_k^{\triangle} + RT \ln\left(\frac{m_k}{m^{\triangle}}\right) \tag{20}$$

In Eqn. (19), we introduce the notation $G^{id,\triangle}$ for meaning the unperturbed expression for the total Gibbs free energy of an ideal molal solution component, $G_{id,\triangle}$, because below, we will introduce modifications to $G_{id,\triangle}$ which will be calling $G_{id,\triangle}^{\mathrm{mod},id,\triangle}$. Plugging this into the general expression for the definition of the chemical potential:

$$\left(\frac{dG}{dn_k}\right)\Bigg|_{T,P,n_{j\neq k}} = \bar{\mu}_k\left(T,P,\boldsymbol{x}\right) = \bar{\mu}_k^{\triangle} + RT \ln\left(\frac{m_k \gamma_k^{\triangle}}{m^{\triangle}}\right) = \frac{dG^{id,\triangle}}{dn_k} + \frac{dG_{ex,\triangle}}{dn_k} \tag{21}$$

$$\begin{aligned}\left(\frac{dG}{dn_o}\right)\Bigg|_{T,P,n_k} &= \bar{\mu}_o\left(T,P,\boldsymbol{x}\right) = \bar{\mu}_o^o - RT\phi\left(\sum_{k\neq o}\frac{n_k}{n_o}\right) = \frac{dG^{id,\triangle}}{dn_o} + \frac{dG_{ex,\triangle}}{dn_o} \\ &= \bar{\mu}_o^o - \tilde{M}_o \sum_{k\neq o} m_k + \frac{dG_{ex,\triangle}}{dn_o}\end{aligned} \tag{22}$$

$$-RT\phi\left(\sum_{k\neq o} m_k\right) = -RT\left(\sum_{k\neq o} m_k\right) + \left(\frac{dG_{ex,\triangle}}{dn_o}\right)\frac{1}{\tilde{M}_o}$$
$$RT\left(1-\phi\right)\left(\sum_{k\neq o} m_k\right) = \left(\frac{dG_{ex,\triangle}}{dn_o}\right)\frac{1}{\tilde{M}_o} \tag{23}$$

Therefore,

$$\frac{dG_{ex,\triangle}}{dn_k} = RT\ln\left(\gamma_k^{\triangle}\right) \quad \text{or} \quad \left.\frac{d\left(\frac{G_{ex,\triangle}}{RT\tilde{M}_o n_o}\right)}{dm_k}\right|_{T,P,n_{j\neq k}} = RT\ln\left(\gamma_k^{\triangle}\right) \tag{24}$$

Eqn. (24) is a reproduction of Pitzer's Eqn. (34) on p. 86 of ref [18]. Rearranging Eqn. (22), we obtain

$$\phi - 1 = -\left(\frac{d\left(\frac{G_{ex,\triangle}}{RT}\right)}{d\left(\tilde{M}_o n_o\right)}\right)\frac{1}{\sum_{k\neq o} m_k} \tag{25}$$

Eqn. (25) is given by Pitzer as Eqn. (35) on p. 86 of ref. [18].

3 Formulation of Standard States within Cantera

To compute the thermodynamic properties of multicomponent solutions, it is necessary to know something about the thermodynamic properties of the individual species present in the solution. Exactly what sort of properties is required depends on the thermodynamic model for the solution. For a gaseous solution (i.e., a gas mixture), the species properties required are usually ideal gas properties at the mixture temperature and at a reference pressure (almost always at 1 bar). For other types of solutions, however, it may not be possible to isolate the species in a "pure" state. For example, the thermodynamic properties of, say, Na^+ and Cl^- in an electrolyte solution are not easily determined from data on the properties of solid NaCl (halite), or solid Na metal, or chlorine gas. In this case, the solvation in water is fundamental to the identity of the species, and some other reference state must be used. One common convention for liquid solutions is to use thermodynamic data for the solutes in the limit of infinite dilution within the pure solvent; another convention is to reference all properties to unit molality. However, in all of these cases the reference states for the fluid mixture are considered asymmetric since some species have reference states based on being in infinite dilution, while other species have reference states based on their undiluted form.

In defining these standard states for species in a phase, we make the following refinement in language pertaining to Cantera. A “reference state” is a standard state of a species whose definition is limited to one particular pressure; the reference pressure. The reference state specifies the dependence of all thermodynamic functions as a function of the temperature in between a minimum temperature and a maximum temperature at the reference pressure. The reference state also specifies the molar volume of the species as a function of temperature. The molar volume is an additional thermodynamic function. In contrast, a Cantera “standard state” does the same as a Cantera “reference state” but specifies these thermodynamics function at all pressures. A standard state may employ a reference state in order to provide the temperature dependence, while it provides the pressure dependence. For example, the ideal gas standard state does this. Or, a standard state may not employ a reference state in its formulation, depending on its needs if it doesn’t make sense to do so. For example the real equation of state of pure water in the liquid state doesn’t employ a reference state formulation, because the equation of state is a complex function of temperature and density that doesn’t benefit from its description at any particular pressure.

The formulation of standard states is done within the `ThermoPhase` object. Objects which inherit directly from the object `ThermoPhase` assume that each species has a reference state associated with it. The class `ThermoPhase` owns a pointer to the class `SpeciesThermo`. The class `SpeciesThermo` is the base class for a family of classes that compute properties of all species in a phase in their reference states, for a range of temperatures. Note, the pressure dependence of the species thermodynamic functions is not handled by this particular species thermodynamic model. `SpeciesThermo` calculates the reference-state thermodynamic values of all species in a single phase during each call.

The class SpeciesThermoInterpType is a pure virtual base class for calculation of thermodynamic functions for a single species in its reference state. All individual reference state classes inherit from SpeciesThermoInterpType. Fig. 1 depicts a description of this relationship along with a listing of the currently available classes that inherit from SpeciesThermo and SpeciesThermoInterpType.

As stated previously, Cantera allows for the use of a variety of standard states. Cantera's primary use is for ideal gases. These have standard states that are just based on temperature, and assume an ideal gas at 1 bar. Also, they are based on the NIST/JANAF table convention [24, 57] where the heats of formation of the elements in their standard states are set to zero. Calculation of standard state properties can be computationally intensive. Therefore, ThermoPhase object relies on the set of SpeciesThermo manager classes to calculate the thermodynamic properties of the reference state for all of the species in the phase at the same time. Different derivative class of SpeciesThermo make assumptions about the identity of the reference state classes for species in the phase, allowing for the grouping together of common operations and for the speedup of standard state calculations. Of particular importance is the class NasaThermo, which assumes that each species in the phase is an ideal gas comprising a NasaPoly2 reference state format. The NasaPoly2 format assumes that the standard state polynomials may be separated into two temperature regions, each with a standard NASA polynomial represented by 7 coefficient polynomials used in the JANAF tables and in the code Chemkin [57,56].

The GeneralSpeciesThermo class, which inherits from SpeciesThermo, is special in the sense that it doesn't make any assumptions about the reference states of the species in its phase. The class, which just contains a list of pointers to SpeciesThermoInterpType classes, which it calls consecutively to calculate thermodynamic properties, should work in all cases.

All classes that employ variable temperature and pressure standard states for their species inherit from the class VPStandardState, which in turn inherits from ThermoPhase. VPStandardState modifies the assumptions of ThermoPhase slightly while still maintaining its interface functions. A variable pressure and temperature standard state is assumed. All pressure dependent standard states inherit from the virtual base class PDSS (pressure dependent standard state) calculator class. VPStandardState maintains a pointer list of PDSS standard state calculator classes. However, in order to calculate a vector of standard state properties for its species, it maintains a Manager class called VPSSMgr, which assumes certain properties of the species standard state classes within the phase in order to create efficiencies in the calculation of those properties by grouping common work.

Fig. 1 contains a current list of all classes that inherit from the PDSS and VPSSMgr classes. Of particular interest to the current work are the PDSS child classes PDSS_HKFT and PDSS_Water. The pressure and temperature equations for the PDSS_HKFT class, described in the next section, are the most common equations used to describe electrolytes in water. The PDSS_Water class is used to describe the liquid portion (liquid and supercritical fluid) of the full equation of state for water from Wagner and Pruβ [32].

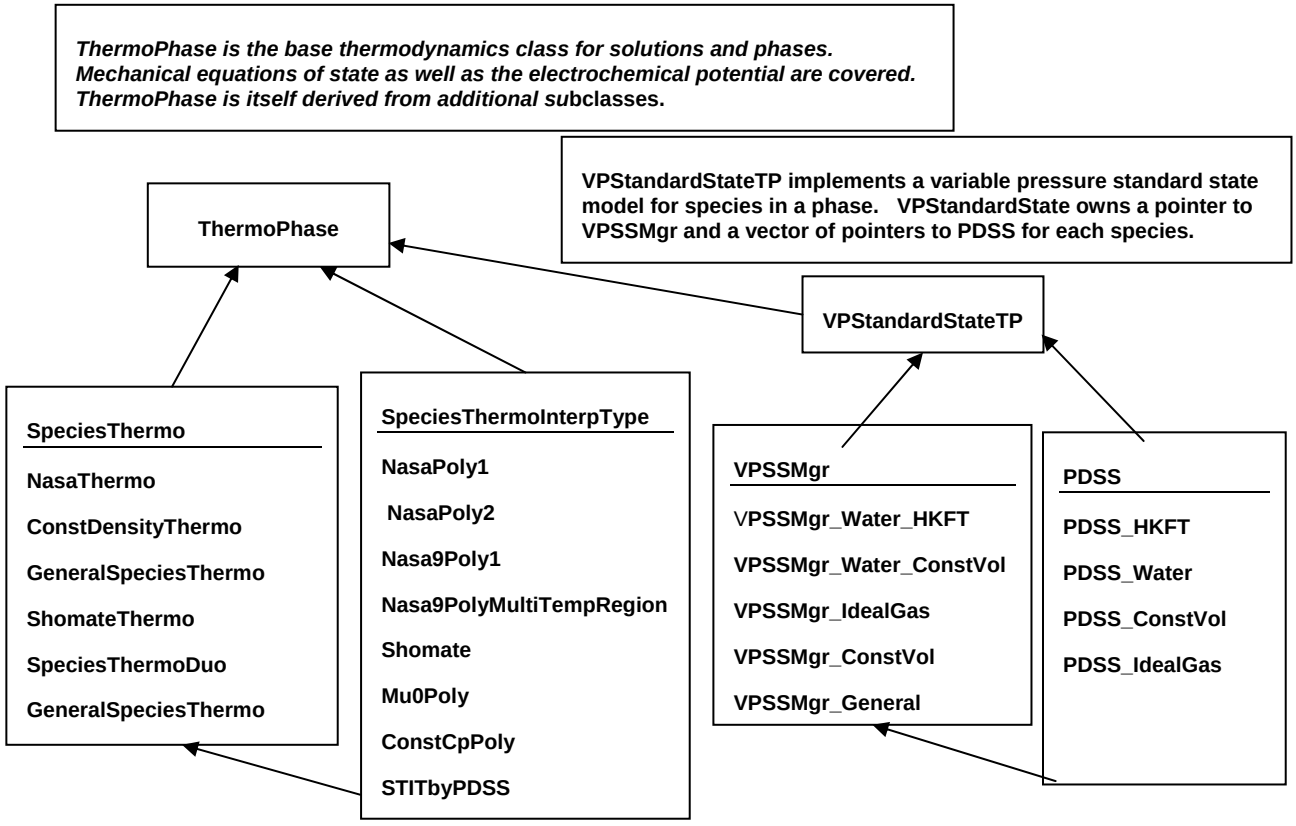

Fig. 1. Pictorial description of Standard State Calculators and Standard State Managers within Cantera

Cantera classes maintains a child `PDSS_IdealGas` class just for internal checking against the alternative and faster class, `NasaPoly2`, described previously. The associated Manager class is `VPSSMgr_IdealGas`. The class `VPSSMgr_General` makes no assumption about the type of `PDSS` classes in the phase, and may be used with any combination of `PDSS` classes. The manager class that is used with the brine thermochemistry capability the most is the `VPSSMgr_Water_HKFT` manager class. This class assumes that species 0 employs a real water equation of state (`PDSS_Water`) and the rest of the species employ an electrolyte equation of state, `PDSS_HKFT`, described in the next section.

3.1 Formulation of the HKFT Standard State

The common standard state adopted for solute ions in electrolyte solutions is designated in this work as the `HKFT` standard state. `HKFT` stands for the four authors who develop the EoS formulations for retrieval of thermodynamic data of aqueous species consistent with this standard state: Harold C. Helgeson, David H. Kirkham, George C. Flowers, and John C. Tanger (IV). Often in the literature,

this EoS is referred as HKF after the seminal works of Helgeson, Kirkham, and Flowers [20 and references therein] or the revised HKF after the work of Tanger and Helgeson [32]. This standard state is defined by unit activity of the ionic species in a hypothetical one molal solution referenced to infinite dilution at any pressure and temperature. The implementation of the HKFT standard state within the Cantera framework [44] is the emphasis of this section. Nothing necessarily new has been developed within Cantera to handle electrode reactions. This capability to model Butler-Volmer electrode reactions has previously been used extensively within Cantera to model solid oxide fuel cells [45]. Wedo, however, explain how this functionality is used within liquid water electrolyte systems.

The HKFT standard state is used extensively within the SUPCRT92 [46] package calculating thermodynamic properties if ions, solids, and gases, and the EQ3/6 software package. Essentially, because this standard state has been widely used as the basis for fitting experimental data on ions in water, this has become the *de facto* standard despite some of the heuristic issues involved with its implementation. The standard state varies with both temperature and pressure. Therefore, it's fundamentally different from other standard states, for example the one adopted in the gas phase literature, and available on the NIST website [24], that are based on a fixed temperature.

The HKFT standard state is similar to the NIST standard state in the fact that it makes an assumption about an idealized standard state. The HKFT assumes an idealized one molal solution of the ions referenced to the infinite dilution state, while the NIST standard state assumes an idealized ideal gas approximation at any temperature and pressure, which is only ideally realized at infinite dilution. Thus, it's assumed that the activity coefficients (on the molality scale) are all one.

3.1.1 Definition of Standard States

There is no such thing as an absolute value of a Gibbs free energy or an Enthalpy of a species. These energies are all based on comparing differences of energies for a set of species relative to a common reference condition, within which differences due to legitimate chemical reactions which conserve elements cancel out. Because Cantera has its roots in the combustion field, we maintain its adherance to the Gibbs free energy reference condition used by NIST and by the JANAF tables based on the $\Delta H^o_{f,298}\left(elements\right)=0$ condition. In this section we will explain how to reconcile this condition with the convention normally invoked for aqueous thermodynamics [47] which uses the apparent standard partial molar Gibbs free energy of formation as its reference condition for its Gibbs free energies.

$\Delta\bar{G}^{\triangle}_j\left(T,P\right)$ is the apparent standard partial molar (or molal[1]) Gibbs free energy of formation from the elements of species *j*. The "apparent" standard partial molal Gibbs free energy of formation at any *T* and *P* may be related to the Gibbs free energy of the formation reaction of the species from its constitutive elements in their stable states at 298 K and 1 bar by Eqn. (26). The "apparent" modifier takes on a special meaning in Eqn. (26). $\Delta\bar{G}^o_{f,j}$ is evaluated at $\left(T_r\,,P_r\right)$. However, only the Gibbs free energy of species *j* is adjusted at a given temperature and pressure.

[1] The distinction between partial molar and partial molal quantities is one based on units only. They are the same up to a multiplicative constant. See the discussion in the nomenclature section concerning the difference between $\Delta\hat{G}^{\triangle}_{f,k}(T,P)$ and $\Delta\bar{G}^{\triangle}_{f,k}(T_r\,,P_r\,)$.

$$\Delta\bar{G}_j^{\triangle}(T,P) = \Delta\bar{G}_{f,j}^{\triangle}(T_r,P_r) + \left(\bar{G}_j^{\triangle}(T,P) - \bar{G}_j^{\triangle}(T_r,P_r)\right) \quad (26)$$

$\Delta\bar{G}_{f,j}^{\triangle}(T_r,P_r)$ is defined as the standard partial molar Gibbs free energies of formation of a species from its elements in their stable forms at the reference pressure P_r and temperature T_r of 1 bar and 298 K. $\bar{G}_j^{\triangle}(T,P) - \bar{G}_j^{\triangle}(T_r,P_r)$ is the difference in the standard partial molal Gibbs free energies of species *j* at (T,P) vs. (T_r,P_r).

There is a further convention applied only to ionic species in aqueous solutions that has far reaching consequences. The apparent standard partial molar Gibbs free energy of formation of those ions are represented on a conventional (i.e., H+ convention) basis rather than an absolute basis via the following formulation [46, 66].

$$\Delta\bar{G}_j^{\triangle}(T,P) = \Delta\bar{G}_j^{\triangle,abs}(T,P) - z_j\Delta\bar{G}_{\mathrm{H+}}^{\Delta,abs}(T,P) \quad (27)$$

$\Delta\bar{G}_{\mathrm{H+}}^{\triangle,abs}(T,P)$ is the absolute standard partial molal Gibbs free energy of formation of the hydrogen ion. z_j is the ionic charge of the ion, *j*. With this definition, ionic species may be defined on a relative basis, in which apparent standard partial molal Gibbs free energy of the hydrogen ion is zero for all temperatures and pressures:

$$\Delta\bar{G}_{\mathrm{H+}}^{\triangle}(T,P) = 0 \quad (28)$$

Lastly, $\Delta\bar{G}_{f,j}^{\triangle}(T_r,P_r)$ may be related to the Gibbs free energy definition used in the JANAF and NIST database, which is referred to here as either $\tilde{G}_j^{o}(T,P)$ or $\tilde{G}_j^{\triangle}(T,P)$ depending upon whether the specific activity coefficient formulation is on the molar or molality scale. This Gibbs free energy formulation is based on the standard state conventions where $\Delta H_{f,298}^{o}(elements) = 0$. This convention, followed by NIST and the JANAF tables, sets the Enthalpy of formation of the elements at T_r and P_r to zero. The two scales may be related by the following equation.

$$\Delta\bar{G}_{f,j}^{\triangle}(T_r,P_r) = \tilde{G}_j^{\triangle}(T_r,P_r) - \sum_i \alpha_{ij}\tilde{G}_i^{o}(T_r,P_r) = \bar{G}_j^{\triangle}(T_r,P_r) + \left(\sum_i \alpha_{i,j}\tilde{S}_i^{o}(T_r,P_r)\right)T_r \quad (29)$$

because

$$\Delta\bar{H}_{f,j}^{\triangle}(T_r,P_r) = \tilde{H}_j^{\triangle}(T_r,P_r) - \sum_i \alpha_{ij}\tilde{H}_i^{o}(T_r,P_r) = \tilde{H}_j^{\triangle}(T_r,P_r) \quad (30)$$

$\alpha_{i,j}$ is the formula matrix for the j^{th} species, with $\alpha_{i,j}$ being the number of atoms of element *i* in species *j*. $\tilde{S}_i^{o}(T_r,P_r)$ is the Entropy per gmol of the i^{th} element in its stable state at T_r and P_r.

To calculate $\tilde{G}_j^{\triangle}(T,P)$, the NIST-scaled Gibbs free energy to be used within Cantera, either of the following formulas, Eqn. (31) or Eqn. (32), may be used.

$$\tilde{G}_j^{\triangle}(T,P) = \tilde{G}_j^{\triangle}(T_r,P_r) + \left(\tilde{G}_j^{\triangle}(T,P) - \tilde{G}_j^{\triangle}(T_r,P_r)\right) \quad (31)$$

$$\tilde{G}_j^{\vartriangle}(T,P) = \left[\Delta\bar{G}_{f,j}^{\vartriangle}(T_r, P_r) - \left(\sum_i \alpha_{i,j} \tilde{S}_i^o(T_r, P_r) \right) T_r \right] + \left(\tilde{G}_j^{\vartriangle}(T,P) - \tilde{G}_j^{\vartriangle}(T_r, P_r) \right) \qquad (32)$$

The first formula, Eqn. (31), assumes the Gibbs free energy is already using the NIST $\Delta\tilde{H}_{j,298}^o(elements) = 0$ absolute scaling convention. The second formula, Eqn. (32), assumes that the base thermodynamic data is given in SUPCRT92 format, i.e., Gibbs free energy of formation, in which case a correction factor based on the entropies of the elements in their standard states needs to be applied before being used within Cantera. For more information see ref. [3]. We provide an explicit example of Eqn. (29) in action in the example section at the end of the memo. It should be noted that the form of equations (26) through (32) applies to any standard molal property of the ion or the bulk electrolyte.

The standard state adopted so far, i.e., the "$_{\vartriangle}$" in the expression, $\tilde{G}_j^{\vartriangle}(T,P)$, is a special one. For ions in solution it is defined as the state of unit activity of the species in a hypothetical one molal solution referenced to infinite dilution at any pressure and temperature [33]. The full expression for the partial molal chemical potential $\tilde{\mu}_j(T,P,\boldsymbol{m})$ may then be calculated from Eqn. (33),

$$\tilde{\mu}_j(T,P,\boldsymbol{m}) = \tilde{G}_j^{\vartriangle}(T,P) + RT\ln\left(\frac{m_j\gamma_j^{\Delta}}{m^{\Delta}}\right) \qquad (33)$$

where m_j is the molality of species *j* in the solution, γ_j^{Δ} is the molality-based activity coefficient of species *j*, and m^{Δ} is the molality in the adopted standard state. Notice that the latter is a constant that makes the logarithm of the expression unitless. The standard state for gases, however, remains a unit fugacity of the gas at 1 bar at any temperature.

Unlike the Gibbs free energies, all other thermodynamic functions don't have to be modified. From Eqn. (30), the absolute-scale enthalpies used by Cantera, $\tilde{H}_j^{\vartriangle}(T,P)$, are equal to the enthalpy of formation of species *j* from elements in their standard states, $\Delta\bar{H}_{f,j}^{\vartriangle}(T_r, P_r)$, used by the computer code SUPCRT92.

For ionic species, within Cantera, we have chosen the case that both $\Delta\bar{G}_{\mathrm{H+}}^{\vartriangle}(T,P) = 0$ and $\tilde{G}_{\mathrm{H+}}^{\vartriangle}(T,P) = 0$ are true [27], implying also that

$$\tilde{G}_{\mathrm{H^+}}^{\vartriangle}(T,P) = \tilde{H}_{\mathrm{H^+}}^{\vartriangle}(T,P) = \tilde{S}_{\mathrm{H^+}}^{\vartriangle}(T,P) = \tilde{V}_{\mathrm{H^+}}^{\vartriangle} = \tilde{C}_{p,\mathrm{H^+}}^{\vartriangle} = 0 \qquad (34)$$

Also, only reactions that ensure charge neutrality in the liquid phase are allowed. Therefore, the H^+ formation reaction may be invoked if an e- species is used:

$$\frac{1}{2}\mathrm{H_2}(g) = \mathrm{H^+} \quad + \quad \mathrm{e^-}(Pt) \qquad (35)$$

It turns out that an additional standard (the standard hydrogen electrode – SHE) is invoked at this point which specifies that the Gibbs free energy of Eqn. (35) is zero when the electron e- is located within platinum metal. In this case we can write out the consequences in Eqn. (36).

$$\Delta\bar{G}^{\triangle}_{H+}(T,P) = \tilde{G}^{\triangle}_{H^+}(T,P) + \tilde{G}^{\triangle}_{e^-}(T,P) - \frac{1}{2}\tilde{G}^{o}_{H_2(g)}(T,P) = 0 \tag{36}$$

implying that

$$\tilde{G}^{\triangle}_{e^-}(T,P) = \frac{1}{2}\tilde{G}^{o}_{H_2(g)}(T,P) = \frac{1}{2}\left(\tilde{H}^{o}_{H_2(g)}(T,P) - \tilde{S}^{o}_{H_2(g)}(T,P)T\right) = \frac{-1}{2}\tilde{S}^{o}_{H_2(g)}(T,P)T \tag{37}$$

The last step in Eqn. (37) is due to the $\Delta H^{o}_{f,298}(elements) = 0$ convention. Note, Eqn. (37) is true for any temperature and pressure. The Pt e^- electron for the NIST-based Gibbs free energy has a pressure and temperature dependence similar to an ideal gas. Eqn. (37) is sometimes helpful in deriving expressions involving electrode reactions [50] which involve the exchange of an electronic charge in a metal electrode with the aqueous phase.[2] In this case a related expression to Eqn. (37) is actually employed for electrons within metals:

$$\tilde{G}^{o}_{e^-,M}(T,P) = -\frac{1}{2}\tilde{G}^{o}_{H_2(g)}(T,P)T + z_{e^-}F\Phi_M \tag{38}$$

Here $\tilde{G}^{o}_{e^-,M}(T,P)$ refers to the chemical potential of an electron within a Metal *M*. It's strictly true only for Pt and for relative measurements between electrodes made up of the same metal, but can be considered to be independent of the type of metal for practical cases not involving large changes in temperature Φ_M refers to the electric potential of Metal *M* with respect to the electrolyte liquid.

3.1.2 HKFT System of Equations

From the theory presented in refs. [47, 66], the change in the standard state Gibbs free energy with respect to temperature and pressure may be written as Eqn. (39).

[2] Work function differences between metal electrodes are absorbed within the Gibbs free energies of the electrode reactions such that all electrons within quoted electrode reactions can be assumed to be in a platinum metal.

$$\begin{aligned}\tilde{G}_j^{\triangle}(T,P)-\tilde{G}_j^{\triangle}(T_r,P_r)=&-\tilde{S}_j^{\triangle}(T_r,P_r)(T-T_r)-c_1\left(T\ln\frac{T}{T_r}-(T-T_r)\right)\\&+\left(a_1(P-P_r)\right)+a_2\ln\left(\frac{\Psi+P}{\Psi+P_r}\right)\\&-c_2\left(\left(\left(\frac{1}{T-\Theta}\right)-\left(\frac{1}{T_r-\Theta}\right)\right)\left(\frac{\Theta-T}{\Theta}\right)-\left(\frac{T}{\Theta^2}\right)\ln\left(\frac{T_r(T-\Theta)}{T(T_r-\Theta)}\right)\right)\\&+\left(\frac{1}{T-\Theta}\right)\left(a_3(P-P_r)+a_4\ln\left(\frac{\Psi+P}{\Psi+P_r}\right)\right)\\&+\omega_j\left(\frac{1}{\varepsilon}-1\right)-\omega_{j,P_r,T_r}\left(\frac{1}{\varepsilon_{P_r,T_r}}-1\right)+\omega_{j,P_r,T_r}\left(Y_{P_r,T_r}\right)(T-T_r)\end{aligned} \tag{39}$$

We note a couple of conventions. First, the constants, c_1, c_2, a_1, a_2, a_3, a_4 and ω_{j,P_r,T_r} are all implicit constant values of the ion, *j*, fit to experimental data. The Born radius, ω_j is a calculated function of the temperature and pressure that only depends on the one constant value, ω_{j,P_r,T_r}. The *j* subscript has just been left out of the expression. These constants are supplied from the input file for each ion.

Some of the variables in Eqn. (39) pertain to the solvent water. The parameters Θ and Ψ are set to 228.0 K and 2600, respectively. They represent universal behavior experienced by ions in water. ε, the dielectric constant of water, is a complicated function of *T* and *P*. The following variables derived from ε, *Z*, *Y*, *Q*, and *X*, are defined and used within Cantera:

$$Z=-\frac{1}{\varepsilon}\ , \tag{40}$$

$$Y=\left.\frac{dZ}{dT}\right|_P=\frac{1}{\varepsilon^2}\left(\frac{\partial\varepsilon}{\partial T}\right)_P,$$

$$Q=\left.\frac{dZ}{dP}\right|_T=\frac{1}{\varepsilon^2}\left(\frac{\partial\varepsilon}{\partial P}\right)_T,$$

$$X=\left.\frac{dY}{dT}\right|_P=\frac{1}{\varepsilon^2}\left(\frac{\partial^2\varepsilon}{\partial T^2}\right)_P-2\varepsilon Y^2$$

The dielectric constant for liquid water and its derivatives have already been implemented within Cantera [4]. However, SUPCRT92 has an alternative form from [49] that is qualitatively the same. Experiments have shown that even the derivatives of the two formulations are quantitatively fairly close to one another.

From Eqn. (39), the development of the equations for the standard state entropies, enthalpies, and standard state volumes follow directly from thermodynamic relations. And, for consistency it must be the case that

$$\tilde{G}_j^{\triangle}(T,P) = \tilde{H}_j^{\triangle}(T,P) - T\,\tilde{S}_j^{\triangle}(T,P) \tag{41}$$

Also, the other thermodynamic function s will be derived from derivatives of Eqn. (39). Therefore, Eqn. (39) represents the complete specification of the standard state HKFT.

3.1.2.1 Entropy Calculation

The entropy may be derived from $d\tilde{G}_j^{\triangle}(T,P) = \tilde{V}_j^{\triangle} dP - \tilde{S}_j^{\triangle}(T,P)\,dT$ to yield:

$$\tilde{S}_j^{\triangle} = \left.\frac{d\tilde{G}_j^{\triangle}(T,P)}{dT}\right|_P . \tag{42}$$

The absolute entropy of species *j* at the reference temperature and pressure (T_r, P_r) is an input parameter. The change in entropy from the reference temperature and pressure is calculated from taking the derivative of Eqn. (39) to yield the following expression.

$$\begin{aligned}\tilde{S}_j^{\triangle}(T,P) - \tilde{S}_j^{\triangle}(T_r,P_r) = {} & c_1\left(\ln\frac{T}{T_r}\right) \\ & -\frac{c_2}{\Theta}\left(\left(\frac{1}{T-\Theta}\right)-\left(\frac{1}{T_r-\Theta}\right)+\left(\frac{1}{\Theta}\right)\ln\left(\frac{T_r(T-\Theta)}{T(T_r-\Theta)}\right)\right) \\ & +\left(\frac{1}{T-\Theta}\right)^2\left(a_3(P-P_r)+a_4\ln\left(\frac{\Psi+P}{\Psi+P_r}\right)\right) \\ & +\left.\frac{d\omega_j}{dT}\right|_P (Z+1) - \left.\frac{d\omega_j}{dT}\right|_{P_r,T_r}\left(Z_{P_r,T_r}+1\right) + \omega_j Y - \omega_{j,P_r,T_r} Y_{P_r,T_r}\end{aligned} \tag{43}$$

Note, this expression is different than Eqn. (61) in [47]. However, the latter is missing the $d\omega_j / dT\left(Z_{P_r,T_r}+1\right)$ term. It may however be the case that the term is missing because it is zero for the cases considered, and therefore was just left out. Numerical experiments indicated that it is small but not zero. Therefore, we have formally left the term in.

3.1.2.2 Enthalpy Calculation

The enthalpy may be calculated from the previous formulas for $\tilde{G}_j^{\triangle}(T,P)$ and $\tilde{S}_j^{\triangle}(T,P)$, and from Eqn. (41).

$$\begin{aligned}\tilde{H}_j^{\triangle}(T,P)-\tilde{H}_j^{\triangle}(T_r,P_r) &= c_1(T-T_r)\\ &+\left(a_1(P-P_r)\right)+a_2\ln\left(\frac{\Psi+P}{\Psi+P_r}\right)\\ &-c_2\left(\left(\frac{1}{T-\Theta}\right)-\left(\frac{1}{T_r-\Theta}\right)\right)\\ &+\left(\frac{2T-\Theta}{(T-\Theta)^2}\right)\left(a_3(P-P_r)+a_4\ln\left(\frac{\Psi+P}{\Psi+P_r}\right)\right)\\ &+T\left(\left(\frac{d\omega_j}{dT}\right)_P(Z+1)-\left(\frac{d\omega_j}{dT}\right)_{T_r,P_r}\left(Z_{T_r,P_r}+1\right)\right)\\ &+\omega_j Y\ T-\omega_{j,P_r,T_r}Y_{P_r,T_r}T_r\\ &-\left(\omega_j(Z+1)-\omega_{j,P_r,T_r}\left(Z_{P_r,T_r}+1\right)\right)\end{aligned} \tag{44}$$

Although this equation may seem redundant, since Eqn. (39) and Eqn. (43) are sufficient as to provide a complete set of thermodynamic properties of interest, it's useful for understanding changes in the standard state enthalpy (measurable quantity) with temperature and pressure.

For purposes of the code, however, $\tilde{H}_j^{\triangle}(T_r,P_r)$ is not a primary quantity, unlike $\tilde{G}_j^{\triangle}(T_r,P_r)$ and $\tilde{S}_j^{\triangle}(T_r,P_r)$. This somewhat arbitrary prioritization is necessary for internal consistency. You can't have three quantities specifying two independent unknowns $\tilde{H}_j^{\triangle}(T_r,P_r)$ is supplied from the input file and checked for consistency, however.

It should also be mentioned that the SUPCRT92 database contains three quantities, $\Delta\bar{G}_j^{\triangle}(T,P)$, $\Delta\bar{H}_j^{\triangle}(T,P)$, and $\Delta\bar{S}_j^{\triangle}(T,P)$, which are not independent quantities. As has been previously mentioned, the heat of formation reaction for species *j* at standard conditions, $\Delta\bar{H}_{f,j}^{o}(298.15K,1\,\text{bar})$, is equal to the absolute enthalpy under the NIST convention, $\tilde{H}_j^{o}(T_r,P_r)$. However, in implementing the database within SUPCRT92, we ignore the $\Delta\bar{H}_j^{o}(T,P)$ entry. Actually, its value is internally checked to make sure that its value is within an acceptance tolerance condition.

3.1.2.3 Heat Capacity Calculation

The constant pressure heat capacity may be calculated from the following expression.

$$\tilde{C}_{p,j}^{\triangle}=\left.\frac{d\tilde{H}_j^{\triangle}(T,P)}{dT}\right|_P \tag{45}$$

Taking the derivative of Eqn. (45) yields:

$$\tilde{C}_{p,j}^{\triangle}(T,P) = c_1 + \frac{c_2}{(T-\Theta)^2} - \left(\frac{2T}{(T-\Theta)^3}\right)\left(a_3\left(P-P_r\right) + a_4 \ln\left(\frac{\Psi+P}{\Psi+P_r}\right)\right) + 2TY\left(\frac{d\omega_j}{dT}\right)_P + \omega_j TX + T(Z+1)\left(\frac{d^2\omega_j}{dT^2}\right)_P \quad (46)$$

3.1.2.4 Standard State Volume

The standard state molar volume may be calculated from the following expression.

$$\tilde{V}_j^{\triangle} = \left.\frac{d\tilde{G}_j^{\triangle}(T,P)}{dP}\right|_T \quad (47)$$

Taking the derivative of Eqn. (39) yields:

$$\tilde{V}_j^{\triangle}(T,P) = a_1 + \frac{a_2}{\Psi+P} + \frac{a_3}{T-\Theta} + \frac{a_4}{(\Psi+P)(T-\Theta)} - \left(\frac{d\omega_j}{dP}\right)_T (Z+1) - \omega_j Q \quad (48)$$

Thus, the standard state volume depends on both *T* and *P*.

3.1.3 Theory

We write down the formation reaction Gibbs free energy as a sum of two terms: a non-solvation term and a solvation term. The absolute standard partial molal Gibbs free energy of solvation, $\Delta_s \bar{G}_j^{o,abs}$, is expressed as [66]

$$\Delta_s \bar{G}_j^{o,abs} = \frac{N_a z_j^2 e^2}{2r_{e,j}}\left(\frac{1}{\varepsilon}-1\right) = \omega_j^{abs}\left(\frac{1}{\varepsilon}-1\right) \quad (49)$$

where ω_j^{abs} is the absolute Born coefficient for the ion, N_a stands for the Avogadro's number, and z_j designates the charge of the ion.

3.1.4 Calculation of the Born Radius

The absolute Born coefficient of the j^{th} ion appears in the expressions above. Following Johnson et al. [46] and Shock et al. [66], the conventional Born coefficient it is given by Eqn. (50).

$$\omega_j = \omega_j^{abs} - Z_j \omega_{\mathrm{H+}}^{abs} \tag{50}$$

We note that this means that $\omega_{\mathrm{H+}} = 0$ by definition. Also, it means that the expression for $\omega_{\mathrm{H+}}^{abs}$ is associated with all other ions in the solution, and it is compatible with the convention that $V_{\mathrm{H+}}^o = H_{\mathrm{H+}}^o = S_{\mathrm{H+}}^o = 0$, as long as all the other coefficients for H^+ (e.g., a_1, a_2, ...) are identically zero, as well. In turn,

$$\omega_{\mathrm{H+}}^{abs} = \frac{\eta Z_j^2}{r_{e,j}} \tag{51}$$

where $\eta = 1.66027 \times 10^5$ Å cal gmol^{-1}. The value of $\omega_{\mathrm{H+}}^{abs}$ at 298 K and 1 bar is taken to be 0.5387×10^5 cal gmol^{-1}, which yields $r_{e,\mathrm{H+},T_r,P_r} = 3.082$ Å. $r_{e,j}$ refers to the effective electrostatic radius of the j^{th} ionic species defined as

$$r_{e,j} = r_{e,\mathrm{H+},T_r,P_r} + |Z_j| g \tag{52}$$

g is a function of the solvent and is dependent on temperature and pressure. It is also an universal function with respect to the identity of the ionic species, and its formulation is described below. Combination of Eqns. (50), (51), and (52) yields the following expression:

$$\omega_j = \omega_j^{abs} - Z_j \omega_{\mathrm{H+}}^{abs} = \eta \left(\frac{Z_j^2}{r_{e,j}} - \frac{1}{3.082 + g} \right) = \eta \left(\frac{Z_j^2}{r_{e,j,T_r,P_r} + |Z_j| g} - \frac{1}{3.082 + g} \right) \tag{53}$$

Eqn. (53) is implemented within the code. An expression for the ionic radius of ion *j* at the standard temperature and pressure, r_{e,j,T_r,P_r}, is needed. Eqn. (53) may be used to determine an expression for r_{e,j,T_r,P_r} in terms of ω_{j,T_r,P_r}.

$$r_{e,j,T_r,P_r} = Z_j^2 \left[\frac{\omega_{j,T_r,P_r}}{\eta} + \frac{Z_j}{r_{e,\mathrm{H+},T_r,P_r}} \right]^{-1} \tag{54}$$

Again, the value of $r_{e,\mathrm{H+},T_r,P_r} = 3.082$ Å is used within Eqn. (54) to calculate the Born radius of ion *j*. All of the fitting therefore has implicitly relied on this number. In practice, ω_{j,T_r,P_r} is used as the fitting parameter for species *j*. Then, Eqn. (54) is used to evaluate r_{e,j,T_r,P_r} at T_r and P_r. Then, Eqn. (53) is used to extrapolate the value of $r_{e,j}$ to other temperatures and pressures. In this process, there is just one fitting parameter, ω_{j,T_r,P_r}, per species.

The function *g* is parameterized as a function of *T* and *P*, and was originally fit from an extensive investigation of the NaCl system [33]. It's form, revised in [34], is given in Eqn. (55).

$$g = a_g \left(1-\hat{\rho}\right)^{b_g} - f \tag{55}$$

where

$$a_g = a_{g,1} + a_{g,2}T + a_{g,3}T^2 \tag{56}$$

$$b_g = b_{g,1} + b_{g,2}T + b_{g,3}T^2$$

and *f* denotes a difference function given by the following expression

$$\begin{aligned} f = &\left[\left(\frac{\left(T-155\,C\right)}{300}\right)^{4.8} + a_{f,1}\left(\frac{\left(T-155\,C\right)}{300}\right)^{16}\right] \\ &\times\left[a_{f,2}\left(1000-P\left(bar\right)\right)^3 + a_{f,3}\left(1000-P\left(bar\right)\right)^4\right] \end{aligned} \tag{57}$$

Non-zero values of g are limited to values of the density, $\hat{\rho}$, which are less than 1 gm cm^{-3}. Non-zero values of *f* are restricted to temperatures greater than 155 and less than 355, and pressures below 1000 bar. The whole procedure is restricted to absolute densities greater than 0.35 g cm^{-3}, due to the lack of fitting data outside this density range. The coefficients in Eqns. (55) through (57) are given in Tables 2 and 3 in [47] and Tables 3 and 4 in [67]. It sould be noted to the user that there are minor discrepancies in these tabulations even when they should be identical. The numerical values for these coefficients as given by [47] are correct and are adopted in the current Cantera implementation of the HKFT EoS. However, the temperature units reported for some of the coefficients in this source is in degree Celsius instead of Kelvin. Shock et al. [67] reports these coefficients in degrees Kelvin, consistent with the usage of temperature units in all these equations. Nevertheless, there is one discrepancy in the numerical value of $a_{g,1}$, which is smaller by a factor 10 relative to that listed in [47] (i.e., 3.66666 instead of 36.66666). The value of 36.66666 given by [47] is the correct one and is adopted in the current Cantera implementation.

3.1.5 Modification for Neutral Species

For the case of neutral species, Eqns. (50) and (53) are essentially replaced by an "effective" Born coefficient $\omega_{e,j}$ that is essentially obtained from a fitting process [51]. These effective ω_e, obtained from regression of experimental data, are assumed to be independent of temperature and pressure. Therefore, the following simplifications in Eqn. (53) can be made.

$$\omega_{e,j} = \omega_{e,j,T_r,P_r} \qquad \frac{d\omega_{e,j}}{dT} = \frac{d\omega_{e,j}}{dP} = 0 \tag{58}$$

These simplifications to $\omega_{e,j}$ modify the equations for the standard state properties given in Eqn. (39) to Eqn. (48). ω_{e,j,T_r,P_r} is input directly from XML file.

```
<species name="Na+">
  <speciesChemFormula> Na+ </speciesChemFormula>
  <atomArray> Na:1 </atomArray>
  <charge +1 </charge>
  <thermo model="HKFT">
  <HKFT Pref="1 atm" Tmax="625.15" Tmin=273.15">
      <DG0_f_Pr_Tr units="cal/gmol"> -62591 </DG0_f_Pr_Tr>
      <DH0_f_Pr_Tr units="cal/gmol"> -57433 </DH0_f_Pr_Tr>
      <S_Pr_Tr units="cal/gmol/K">   13.96  </S_Pr_Tr>
  </HKFT>
  </thermo>
  <standardState model="HKFT">
    <a1 units="cal/mol/bar"> 0.1839 </a1>
    <a2 units="cal/mol"> -228.5 </a2>
    <a3 units="cal K/mol/bar"> 3.256 </a3>
    <a4 units="cal K/mol"> -27260 </a4>
    <c1 units="cal/mol/K"> 18.18 </c1>
    <c2 units="cal K/mol"> -29810 </c2>
    <omega_Pr_Tr units="cal/mol"> 33060 </omega_Pr_Tr>
  </standardState>
  <source> ref:G9 </source>
</species>
```

Fig. 2. XML Format for an HKFT standard state

Values of ω_{e,j,T_r,P_r} regressed from experimental data are negative. This is due to the disruptive effect of a neutral molecule on the electrostatic forces of attraction among the solvent dipoles [52].

3.1.6 Implementation within Cantera

The standard state is implemented as a derivative of the `PDSS` (pressure dependent standard state) base class. The form of the XML data file entry is provided in Fig. 2. The example used is for the ion, Na^+. The units are native to `SUPCRT92`. Within Cantera, the units are translated into MKS format. It's assumed that $T_r = 298.15\ K$ and $P_r = 1$ atm within Fig. 2.

More must be said about the specification of $\Delta\bar{G}^o_{f,j}\left(T_r, P_r\right)$ within Cantera given its roots as a gas-phase constitutive modeling package. Cantera works with absolute Gibbs free energies, G^o_j, not $\Delta\bar{G}^o_{f,j}\left(T_r, P_r\right)$, which is the norm within the combustion community. Therefore, the $\Delta\bar{G}^o_{f,j}\left(T_r, P_r\right)$ values input from the input file, an example of which is Fig. 2, must be translated into G^o_j. This is done automatically within Cantera using Eqn. (59). Eqn. (59) is written in two forms: one for species *j* whose standard state is on the molar basis and one for species *j* whose standard state is on the molality basis; the equation is equivalent for the two forms.

$$\tilde{G}^o_j\left(T_r, P_r\right) = \Delta\bar{G}^o_{f,j}\left(T_r, P_r\right) + \left(\sum_e \alpha_{e,j}\tilde{G}^o_e\left(T_r, P_r\right)\right) - \frac{Z_j}{2}\tilde{G}^o_{\mathrm{H2(g)}}\left(T_r, P_r\right) \tag{59}$$

$$\tilde{G}_j^{\triangle}\left(T_r, P_r\right) = \Delta\bar{G}_{f,j}^{\triangle}\left(T_r, P_r\right) + \left(\sum_e \alpha_{e,j}\tilde{G}_e^o\left(T_r, P_r\right)\right) - \frac{Z_j}{2}\tilde{G}_{\mathrm{H2(g)}}^o\left(T_r, P_r\right)$$

$\alpha_{e,j}$ is the element stoichiometry within species *j* for element *e*. $\tilde{G}_e^o\left(T_r, P_r\right)$ is the Gibbs energy for the element *e* in its stable state at $\left(T_r, P_r\right)$. Z_j is the charge for species *j*. Within Cantera, the values of $\tilde{G}_e^o\left(T_r, P_r\right)$ have been added to the element database, so that Eqn. (59) may be applied automatically within the initialization process.

Let's go through an example of applying Eqn. (59) to the case of Na^+. CODATA [29], which follows the NIST standards for representing heats of formation and Gibbs free energies, has the following entries for Na^+:

$$\tilde{H}_j^{\triangle}\left(298.15, P_r\right) = -240.34 \pm .06 \text{ kJ gmol}^{-1}$$

$$\tilde{S}_j^{\triangle}\left(298.15, P_r\right) = 58.45 \pm .15 \text{ J gmol}^{-1}\text{ K}^{-1}$$

This implies that

$$\tilde{G}_j^{\triangle}\left(298.15, P_r\right) = -257.7668 \text{ kJ gmol}^{-1}$$

The SUPCRT92 database developed for the YMP (SPEQ06.dat) has the standard partial molal Gibbs free energies of formation of the Na^+ ion species set at

$$\Delta\bar{G}_{f,\mathrm{Na+}}^{\triangle}\left(T_r, P_r\right) = -62.591 \text{ kcal gmol}^{-1} = -261.88 \text{ kJ gmol}^{-1}$$

Let's go through the exercise of reconciling the two values, which differ by 4.113 kJ gmol^{-1}. $\Delta\bar{G}_{f,\mathrm{Na+}}^{\triangle}\left(T_r, P_r\right)$ refers to the formation reaction below

$$\mathrm{H^+ + Na(s) \rightarrow Na^+ + \frac{1}{2}H_2(g)}$$

Then, we can formulate the Gibbs free energy of formation reaction in terms of the NIST-scaled Gibbs free energies as

$$\Delta\bar{G}_{f,\mathrm{Na^+}}^{\triangle}\left(T_r, P_r\right) = \tilde{G}_{\mathrm{Na^+}}^{\triangle} + \frac{1}{2}\tilde{G}_{\mathrm{H_2(g)}}^o - \tilde{G}_{\mathrm{Na(s)}}^o - \tilde{G}_{\mathrm{H^+}}^{\triangle}$$

Note, this is an explicit example of Eqn. (59) applied at the reference state conditions of $\left(T_r, P_r\right)$. Now, obtaining entropies from the JANAF tables, we obtain for NIST-scaled Gibbs free energies of the elements:

$$\tilde{G}_{\mathrm{H_2(g)}}^{\triangle} = -\tilde{S}_{\mathrm{H_2(g)}}^{\triangle}\left(298\right) = -\left(130.68 \text{ J gmol}^{-1}\text{ K}^{-1}\right)\left(298\,\mathrm{K}\right)$$

$$\frac{1}{2}\tilde{G}_{\mathrm{H_2(g)}}^{\triangle} = -19.48112 \text{ kJ gmol}^{-1}$$

and

$$\tilde{G}^{\triangle}_{\mathrm{Na(s)}} = -\tilde{S}^{\triangle}_{\mathrm{Na(s)}}\left(298.15\right) = -\left(51.30\ \mathrm{J\ gmol^{-1}\ K^{-1}}\right)\left(298.15\ \mathrm{K}\right)$$
$$= -15.29509\ \mathrm{kJ\ mol^{-1}}$$

Therefore, since the definition, $\tilde{G}^{\triangle}_{\mathrm{H+}} = 0$, is used:

$$\Delta\tilde{G}^{\triangle}_{f,\mathrm{Na+}}\left(T_r, P_r\right) = \tilde{G}^{\triangle}_{\mathrm{Na+}}\left(T_r, P_r\right) - 4.18606\ \mathrm{kJ\ gmol^{-1}}$$

Therefore, the SUPCRT92 Gibbs free energy value is consistent with an absolute scaled Gibbs free energy of $\tilde{G}^{\triangle}_{\mathrm{Na+}}\left(T_r, P_r\right) = -257.6904\ \mathrm{kJ\ gmol^{-1}}$. The SUPCRT92 value is 0.07 kJ gmol^{-1} which is larger than the CODATA value. This is typical (actually, one of the better cases) for the types of accuracies/discrepancies between the CODATA/JANAF and the SUPCRT92 thermodynamic databases.

3.2 Water Standard State

The PDSS_Water object employs the real EoS formulation of water given by Wagner and Pruß et al. [32], a complicated function of the Helmholtz free energy (not repeated here). The EoS expression advanced by these authors is also referred as the Internationation Association for the Properties of Water and Steam (IAPWS) 1995 formulation.

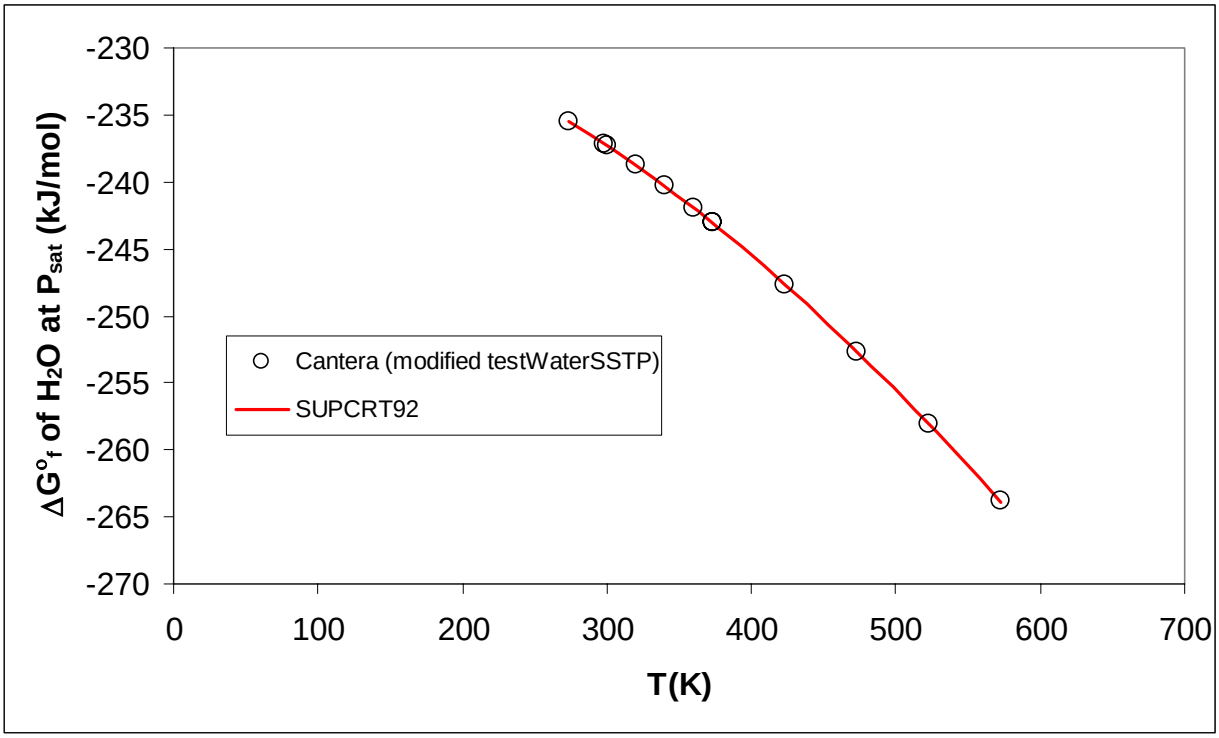

Fig. 3. Comparison of $\Delta\overline{G}^{a}_{f}\left(T,P\right)$ of H_2O between SUPCRT92 and the IAPWS implentation

in Cantera as a function of temperature along $P_{sat}(T)$.

Fig. 3 is a graph comparing the values computed using `SUPCRT92` and Cantera for the apparent Gibbs free energy of formation $\Delta\overline{G}_f^a(T,P)$ of H_2O as a function of temperature along $P_{sat}(T)$. The differences are very small (in the order of 0.01 to 0.02 percent). The consistency in results from two different sources (although similar sources of data) provides almost identical results.

The independent variables in the formulation are density and temperature. The `PDSS_Water` object translates the independent variables into pressure and temperature, by solving for the pressure at every density and temperature point. The pressure is a multivalued function at some points. For the purposes of calculating liquid equations of state, we have employed an algorithm that always chooses the liquid branch even if it is unstable compared to the gas branch as long as it is on the correct side of the spinodal curve, where

$$\left.\frac{d\rho}{dp}\right|_T = 0 \quad . \tag{60}$$

The spinodal curve as well as the liquid-vapor saturation curve are depicted in Fig. 4. Always choosing the liquid branch is necessary because the water standard state is calculated for conditions where the pure liquid water is unstable relative to pure steam yet the addition of electrolyte stabilizes the water phase. Complications associated with convergence of the pressure calculation very near the critical point have been deferred in this initial implementation.

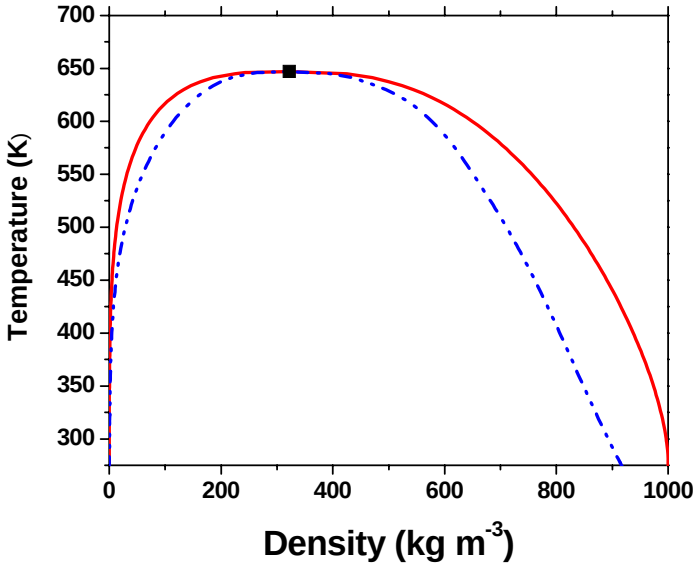

Fig. 4. Saturation curve from calculated from Wagner and Pruβ's equation of state is

displayed in red. Blue curve is the spinodal curve calculated within Cantera.

Additionally, the basis for the thermodynamic functions, both with respect to the entropy and the enthalpy, must be adjusted from zero value corresponding to liquid water at the water triple point to Cantera's current standard which follows the NIST/Chemkin standard of zero heat of formation for elements in their standard states and the absolute entropy. This transfer of basis is done within the `PDSS_Water` object.

3.2.1 Dielectric Constant

The dielectric constant of water is a full function of the temperature and pressure obtained from Bradley and Pitzer [38]. Fig. 5 confirms that the equations in Cantera are implemented correctly. The equations and coefficients in `WaterC` are fitted to the values given by the equation of Uematsu & Franck (1980) [39], another standard for obtaining H_2O dielectric constant as a *f(P,T)* for the dielectric constant of H_2O below 550°C. The `WaterC` code is a C implementation of a FORTRAN subroutine called 'H2O88' and was developed by Prof. Denis L. Norton and Loki Demsey at the Department of Geosciences, University of Arizona. This FORTRAN subroutine was written by James W. Johnson (LLNL) and Denis L. Norton for calculating the thermodynamic properties of H_2O. Details on the implementation of EoS formulations are described in Johnson and Norton [49].

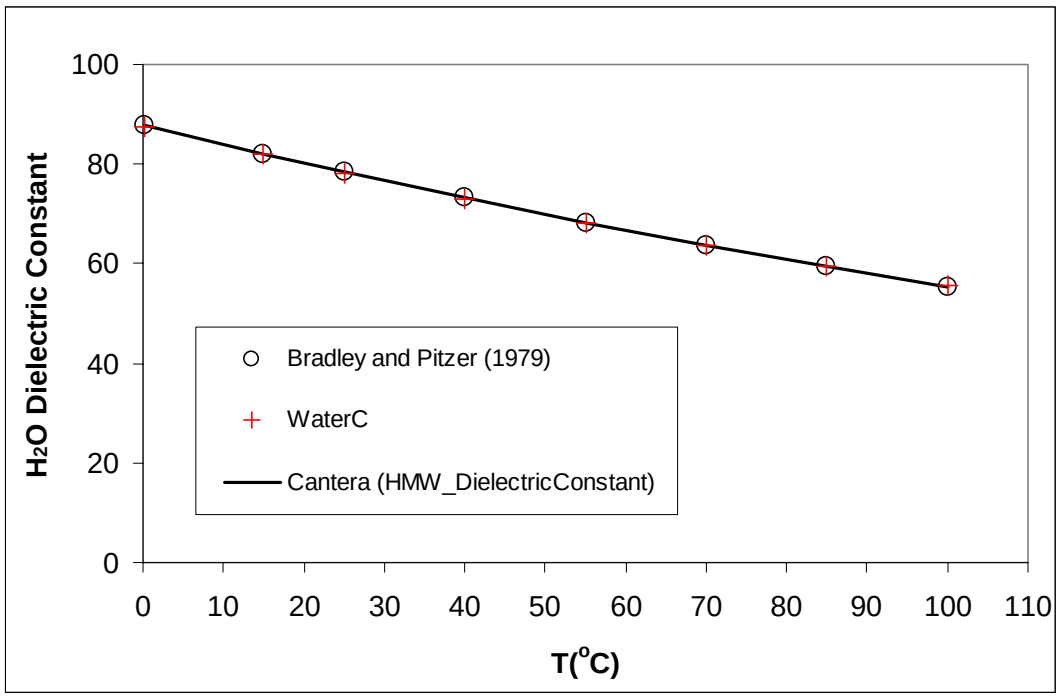

Fig. 5. Dielectric constants for water from Bradley and Pitzer [38], implementation of 'H2O88' in `WaterC` code (see text; Johnson and Norton, 1991) [49], and Cantera.

3.3 Other Standard State Implementations with Cantera

Several other types of standard states have been implemented within Cantera to support the database format used to generate the needed thermodynamic data to feed EQ3NR.

Aqueous species that are not ions are still handled by the `PDSS_HKFT` object. These have been covered in Section 3.1.5. However, there are a variety of minerals in the database used for EQ3NR which may be fit to the Shomate polynomial form (see Fig. 1 for a listing of the Thermodynamic objects).

Fig. 6 provides an example of the `MineralEQ3` format for specifying the formulation of a stoichiometric phase within Cantera, i.e., a phase whose composition can not vary. The thermodynamic model `MineralEQ3` is inherited from other existing models within Cantera that have previously emulated stoichiometric solids, specifically `StoichSubstanceSSTP`. However, `MineralEQ3` differs from the existing implementation in the sense that the Gibbs free energy, enthalpy and entropy at the T_r and P_r are specified via the Gibbs free energy of formation, the Enthalpy of formation and the Entropy, just as the ionic species in the aqueous phase are. Within Fig. 6, the first three entries, `DG0_f_Pr_Tr`, `DH0_f_Pr_Tr`, and `S0_Pr_Tr`. specify these quantities. Internally within Cantera, these are converted to the NIST absolute chemical potential standard, following the discussion in Section 3.1.1.

```
<?xml version="1.0" ?>
  <ctml>
    <validate reactions="yes" species="yes" />
    <!--
          phase NaCl(S)
      -->
    <phase dim="3" id="NaCl(S)">
      <elementArray datasrc="elements.xml">Na Cl</elementArray>
      <speciesArray datasrc="#species_NaCl(S)">NaCl(S)</speciesArray>
      <thermo model="MineralEQ3" />
      <transport model="None" />
      <kinetics model="none" />
    </phase>
    <!--
       species definitions
      -->
    <speciesData id="species_NaCl(S)">
       <species name="NaCl(s)">
         <atomArray>Na:1 Cl:1</atomArray>
         <charge>0</charge>
         <thermo model="MineralEQ3">
           <MinEQ3 Pref="1 atm" Tmax="1073." Tmin="200.">
             <DG0_f_Pr_Tr units="cal/gmol">-91807</DG0_f_Pr_Tr>
             <DH0_f_Pr_Tr units="cal/gmol">-98260</DH0_f_Pr_Tr>
             <S0_Pr_Tr units="cal/gmol/K">17.24</S0_Pr_Tr>
             <a units="cal/gmol/K">10.98</a>
             <b units="cal/gmol/K2">3.9E-3</b>
```

```
          <c units="cal K/gmol">0.0E5</c>
        </MinEQ3>
      </thermo>
      <standardState model="constantVolume">
        <V0_Pr_Tr units="cm3/gmol">27.015</V0_Pr_Tr>
      </standardState>
    </species>
  </speciesData>
</ctml>
```

Fig. 6. Example of the `MineralEQ3` database format. Example is for the stoichiometric solid NaCl(S).

The heat capacity is given by Eqn. (61). The form of this equation is consistent with that used in SUPCRT92 as given by Eq. 81 in Johnson et al. [47]. This turns out to be a subset of the Shomate polynomial representation already existing within Cantera. The coefficients for the heat capacity are given in the `MinEQ3` block within Fig. 6.

$$\tilde{C}^o_{p,j}(T,P) = a + bT + \frac{c}{T^2} \tag{61}$$

For the `MineralEQ3` stoichiometric solid, it is assumed that the phase has a constant molar volume, V^o_j, which is specified within Fig. 6. We have assumed that the enthalpy is adjusted as a function of pressure in order to make this assumption thermodynamically rigorous. The enthalpy is therefore given by

$$\tilde{H}^o_j(T,P) - \tilde{H}^o_j(T_r,P_r) = a(T - T_r) + \frac{b}{2}(T - T_r)^2 - \frac{c}{(T - T_r)} + V^o_j(P - P_r) \tag{62}$$

The entropy is given by

$$\tilde{S}^o_j(T,P) - \tilde{S}^o_j(T_r,P_r) = a\ln\left(\frac{T}{T_r}\right) + b(T - T_r) - \frac{c}{2(T - T_r)^2} \tag{63}$$

The Gibbs free energy is then given by

$$\begin{aligned}\tilde{G}^o_j(T,P) - \tilde{G}^o_j(T_r,P_r) &= \tilde{H}^o_j(T,P) - \tilde{H}^o_j(T_r,P_r) \\ &\quad - T\left(\tilde{S}^o_j(T,P) - \tilde{S}^o_j(T_r,P_r)\right) - (T - T_r)\tilde{S}^o_j(T_r,P_r)\end{aligned} \tag{64}$$

The `MineralEQ3` object helps to implement exact comparison of Cantera against other codes as a function of temperature and pressure. Due to the effect of small differences in Gibbs free energies on the solubility of minerals in aqueous systems, which we will demonstrate in Chapter 7, we have found implementing exact representations instead of approximate representations, to be necessary.

4 Multicomponent Formulation of the Pitzer Formulation

The starting point for the formulation of Pitzer's model is the equation for the excess Gibbs free energy, G^{ex}, described in the previous section. All other formulas are derived by taking suitable derivatives.

The formulae are based around a combination of the Debye-Hückel theory for long range ionic interactions with a second and third order virial coefficient expansion to take into account of short range interactions that dominate strong electrolytes. A review paper [18] contains the most complete description of Pitzer's model. The equations described below come from this paper, unless otherwise stated. The general expression for the excess Gibbs free energy, adopted by Pitzer, is Eqn. (65).

$$\begin{aligned}\frac{G_{ex,\triangle}}{\tilde{M}_o n_o RT} &= -\left(\frac{4AI}{3b}\right)\ln\left(1+b\sqrt{I}\right) + 2\sum_c\sum_a m_c m_a B_{ca} + \sum_c\sum_a m_c m_a \left(ZC_{ca}\right) \\ &+\sum_{c<c'}\sum m_c m_{c'}\left[2\Phi_{cc'} + \sum_a m_a \psi_{cc'a}\right] + \sum_{a<a'}\sum m_a m_{a'}\left[2\Phi_{aa'} + \sum_c m_c \psi_{aa'c}\right] \\ &+2\sum_n\sum_c m_n m_c \lambda_{nc} + 2\sum_n\sum_a m_n m_a \lambda_{na} + 2\sum_{n<n'}\sum m_n m_{n'} \lambda_{nn'} \\ &+\sum_n m_n^2 \lambda_{nn} + \sum_n m_n^3 \mu_{nnn} + \sum_n\sum_c\sum_a m_n m_c m_a \zeta_{nca}\end{aligned} \tag{65}$$

a is a subscript over all anions, *c* is a subscript extending over all cations, and *i* is a subscript that extends over all anions and cations. *n* is a subscript that extends only over neutral solute molecules. The second line contains cross terms where cations affect cations and/or cation/anion pairs, and anions affect anions or cation/anion pairs. Note, part of the coefficients, $\Phi_{cc'}$ and $\Phi_{aa'}$, stem from the theory of unsymmetrical mixing of electrolytes with different charges. This theory depends on the total ionic strength of the solution, and therefore, $\Phi_{cc'}$ and $\Phi_{aa'}$ will depend on *I*, the ionic strength. B_{ca} is a strong function of the total ionic strength, *I*, of the electrolyte. The rest of the coefficients are assumed to be independent of molalities or ionic strengths.

A, the Debye-Hückel constant, with a value of 1.1744 $\text{kg}^{1/2}\,\text{gmol}^{-1/2}$ at 25 °C and 1 atm, is given by the following expression in SI units:

$$A = \frac{1}{8\pi}\left(\frac{2N_a\rho_w}{1000}\right)^{1/2}\left(\frac{e^2}{\varepsilon RT}\right)^{3/2}, \tag{66}$$

where N_a is Avogadro's number, ρ_w is the density of water, e is the electronic charge, $\varepsilon = K\varepsilon_o$ is the permittivity of water, ε_o is the permittivity of free space, *K* is the dielectric constant of water, *R* is the gas constant, and *T* is the temperature in Kelvin. ρ_w is a function of both *T* and *P*. Within the Cantera implementation, ρ_w, and its derivatives, are evaluated from the IAPWS formulation for the equation

of state for water [32]. *K*, the dielectric constant for water, is also a large function of temperature and pressure. Its functional form and associated derivatives were taken from Bradley and Pitzer [38].

The ionic strength of the solution, *I*, is defined on the molality concentration scale as

$$I = \frac{1}{2}\left(\sum_i m_i z_i^2 \right) \tag{67}$$

In contrast to several other Debye-Hückel implementations, the parameter *b* in Eqn. (65) is a constant that does not vary with respect to ion identity. This is an important simplification as it avoids troubles with satisfaction of the Gibbs-Duhem analysis, mentioned in ref. [4]. A Gibbs -Duhem analysis checks to make sure that the Gibbs-Duhem equation, which expresses the interdependence of the activity coefficients, is satisfied for all possible cases. When variable *b*'s are used, the Debye-Hückel equations don't satisfy a Gibbs-Duhem analysis [4].

A few of the other terms used in Eqn. (65) are defined as follows:

$$Z = \sum_i m_i \left| z_i \right| \tag{68}$$

$$B_{ca} = \beta_{ca}^{(0)} + \beta_{ca}^{(1)} g\left(\alpha_1 \sqrt{I}\right) + \beta_{ca}^{(2)} g\left(\alpha_2 \sqrt{I}\right) \tag{69}$$

where

$$g\left(x\right) = 2\frac{\left(1-\left(1+x\right)\exp\left[-x\right]\right)}{x^2} \tag{70}$$

The formulation for B_{ca}, combined with the formulation of the Debye-Hückel term in Eqn. (65), stems essentially from an empirical fit to ionic strength dependent data based over a wide sampling of binary electrolyte systems. C_{ca}, λ_{nc}, λ_{na}, λ_{nn}, $\psi_{cc'a}$, and $\psi_{aa'c}$ are experimentally derived coefficients that may have pressure and/or temperature dependencies. $\Phi_{cc'}$ and $\Phi_{aa'}$ formulations are slightly more complicated; their formulation is described in a later section. *b* is a constant, in contrast to some Debye-Hückel implementations, defined to be equal to 1.2 $\text{kg}^{1/2}\ \text{gmol}^{-1/2}$. The exponential coefficient α_1 is usually fixed at $\alpha_1 = 2.0\ \text{kg}^{1/2}\ \text{gmol}^{-1/2}$, except for 2-2 electrolytes, while other parameters were fit to experimental data [18]. However, recent formulations have fit α_1 to experimental data [16]; within Cantera, it's treated as an input parameter. For 2-2 electrolytes, $\alpha_1 = 1.4\ \text{kg}^{1/2}\ \text{gmol}^{-1/2}$ was used in combination with either $\alpha_2 = 12\ \text{kg}^{1/2}\ \text{gmol}^{-1/2}$ or $\alpha_2 = kA_\phi$, where *k* is a constant. For electrolytes other than 2-2 electrolytes the $\beta_{ca}^{(2)} g\left(\alpha_2 \sqrt{I}\right)$ term is not used in the fitting procedure; it is only used for divalent metal sulfates and other high- valence electrolytes which exhibit significant association at low ionic strengths.

The $\beta_{ca}^{(0)}$ $\beta_{ca}^{(1)}$, $\beta_{ca}^{(2)}$, and C_{ca} binary coefficients are referred to as ion-interaction or Pitzer parameters. These Pitzer parameters may vary with temperature and pressure, but they do not depend on the ionic

strength. The ionic strength dependence is built in through Eqn. (69). Their values and temperature derivatives of their values are tabulated for a range of electrolytes at 25°C in ref. [18]. Additionally, their values are tabulated in the YMP Pitzer database documentation [43]. In general, the temperature and pressure dependencies of these coefficients must be measured and experimentally fit to each binary electrolyte system independently. Later, wewill show results for the NaCl system, where the Pitzer parameters have been exhaustively measured for a full range of temperatures and pressures up to and actually beyond the critical point for water.

The $\Phi_{cc'}$ and $\Phi_{aa'}$ contributions, which capture cation-cation and anion-anion interactions, also have an ionic strength dependence to be described later.

Ternary contributions, $\psi_{cc'a}$, and $\psi_{aa'c}$, are reported for some systems at 25 °C in ref. [18, 14, 15]. In general, these contributions are fairly highly correlated with the $\theta_{aa'}$ and $\theta_{cc'}$ values are input in the same block as their $\psi_{aa'c}$ and $\psi_{cc'a}$ counterparts in the XML input file. The success of the Pitzer method lies in its ability to model nonlinear activity coefficients of complex multicomponent systems with just binary and minor ternary contributions, which can be independently measured in binary or ternary subsystems [14, 15]. Nonionic species are represented by the last terms in Eqn. (65).

4.1 Temperature Dependence of Coefficients

A key feature is the temperature dependence of the Pitzer coefficient when calculating excess Gibbs energies and activity/osmotic coefficients of electrolyte solutions. A key underlying issue is the decision as to which coefficients need to be dependent on the temperature and what functional formalism will be used to describe that temperature dependence and to describe its dependence on the ionic strength. These issues have already been decided by the original authors (Pitzer, Helgeson, et al.) within the field.

What we have chosen to do is to establish sets of parameterizations and label them with string names. Conceptually, all of the coefficients in Eqn. (65) can have temperature and pressure dependencies within a parameterization.

Silvester and Pitzer [31] described one set of numerical fitting data where he fit much of the experimental data for NaCl over an extensive data range, below the critical temperature. They found a temperature functional form, Eqn. (71), for fitting the 3 coefficients that describe the Pitzer parameterization for a single salt that can adequately describe how those three coefficients change with respect to temperature. In Pitzer's cumulative paper [18], he presents tables of derivatives of these three quantities at the reference temperature of 25°C for a range of binary salt systems. Therefore, it seems prudent to generate functional dependencies which parameterize the temperature dependence of the three Pitzer coefficients, $\beta^{(0)}$, $\beta^{(1)}$, C^{ϕ}, as a way to handle the general case. Additionally, there are temperature dependencies involved with specification of the standard states. But conceptually, these may be found independently of the Pitzer coefficients.

The YMP Pitzer database [43] developed for use with the code EQ3/6 somewhat follows the parameterization used in Silvester and Pitzer. In our initial treatment we use a slightly expanded form of the EQ3/6 parameterization that is a superset of the two. We call this parameterization, which only depends on temperature, as `COMPLEX1`. This formulation is given below.

Also, in later papers, Pitzer has added additional temperature dependencies to all of the other remaining second and third order virial coefficients. Some of these dependences are justified and motivated by theory. Therefore, a formalism wherein all of the coefficients in the base theory have temperature dependences associated with them.

$$\beta^{(0)} = q_0^{\beta(0)} + q_1^{\beta(0)}\left(T - T_r\right) + q_2^{\beta(0)}\left(T^2 - T_r^2\right) + q_3^{\beta(0)}\left(\frac{1}{T} - \frac{1}{T_r}\right) + q_4^{\beta(0)} \ln\left(\frac{T}{T_r}\right) \tag{71}$$

$$\beta^{(1)} = q_0^{\beta(1)} + q_1^{\beta(1)}\left(T - T_r\right) + q_2^{\beta(1)}\left(T^2 - T_r^2\right) + q_3^{\beta(1)}\left(\frac{1}{T} - \frac{1}{T_r}\right) + q_4^{\beta(1)} \ln\left(\frac{T}{T_r}\right)$$

$$\beta^{(2)} = q_0^{\beta(2)} + q_1^{\beta(2)}\left(T - T_r\right) + q_2^{\beta(2)}\left(T^2 - T_r^2\right) + q_3^{\beta(2)}\left(\frac{1}{T} - \frac{1}{T_r}\right) + q_4^{\beta(2)} \ln\left(\frac{T}{T_r}\right)$$

$$C^{\phi} = q_0^{C\phi} + q_1^{C\phi}\left(T - T_r\right) + q_2^{C\phi}\left(T^2 - T_r^2\right) + q_3^{C\phi}\left(\frac{1}{T} - \frac{1}{T_r}\right) + q_4^{C\phi} \ln\left(\frac{T}{T_r}\right)$$

$$\theta_{cc'} = q_0^{\theta cc} + q_1^{\theta cc}\left(T - T_r\right) + q_2^{\theta cc}\left(T^2 - T_r^2\right) + q_3^{\theta cc}\left(\frac{1}{T} - \frac{1}{T_r}\right) + q_4^{\theta cc} \ln\left(\frac{T}{T_r}\right)$$

$$\theta_{aa'} = q_0^{\theta aa} + q_1^{\theta aa}\left(T - T_r\right) + q_2^{\theta aa}\left(T^2 - T_r^2\right) + q_3^{\theta aa}\left(\frac{1}{T} - \frac{1}{T_r}\right) + q_4^{\theta aa} \ln\left(\frac{T}{T_r}\right)$$

$$\psi_{cc'a} = q_0^{\psi cc'a} + q_1^{\psi cc'a}\left(T - T_r\right) + q_2^{\psi cc'a}\left(T^2 - T_r^2\right) + q_3^{\psi cc'a}\left(\frac{1}{T} - \frac{1}{T_r}\right) + q_4^{\psi cc'a} \ln\left(\frac{T}{T_r}\right)$$

$$\psi_{aa'c} = q_0^{\psi aa'c} + q_1^{\psi aa'c}\left(T - T_r\right) + q_2^{\psi aa'c}\left(T^2 - T_r^2\right) + q_3^{\psi aa'c}\left(\frac{1}{T} - \frac{1}{T_r}\right) + q_4^{\psi aa'c} \ln\left(\frac{T}{T_r}\right)$$

$$\lambda_{ni} = q_0^{\lambda ni} + q_1^{\lambda ni}\left(T - T_r\right) + q_2^{\lambda ni}\left(T^2 - T_r^2\right) + q_3^{\lambda ni}\left(\frac{1}{T} - \frac{1}{T_r}\right) + q_4^{\lambda ni} \ln\left(\frac{T}{T_r}\right)$$

$$\mu_{nnn} = q_0^{\mu nnn} + q_1^{\mu nnn}\left(T - T_r\right) + q_2^{\mu nnn}\left(T^2 - T_r^2\right) + q_3^{\mu nnn}\left(\frac{1}{T} - \frac{1}{T_r}\right) + q_4^{\mu nnn} \ln\left(\frac{T}{T_r}\right)$$

$$\zeta_{nca} = q_0^{\zeta nca} + q_1^{\zeta nca}\left(T - T_r\right) + q_2^{\zeta nca}\left(T^2 - T_r^2\right) + q_3^{\zeta nca}\left(\frac{1}{T} - \frac{1}{T_r}\right) + q_4^{\zeta nca}\ln\left(\frac{T}{T_r}\right)$$

where

$$\Phi_{cc'} = \theta_{cc'} + {}^{E}\theta_{cc'}\left(I\right) \text{ and } \Phi_{aa'} = \theta_{aa'} + {}^{E}\theta_{aa'}\left(I\right) \tag{72}$$

And

$$C_{ca} = \frac{C_{ca}^{\phi}}{2\left|z_c z_a\right|^{1/2}} \tag{73}$$

Thus, $\theta_{cc'}$ is obtained from fitting data, and ${}^{E}\theta_{cc'}\left(I\right)$ is obtained from a theoretical expression to be presented later. The temperature-dependent parameterization adopted in EQ3/6 is centric to $T_r = 298.15K$ and can be described by the following equations.

$$\beta^{(0)} = a_1^{\beta(0)} + a_2^{\beta(0)}\left(\frac{1}{T} - \frac{1}{T_r}\right) + a_3^{\beta(0)}\ln\left(\frac{T}{T_r}\right) + a_4^{\beta(0)}\left(T - T_r\right) \tag{74}$$

$$\beta^{(1)} = a_1^{\beta(1)} + a_2^{\beta(1)}\left(\frac{1}{T} - \frac{1}{T_r}\right) + a_3^{\beta(1)}\ln\left(\frac{T}{T_r}\right) + a_4^{\beta(1)}\left(T - T_r\right)$$

$$\beta^{(2)} = a_1^{\beta(2)} + a_2^{\beta(2)}\left(\frac{1}{T} - \frac{1}{T_r}\right) + a_3^{\beta(2)}\ln\left(\frac{T}{T_r}\right) + a_4^{\beta(2)}\left(T - T_r\right)$$

$$C^{\phi} = a_1^{C\phi} + a_2^{C\phi}\left(\frac{1}{T} - \frac{1}{T_r}\right) + a_3^{C\phi}\ln\left(\frac{T}{T_r}\right) + a_4^{C\phi}\left(T - T_r\right)$$

$$\theta_{cc'} = a_1^{\theta cc'} + a_2^{\theta cc'}\left(\frac{1}{T} - \frac{1}{T_r}\right) + a_3^{\theta cc'}\ln\left(\frac{T}{T_r}\right) + a_4^{\theta cc'}\left(T - T_r\right)$$

$$\theta_{aa'} = a_1^{\theta aa'} + a_2^{\theta aa'}\left(\frac{1}{T} - \frac{1}{T_r}\right) + a_3^{\theta aa'}\ln\left(\frac{T}{T_r}\right) + a_4^{\theta aa'}\left(T - T_r\right)$$

$$\psi_{c'ca} = a_1^{\psi c'ca} + a_2^{\psi c'ca}\left(\frac{1}{T} - \frac{1}{T_r}\right) + a_3^{\psi c'ca}\ln\left(\frac{T}{T_r}\right) + a_4^{\psi c'ca}\left(T - T_r\right)$$

$$\psi_{aa'c} = a_1^{\psi aa'c} + a_2^{\psi aa'c}\left(\frac{1}{T} - \frac{1}{T_r}\right) + a_3^{\psi aa'c}\ln\left(\frac{T}{T_r}\right) + a_4^{\psi aa'c}\left(T - T_r\right)$$

$$\lambda_{ni} = a_1^{\lambda ni} + a_2^{\lambda ni}\left(\frac{1}{T} - \frac{1}{T_r}\right) + a_3^{\lambda ni}\ln\left(\frac{T}{T_r}\right) + a_4^{\lambda ni}\left(T - T_r\right)$$

$$\mu_{nnn} = a_1^{\mu nnn} + a_2^{\mu nnn}\left(\frac{1}{T} - \frac{1}{T_r}\right) + a_3^{\mu nnn}\ln\left(\frac{T}{T_r}\right) + a_4^{\mu nnn}\left(T - T_r\right)$$

$$\zeta_{nca} = a_1^{\zeta nca} + a_2^{\zeta nca}\left(\frac{1}{T} - \frac{1}{T_r}\right) + a_3^{\zeta nca}\ln\left(\frac{T}{T_r}\right) + a_4^{\zeta nca}\left(T - T_r\right)$$

We have written Perl scripts routines to translate from the EQ3/6 database format into the `COMPLEX1` description, in order to port the database into Cantera. These Perl scripts take a text file containing comma-separated values of Pitzer interaction parameters for all aqueous species and convert them in the xml file format used by Cantera. See Section 6.4 for more details on the xml file format used by Cantera.

There are other parameterizations other than `COMPLEX1` within Cantera. The parameterization `CONSTANT` may be used, in which case only the first non-temperature dependent parameter in each of the equations in Eqn. (71) is used. The parameterization `LINEAR` may be used also, in which case only the first two terms (the second one being a linear term in temperature) in each of the equations in Eqn. (71) is used. In the future, it should be possible to add additional (*T, P, I*) parameterizations of the Pitzer coefficients, as warranted by the physical system.

4.2 Multicomponent Osmotic Coefficient

The osmotic coefficient may be obtained from the following formula applied to Eqn. (65).

$$\phi - 1 = -\left(\frac{d\frac{G_{ex,\Delta}}{RT}}{d\left(\tilde{M}_o n_o\right)}\right)\frac{1}{\sum_{k\neq o} m_k} \tag{75}$$

The result is Eqn. (76).

$$\phi - 1 = \frac{2}{\sum_{k \neq o} m_k}\Bigg[-A_\phi \frac{I^{3/2}}{1 + b\sqrt{I}} + \sum_c \sum_a m_c m_a \left(B_{ca}^{\phi} + ZC_{ca} \right) + \sum_{c<c'} \sum m_c m_{c'} \left[\Phi_{cc'}^{\phi} + \sum_a m_a \psi_{cc'a} \right] + \sum_{a<a'} \sum m_a m_{a'} \left[\Phi_{aa'}^{\phi} + \sum_c m_c \psi_{aa'c} \right] + \sum_n \sum_c m_n m_c \lambda_{nc} + \sum_n \sum_a m_n m_a \lambda_{na} + \sum_{n<n'} \sum m_n m_{n'} \lambda_{nn'} + \frac{1}{2}\left(\sum_n m_n^2 \lambda_{nn} \right) + \left(\sum_n m_n^3 \mu_{nnn} \right) + \sum_n \sum_c \sum_a m_n m_c m_a \zeta_{nca} \Bigg] \tag{76}$$

We have employed the definition of A_ϕ, also used by Pitzer, which is equal to

$$A_\phi = \frac{A}{3} \ . \tag{77}$$

It can also be shown that the expression,

$$B_{ca}^{\phi} = B_{ca} + I \frac{dB_{ca}}{dI} = \beta_{ca}^{(0)} + \beta_{ca}^{(1)} \exp\left(-\alpha_1 \sqrt{I}\right) + \beta_{ca}^{(2)} \exp\left(-\alpha_2 \sqrt{I}\right) \ , \tag{78}$$

is consistent with the expression B_{ca} of Eqn. (69) after carrying out the derivative in Eqn. (75). Demonstration of this is left to the notes [5].

Also, taking into account that $\Phi_{cc'}$ and $\Phi_{aa'}$ has an ionic strength dependence,

$$\Phi_{cc'}^{\phi} = \Phi_{cc'} + I \frac{d\Phi_{cc'}}{dI} \quad \text{and} \quad \Phi_{aa'}^{\phi} = \Phi_{aa'} + I \frac{d\Phi_{aa'}}{dI} \tag{79}$$

4.3 Multicomponent Activity Coefficients for Solutes

The full osmotic coefficient formulation can be obtained by applying the previously derived relation,

$$\ln \gamma_m^{\triangle} = -\left(\frac{d\left(\dfrac{G_{ex,\triangle}}{\tilde{M}_o n_o RT} \right)}{d\left(m_m \right)} \right)_{n_i} \ , \tag{80}$$

to Eqn. (65). The full result, with derivation left to the notes [5], is Eqns. (81)-(83). The subscript *M*, refers to the particular cation, whose activity coefficient is being evaluated, while the subscript, *X*, refers to the particular anion whose activity coefficient is being currently evaluated.

$$\ln\gamma_M^{\triangle} = z_M^2\left(F\right)+\sum_a m_a\left(2B_{Ma}+ZC_{Ma}\right)+z_M\left(\sum_c\sum_a m_c m_a C_{ca}\right)$$
$$+\sum_c m_c\left[2\Phi_{Mc}+\sum_a m_a\psi_{Mca}\right]+\sum_{a<a'}\sum m_a m_{a'}\psi_{Maa'}+2\sum_n m_n\lambda_{nM}+\sum_n\sum_a m_n m_a\zeta_{nMa} \quad (81)$$

$$\ln\gamma_X^{\triangle} = z_X^2\left(F\right)+\sum_c m_c\left(2B_{cX}+ZC_{cX}\right)+\left|z_X\right|\left(\sum_a\sum_c m_a m_c C_{ca}\right)$$
$$+\sum_a m_a\left[2\Phi_{Xa}+\sum_c m_c\psi_{cXa}\right]+\sum_{c<c'}\sum m_c m_{c'}\psi_{cc'X}+2\sum_n m_n\lambda_{nX}+\sum_n\sum_c m_n m_c\zeta_{ncX} \quad (82)$$

where

$$F=-A_\phi\left[\frac{\sqrt{I}}{1+b\sqrt{I}}+\frac{2}{b}\ln\left(1+b\sqrt{I}\right)\right]+\sum_a\sum_c m_c m_a\frac{dB_{ca}}{dI}$$
$$+\sum_{c<c'}\sum m_c m_{c'}\frac{d\Phi_{cc'}}{dI}+\sum_{a<a'}\sum m_a m_{a'}\frac{d\Phi_{aa'}}{dI} \quad (83)$$

$Z=\sum m_i\left|z_i\right|$. $d\Phi_{cc'}/dI$ and $d\Phi_{aa'}/dI$ are the ionic strength derivatives of the mixing functions, $\Phi_{cc'}$ and $\Phi_{aa'}$, respectively. The formulation for the mixing functions is described in the next section. The function dB_{MX}/dI may be calculated by taking the derivative of Eqn. (69).

$$\frac{dB_{MX}}{dI}=\left(\frac{\beta_{MX}^1 h\left(\alpha\sqrt{I}\right)}{I}\right)+\left(\frac{\beta_{MX}^2 h\left(\alpha\sqrt{I}\right)}{I}\right), \quad (84)$$

where $h\left(x\right)$ is defined as

$$h\left(x\right)=g'\left(x\right)\frac{x}{2}=-\frac{2\left(1-\left(1+x+\frac{x^2}{2}\right)\exp\left[-x\right]\right)}{x^2}. \quad (85)$$

The activity coefficient for neutral species *N* is given by Eqn. (86).

$$\ln\gamma_N^{\triangle}=2\sum_i m_i\lambda_{Ni}+3m_N^2\mu_{NNN} \quad (86)$$

The sum over *i* refers to a full sum over all solute species (charged and uncharged), even *N*.

4.4 Mixing Functions

The previous equations contain the functions, $\Phi_{aa'}$ $\Phi_{cc'}$, and their derivatives with respect to the ionic

strength. Since like charged ions repel each other and are thus generally not near each other, the virial coefficients for same-charged ions are small. However, Pitzer doesn't ignore these in his formulation. An exception to this is the long-range electrical force which appears only for unsymmetrical mixing of same-sign charged ions with different charges. Φ_{ij}, where *ij* is either aa' or cc', is given by

$$\Phi_{ij} = \theta_{ij} + {}^{E}\theta_{ij}(I) \qquad . \tag{87}$$

θ_{ij} is the small virial coefficient expansion term. Dependent in general on temperature and pressure, its ionic strength dependence is ignored in Pitzer's approach. ${}^{E}\theta_{ij}(I)$ accounts for the electrostatic unsymmetrical mixing effects and is dependent only on the charges of the ions *i*, *j*, the total ionic strength and on the dielectric constant and density of the solvent. This seems to be a relatively well-documented part of the theory. The theory below comes from Pitzer summation [18], where it constitutes an entire appendix [pp. 122-124]. It's also mentioned in Bethke's book [11], and the equations are summarized in Harvie and Weare (1980) [15].

Within the code, ${}^{E}\theta_{ij}(I)$ is evaluated according to the algorithm described in Appendix B of ref. [18]. Eqn. B-15 of ref. [18] is reproduced below as Eqn. (88).

$${}^{E}\theta_{ij}(I) = \left(\frac{z_i z_j}{4I}\right)\left(J\left(x_{ij}\right) - \frac{1}{2}J\left(x_{ii}\right) - \frac{1}{2}J\left(x_{jj}\right)\right) \tag{88}$$

where

$$x_{ij} = 6 z_i z_j A_\phi \sqrt{I} \ ,$$

and,

$$J\left(x\right) = \frac{1}{x}\int_0^\infty \left(1 + q + \frac{1}{2}q^2 - e^q\right) y^2 dy \ \text{ and } \ {}^{E}\theta_{ij}(I) = \left(\frac{z_i z_j}{4I}\right)\left(J\left(x_{ij}\right) - \frac{1}{2}J\left(x_{ii}\right) - \frac{1}{2}J\left(x_{jj}\right)\right) \tag{89}$$

where

$$x_{ij} = 6 z_i z_j A_\phi \sqrt{I} \ ,$$

and,

$$J\left(x\right) = \frac{1}{x}\int_0^\infty \left(1 + q + \frac{1}{2}q^2 - e^q\right) y^2 dy \ \text{ and } \ q = -\left(\frac{x}{y}\right)e^{-y} \tag{90}$$

$J\left(x\right)$ is evaluated by numerical integration.

4.5 Simplification of the Pitzer Formulation for Binary Solutions of a Single Strong Electrolyte

A binary electrolyte has the following simplifications. Let's call the cation *M*, and the anion *X*. The cation, *M*, has charge, z_M. The anion has charge, z_X. There are ν_M cations in solution and ν_X anions in solution. Charge neutrality constraints require that Eqn. (91) holds for a single strong electrolyte.

$$z_M \nu_M = |z_X| \nu_X \tag{91}$$

A few other formulas are important

$$m_M = m\nu_M \qquad m_X = m\nu_X \qquad \nu_{MX} = \nu_M + \nu_X \tag{92}$$

Individual activity coefficients cannot be independently measured due to the charge neutrality constraint requiring that any real solution be electrically balanced. Thus, activity coefficients of aqueous ions can only be measured in electrically neutral combinations The mean activity coefficient, $\gamma_{MX}^{\pm}$, Eqn. (93), for every cation M and anion X can be defined and measured. The osmotic coefficient may also always be measured.

$$\ln \gamma_{MX}^{\pm} = \frac{\nu_M \ln \gamma_M + \nu_X \ln \gamma_X}{\nu_{MX}} \tag{93}$$

4.5.1 Excess Gibbs Free Energy

Let's simplify Eqn. (65), the multicomponent excess Gibbs free energy for the case where there is just a single cation M and anion X.

$$\frac{G_{ex,\triangle}}{\tilde{M}_o n_o RT} = -\left(\frac{4AI}{3b}\right)\ln\left(1+b\sqrt{I}\right) + 2m_M m_X B_{MX} + m_M m_X \left(ZC_{MX}\right) \tag{94}$$

This expression is often rearranged in Pitzer's papers into the following form. First, for a binary electrolyte:

$$2m\left(\nu_M z_M\right) = m\nu_M z_M + m\nu_X |z_X| = mz_M + m|z_X| = Z \tag{95}$$

And, using the definition often used in Pitzer's papers:

$$C_{MX} = \frac{C_{MX}^{\phi}}{2\left|z_m z_x\right|^{1/2}} \qquad , \tag{96}$$

Eqn. (94) turns into

$$\frac{G_{ex,\triangle}}{\tilde{M}_o n_o RT} = -\left(\frac{4AI}{3b}\right)\ln\left(1+b\sqrt{I}\right) + m^2\left(2\nu_M\nu_X B_{MX}\right) + m^3\left(\left(\nu_M\nu_X\right)^{3/2} C^{\phi}_{MX}\right) \tag{97}$$

4.5.2 Osmotic Coefficient

Let's reduce the expression (Eqn. (76)) for the osmotic coefficient to the case of one cation *M* and one anion *X*, Eqn. (98).

$$\phi - 1 = \frac{2}{\nu_{MX} m}\left(-A_\phi \frac{I^{3/2}}{1+b\sqrt{I}} + m_M m_X B^{\phi}_{MX} + m_M m_X Z C_{MX}\right) \tag{98}$$

The first term may be simplified by noting the relation, Eqn. (99), which holds for binary electrolytes:

$$\frac{I}{\nu_{MX}} = \frac{1}{2} m z_M \left|z_X\right| \tag{99}$$

The third term in Eqn. (98) may be simplified by employing Eqn. (95) and (96) to yield:

$$\phi - 1 = -\left(z_M \left|z_X\right| A_\phi\right)\frac{\sqrt{I}}{1+b\sqrt{I}} + m\left(2\frac{\nu_M\nu_X}{\nu_{MX}}\right)B^{\phi}_{MX} + m^2 2\frac{\left(\nu_M\nu_X\right)^{3/2}}{\nu_{MX}} C^{\phi}_{MX} \tag{100}$$

B^{ϕ}_{MX} is given by Eqn. (78). C^{ϕ}_{MX} is given by Eqn. (74).

4.5.3 Solute Activity Coefficient for a Single Strong Electrolyte

Reducing Eqn. (81) - (83) for the case of a binary electrolytes produces Eqns. (101) to (103).

$$\ln\left(\gamma^{\triangle}_M\right) = z_M^2 F + 2m_X B^{\phi}_{MX} + 2m_X Z C_{MX} + z_M m_M m_X C_{MX} \tag{101}$$

$$\ln\left(\gamma^{\triangle}_X\right) = z_X^2 F + 2m_X B^{\phi}_{MX} + 2m_M Z C_{MX} + z_X m_M m_X C_{MX} \tag{102}$$

where

$$F = -A_\phi\left[\frac{\sqrt{I}}{1+b\sqrt{I}} + \frac{2}{b}\ln\left(1+b\sqrt{I}\right)\right] + m_M m_X B^{'}_{MX} \tag{103}$$

These may be rearranged and combined to yield:

$$\ln\left(\gamma_M^{\triangle}\right) = z_M^2\left(-A_\phi\left[\frac{\sqrt{I}}{1+b\sqrt{I}}+\frac{2}{b}\ln\left(1+b\sqrt{I}\right)\right]+m_M m_X B_{MX}^{'}\right) \\ +2m_X B_{MX}+\frac{3}{2\nu_M}m^2\left(\left(\nu_M\nu_X\right)^{3/2}C_{MX}^{\phi}\right) \tag{104}$$

$$\ln\left(\gamma_X^{\triangle}\right) = z_X^2\left(-A_\phi\left[\frac{\sqrt{I}}{1+b\sqrt{I}}+\frac{2}{b}\ln\left(1+b\sqrt{I}\right)\right]+m_M m_X B_{MX}^{'}\right) \\ +2m_M B_{MX}+\frac{3}{2\nu_X}m^2\left(\left(\nu_M\nu_X\right)^{3/2}C_{MX}^{\phi}\right) \tag{105}$$

We note that this implies that $\gamma_M^{\triangle} = \gamma_X^{\triangle}$ for the case where $\nu_M = \nu_X$, because $m_M = m_X$.

4.5.4 Mean Solute Activity Coefficient

The mean activity coefficient is given by Eqn. (93). We seek the expression for the mean activity coefficient of a pure binary electrolyte. First we note the following relation holds:

$$\frac{z_M^2\nu_M + z_X^2\nu_X}{\nu_{MX}} = z_M\left|z_X\right| \qquad \text{and } I=\frac{1}{2}_M\, m\ \nu_{MX} z_M\left|z_X\right| \tag{106}$$

Then, combining Eqns. (104) and (105) yields Eqn. (107).

$$\ln\left(\gamma_{\pm}^{\triangle}\right) = z_M\left|z_X\right|\left(-A_\phi\left[\frac{\sqrt{I}}{1+b\sqrt{I}}+\frac{2}{b}\ln\left(1+b\sqrt{I}\right)\right]+z_M\left|z_X\right|m_M m_X B_{MX}^{'}\right) \\ +2m_M\left(\frac{\nu_M\nu_X}{\nu_{MX}}\right)\left(2B_{MX}\right)+3m^2\left(\frac{\left(\nu_M\nu_X\right)^{3/2}}{\nu_{MX}}C_{MX}^{\phi}\right) \tag{107}$$

These relations simplify the first term in the mean activity coefficient formulation. Then, rearranging and using Eqn. (106) yields:

$$\ln\left(\gamma_{\pm}^{\triangle}\right) = z_M\left|z_X\right|\left(-A_\phi\left[\frac{\sqrt{I}}{1+b\sqrt{I}}+\frac{2}{b}\ln\left(1+b\sqrt{I}\right)\right]\right)+2m\left(2\frac{\nu_M\nu_X}{\nu_{MX}}\beta_{MX}^{(0)}\right)$$
$$+2m\left(2\frac{\nu_M\nu_X}{\nu_{MX}}\beta_{MX}^{(1)}g\left(\alpha_1\sqrt{I}\right)\right)+2m\left(2\frac{\nu_M\nu_X}{\nu_{MX}}\beta_{MX}^{(2)}g\left(\alpha_2\sqrt{I}\right)\right)$$
$$+2m\left(\frac{\nu_M\nu_X}{\nu_{MX}}\beta_{MX}^{(1)}h\left(\alpha_1\sqrt{I}\right)\right)+2m\left(\frac{\nu_M\nu_X}{\nu_{MX}}\beta_{MX}^{(2)}h\left(\alpha_2\sqrt{I}\right)\right) \quad . \qquad (108)$$
$$+3m^2\left(\frac{\left(\nu_M\nu_X\right)^{3/2}}{\nu_{MX}}C_{MX}^{\phi}\right)$$

Then, using the relation,

$$h\left(\alpha_1\sqrt{I}\right)+g\left(\alpha_1\sqrt{I}\right)=\exp\left[-\alpha_1\sqrt{I}\right],$$

yields:

$$\ln\left(\gamma_{\pm}^{\triangle}\right) = z_M\left|z_X\right|\left(-\frac{\alpha}{3}\left[\frac{\sqrt{I}}{1+b\sqrt{I}}+\frac{2}{b}\ln\left(1+b\sqrt{I}\right)\right]\right)+2m\left(2\frac{\nu_M\nu_X}{\nu_{MX}}\beta_{MX}^{(0)}\right)$$
$$+2m\left(2\frac{\nu_M\nu_X}{\nu_{MX}}\beta_{MX}^{(1)}g\left(\alpha_1\sqrt{I}\right)\right)+2m\left(2\frac{\nu_M\nu_X}{\nu_{MX}}\beta_{MX}^{(2)}g\left(\alpha_2\sqrt{I}\right)\right)$$
$$+2m\left(\frac{\nu_M\nu_X}{\nu_{MX}}\beta_{MX}^{(1)}h\left(\alpha_1\sqrt{I}\right)\right)+2m\left(\frac{\nu_M\nu_X}{\nu_{MX}}\beta_{MX}^{(2)}h\left(\alpha_2\sqrt{I}\right)\right) \quad . \qquad (109)$$
$$+3m^2\left(\frac{\left(\nu_M\nu_X\right)^{3/2}}{\nu_{MX}}C_{MX}^{\phi}\right)$$

Eqn. (109) is the same as Pitzer's Eqn. (58), p.88, ref [18]. Assuming $\beta_{MX}^{(2)}=0$ for the moment, Eqn. (109)is often rewritten by expanding the $g\left(x\right)$ term to yield:

$$\ln\left(\gamma_{\pm}^{\triangle}\right) = z_M\left|z_X\right|\left(-A_\phi\left[\frac{\sqrt{I}}{1+b\sqrt{I}}+\frac{2}{b}\ln\left(1+b\sqrt{I}\right)\right]\right)$$
$$+2m\left(\frac{\nu_M\nu_X}{\nu_{MX}}\left(2\beta_{MX}^{(1)}+\frac{2\beta_{MX}^{(1)}}{\alpha_1^2 I}\left(1-\left(1+\alpha_1\sqrt{I}-\frac{\alpha_1^2 I}{2}\right)\exp\left[-\alpha_1\sqrt{I}\right]\right)\right)\right) . \qquad (110)$$
$$+3m^2\left(\frac{\left(\nu_M\nu_X\right)^{3/2}}{\nu_{MX}}C_{MX}^{\phi}\right)$$

For example, Eqn. (110) is used in ref [31].

4.6 Implementation of pH Scaling

Single ion activity coefficients are not unique. The following transformation described in Eqn. (111) may be carried out on a set of single-ion activity coefficients ${}^{s1}\gamma_k^{\triangle}$ to transform those activity coefficients into a new set, ${}^{s2}\gamma_k^{\triangle}$, such that all observables are the same.

$$ {}^{s2}\gamma_k^{\triangle} = {}^{s1}\gamma_k^{\triangle} + \frac{c_k}{c_j}\left({}^{s2}\gamma_j^{\triangle} - {}^{s1}\gamma_j^{\triangle} \right) \tag{111} $$

${}^{s1}\gamma_j^{\triangle}$ and ${}^{s2}\gamma_j^{\triangle}$ are the old and new single ion activity coefficients for any one specific species, and c_k is the charge on the species *k*. However, the specification of the pH and other p-type standards is actually a single-ion calculation as the pH is defined from the following Eqn. (112).

$$ pH = -\log_{10} a_{H+}^{\triangle} = -\log_{10} \gamma_{H+}^{\triangle} m_{H+} \tag{112} $$

The NBS standard for the calculation single-ion activity coefficients is the Bates-Guggenheim equation (1973) [70]. In that standard, the chloride ion (Cl^-) is specified to have the following activity coefficient.

$$ {}^{s2}\gamma_{Cl-}^{\triangle} = \frac{-A\sqrt{I}}{1+1.5\sqrt{I}} \tag{113} $$

Then, from Eqn. (111) all other single-ion activity coefficients including the hydrogen ion activity coefficient are specified.

The scaling carried out by Eqn. (112) in aqueous speciation calculations in EQ3/6 is generally referred as the pH scaling [see Appendix B, ref. 7]. The pH scaling as originally laid out in Eqn. (81) and Eqn. (82) is referred as the 'internal' or Pitzer pH scaling when adopting the Pitzer formulation for computing activity coefficients. However, it should be noted that this is not an officially-sanctioned definition for this type of pH scaling. In the Pitzer pH scaling, the activity coefficients for the anion and cation of a single binary electrolyte are equal to each other, if the absolute value of their charges are equal. The pH scaling determined by Eqn. (113) is called the "NBS" pH scaling in EQ3/6. For concentrated solutions, the scaling options may radically alter the values of the single-ion activity coefficients. For dilute solutions, the limiting for of the Debye-Huckel term is essentially the same as the Pitzer scaling form so deviations are very minor.

All single-ion values returned by Cantera including partial molar enthalpies are affected by the choice of the pH scaling. Note, also that electrode reactions are also affected by pH scaling, because they involve single-ion activity coefficients. Numerical experiments have shown that the scaling introduced by Eqn. (113) is numerically stable, because the expression depends on the total ionic strength. Note, the "NBS" scaling isn't currently possible if Cl^- isn't an active ion in the solution.

5 Elimination of Singularities in the Thermodynamic functions

We analyze the equations from the point of view of the molar activity coefficients, the best way to analyze the equations for their singularities. First we will fix up the ideal molal solution approximation. This is at the heart of the singularities. We then show how to apply this to the Pitzer equation. Lastly, we demonstrate our method of modifying the Pitzer formulation for the Gibbs molality-based excess free energy to ensure that these terms are nonsingular.

Most of these modifications don't affect the actual physical results, because they occur in regions of the parameter space that are unphysical. However, they do affect the numerical software, because frequently the numerical software will query physically inaccessible regimes as it searches for stable phases.

5.1 Values for the Molality-Based Activity Coefficients.

In order to understand stability issues inside equilibrium solvers, we seek to understand what the formulas for the molar based activity coefficients are, especially in the limits of the solvent, water species, going to zero. The equilibrium solver effectively uses the molar based activity coefficients. In Eqn. (114), we have written the molality-based activity coefficients in terms of the molar-based coefficients.

$$\overline{\mu}_k\left(T,P,\boldsymbol{x}\right)=\overline{\mu}_k^{\triangle}+RT\ln\left(\frac{m_k\gamma_k^{\triangle}}{m^{\triangle}}\right)=\overline{\mu}_k^{o}+RT\ln\left(\gamma_k X_k\right)\qquad k=1,...,N \tag{114}$$

$$\overline{\mu}_o\left(T,P,\boldsymbol{x}\right)=\overline{\mu}_o^{o}+RT\ln\left(a_o\right)=\overline{\mu}_o^{o}-RT\tilde{M}_o\left(\sum_{j\neq 0}m_j\right)\phi=\overline{\mu}_o^{o}+RT\ln\left(\gamma_o X_o\right)$$

$$\text{where}\quad \overline{\mu}_k^{\triangle}=\overline{\mu}_k^{o}+RT\ln\left(\tilde{M}_o m^{\triangle}\right)\ \text{ and }\ \gamma_k=\frac{\gamma_k^{\triangle}}{X_o}$$

The requirements for the equilibrium solver are that the Henry's law constants asymptote to constant positive definite values in all accessible limits [28]. This is easily true except for the limit of the solvent disappearing. This means that even the ideal molality solution behavior has to be modified in order to accommodate the requirement. What this explicitly means in the context of Eqn. (114) is the following.

$$\gamma_k\rightarrow\gamma_k^{solvent=0}\ \text{ as }\ X_s\rightarrow 0 \tag{115}$$

$$\gamma_o\rightarrow\gamma_o^{solvent=0}\ \text{ as }\ X_s\rightarrow 0$$

Perhaps, the constraints on the activity coefficient models inherent in Eqn. (115) are more severe than necessary. However, these constraints may be shown to be sufficient to allow for a successful equilibrium solution of nonideal multiphase equilibrium problems [28].

We take it piece by piece. The ideal molality solution piece can be handled by taking a look at the Gibbs excess free energy of an ideal molality solution and inventing alterations to make sure the limiting behavior is appropriate. Eqn. (116) represents the Gibbs free energy of mixing on the molality scale, assuming an ideal molal solution.

$$\Delta G_{mix,\vartriangle}^{id,\vartriangle} = \tilde{M}_o n_o \left(\sum_{k\neq 0} m_k \left(\ln\left(\frac{m_k}{m^{\vartriangle}} \right) - 1 \right) \right) \tag{116}$$

Then, Eqn. (117) represents the total excess Gibbs free energy of the "ideal molality" solution. To note, an ideal solution would have an excess Gibbs free energy of zero.

$$\begin{aligned}
\frac{G_{ex}^{id,\vartriangle}}{RT} &= G^{id,\vartriangle} - G^{id} \\
&= \left(n_o \mu_o + \sum_{k\neq 0} n_k \mu_o^{\vartriangle} + \tilde{M}_o n_o \left(\sum_{k\neq 0} m_k \left(\ln\left(\frac{m_k}{m^{\vartriangle}} \right) - 1 \right) \right) \right) \\
&\quad - \left(\sum_{k=o} n_k \mu_o^o + \sum_{k=0} n_k \ln\left(X_k \right) \right) \\
&= \tilde{M}_o n_o \left(\sum_{k\neq 0} m_k \left(\ln\left(\frac{m_k}{m^{\vartriangle}} \right) - 1 \right) \right) - \left(\sum_{k=0} n_k \ln\left(X_k \right) \right) + \sum_{k\neq 0} n_k \ln\left(\tilde{M}_o m^{\vartriangle} \right) \\
&= \sum_{k\neq 0} n_k \left(\ln\left(\frac{n_k}{n_o} \right) - 1 \right) - \sum_{k=0} n_k \ln\left(X_k \right) \\
&= -\sum_{k\neq 0} n_k - \sum_{k\neq 0} n_k \ln\left(X_o \right) - n_o \ln\left(X_o \right) \\
&= -\sum_{k\neq 0} n_k - n \ \ln\left(X_o \right)
\end{aligned} \tag{117}$$

The molar based activity coefficients may be obtained by differentiating Eqn. (117).

$$\ln\left(\gamma_k \right) = \frac{d\left(G_{ex}^{id,\vartriangle} / RT \right)}{dn_k} = \ln\left(\frac{1}{X_o} \right) \tag{118}$$

$$\ln\left(\gamma_o \right) = \frac{d\left(G_{ex}^{id,\vartriangle} / RT \right)}{dn_o} = \ln\left(\frac{1}{X_o} \right) + 1 - \frac{1}{X_o}$$

Implying that

$$\gamma_k = \frac{1}{X_o} \tag{119}$$

$$\gamma_o = \frac{1}{X_o}\exp\left(-\frac{1-X_o}{X_o}\right)$$

Thus, the resulting activity coefficients violate Eqn. (115) and leads to problems within the equilibrium solver. A first thought would be to use the following equation for the total Gibbs free energy for a modified ideal molal solution, $G^{mod,id,\vartriangle}$.

$$\frac{G^{mod,id,\vartriangle}}{RT} = n_o\mu_o^o + \sum_{j\neq 0} n_j\left(\mu_j^{\vartriangle} - \ln\tilde{M}_o m^{\vartriangle}\right) + \sum_{j\neq 0} n_j\left(\ln\left(\frac{X_j}{f\left(X_o\right)}\right) - 1\right), \tag{120}$$

$$\text{with } f\left(X_o\right) = \begin{cases} X_o & , x > X_o \\ X_o^{\min} & , x < X_o \end{cases},$$

which implies:

$$\frac{G_{ex}^{mod,id,\vartriangle}}{RT} = \left(\sum_{k\neq 0} n_k\left(\ln\left(\frac{X_k}{f\left(X_o\right)}\right) - 1\right)\right) - \left(\sum_{k=0} n_k \ln\left(X_k\right)\right) \tag{121}$$

$$\frac{G_{ex}^{mod,id,\vartriangle}}{RT} = -\sum_{k\neq 0} n_k \ln\left(f\left(X_o\right)\right) - n_o \ln\left(X_o\right) - \sum_{k\neq 0} n_k$$

So that the molar activity coefficients for $x > X_o$ are the same as Eqn. (119). For $x < X_o$, they are given by Eqn. (122).

$$\gamma_k = \frac{1}{eX_o^{\min}} \tag{122}$$

$$\gamma_o = \frac{\exp\left(X_o\right)}{eX_o}$$

The γ_k value is now stable as the solvent disappears, but the γ_o value still blows up as $X_o \to 0$. Another approach would be to use Eqn. (123).

$$\frac{G_{ex}^{mod,id,\vartriangle}}{RT} = -\sum_{j\neq 0} n_k \ln\left(f\left(X_o\right)\right) - n_o \ln\left(f\left(X_o\right)\right) - \sum_{j\neq 0} n_k \tag{123}$$

$$\text{where } f\left(X_o\right) = \begin{cases} X_o & , x > X_o \\ X_o^{\min} & , x < X_o \end{cases}$$

which is derived from the following total Gibbs free energy.

$$\frac{G^{mod,id,\vartriangle}}{RT} = n_o \mu_o^o + \sum_{j\neq 0} n_j \left(\mu_j^{\vartriangle} - \ln \tilde{M}_o\right) + \sum_{j\neq 0} n_j \left(\ln\left(\frac{X_j}{f\left(X_o\right)}\right) - 1\right) - n_o \ln\left(f\left(X_o\right)\right) + n_o \ln\left(X_o\right)$$

Then, for $x > X_o$, the values for the activity coefficients are the same as Eqn. (119). For $x < X_o$, they are given by Eqn. (124).

$$\gamma_k = \frac{1}{eX_o^{\min}} \tag{124}$$

$$\gamma_o = \frac{1}{X_o^{\min}}$$

Now, both γ_k and γ_o values are bounded as $X_o \to 0$. Unfortunately, the problem with this is that the activity coefficients aren't continuous. It turns out that the Gibbs excess energy must be at least a C1 function for the equilibrium solver to function properly [28]. Therefore, in the next two sections we will seek a more complicated alteration to the ideal molal Gibbs free energy that satisfies the C1 continuity requirements.

5.1.1 Search for an Appropriate Exponential Polynomial function.

We seek the right value of *f* and *g*, starting with Eqn. (125) and breaking the domain up into two regions depending on the value of X_o the solvent mole fraction. $f\left(X_o\right)$ and $g\left(X_o\right)$ are arbitrary functions of the solvent mole fraction, whose form we will generate to fit the requirements described below. For $X_o > X_o^*$, the ideal molal solution approximation will hold. For $X_o < X_o^*$, a C1 approximation will be assumed that employs an exponential function multiplied by a polynomial in X_o^*.

$$\frac{G_{ex}^{mod,id,\vartriangle}}{RT} = -\sum_{j\neq 0} n_k - \sum_{j\neq 0} n_k \ln\left(f\left(X_o\right)\right) - n_o \ln\left(g\left(X_o\right)\right) \tag{125}$$

This implies a Gibbs free energy of mixing on the molar scale, $\Delta G_{mix}^{\mathrm{mod},id,\vartriangle}$, given by Eqn. (126),

$$\Delta G_{mix}^{\mathrm{mod},id,\vartriangle} = \left(\sum_{k\neq 0} n_k \left(\ln\left(\frac{X_k}{f\left(X_o\right)}\right) + n_o \ln\left(\frac{X_o}{g\left(X_o\right)}\right)\right)\right) \tag{126}$$

And a Gibbs free energy of mixing on the molal scale, $\Delta G_{mix,\vartriangle}^{\mathrm{mod},id,\vartriangle}$, given by Eqn. (127).

$$\Delta G_{mix,\triangle}^{\mathrm{mod},id,\triangle} = \left(\sum_{k\neq 0} n_k \left(\ln\left(\frac{m_k X_o}{m^{\triangle} f\left(X_o\right)} \right) + n_o \ln\left(\frac{X_o}{g\left(X_o\right)} \right) \right) \right) \tag{127}$$

Mathematically, this problem may be specified in the following way. For $X_o > X_o^*$,

$$f\left(X_o\right) = g\left(X_o\right) = X_o$$

For the $X_o = 0$ limit, we require that $f\left(X_o\right)$ and $g\left(X_o\right)$ have the following form so that the activity coefficients are finite in this limit.

$$f\left(0\right) = \frac{1}{e\gamma_k^{\min}} \text{ and } g\left(0\right) = \frac{1}{\gamma_o^{\min}}$$

In the middle region, $0 < X_o < X_o^*$, we will require that

1) High condition on value $\quad f\left(X_o = X_o^*\right) = X_o^* \quad g\left(X_o = X_o^*\right) = X_o^*$ (128)

2) High condition on derivative $\quad f'\left(X_o^*\right) = 1 \quad g'\left(X_o^*\right) = 1$

3) Low condition on value $\quad f\left(0\right) = \frac{1}{e\gamma_k^{\min}} \quad g\left(0\right) = \frac{1}{\gamma_o^{\min}}$

4) Low condition on derivative $\quad f'\left(0\right) = S_o^f \quad g'\left(0\right) = S_o^g$

S_o^f is the limiting value of derivative of *f*, while S_o^g is the limiting value of derivative of *g*. Note, S_o^f appears prominently in the value of $\gamma_o^{\min}$, and a non-zero value S_o^f appears to be essential for creating a well-behaved solution of the problem. Within the lower interval, the following holds:

$$\ln\gamma_k = -1 - \ln f - \left(\frac{n_o}{g}\frac{dg}{dX_o} + \sum \frac{n_k}{f}\frac{df}{dX_o} \right)\left(\frac{-X_o}{n^T} \right) \tag{129}$$

$$\ln\gamma_o = -\ln g - \left(\frac{n_o}{g}\frac{dg}{dX_o} + \sum \frac{n_k}{f}\frac{df}{dX_o} \right)\left(\frac{1-X_o}{n^T} \right)$$

At the top of the domain, the following boundary conditions hold:

$$\ln\gamma_k = -1 - \ln f + 1 = -\ln f = \ln\frac{1}{X_o}$$

$$\ln\gamma_o = -\ln g - \left(\frac{1-X_o}{X_o} \right) = \ln\frac{1}{X_o} - \left(\frac{1-X_o}{X_o} \right)$$

These agree with the ideal molality solution in Eqn. (119). With the aid of the following two functions, $f(X)$ and, $g(X)$, we may solve this problem.

$$f(X_o) = X_o + e_f + \exp\left[\frac{-X_o}{c_f}\right]\left(a_f + b_f X_o + d_f X_o^2\right) \tag{130}$$

$$g(X_o) = X_o + e_g + \exp\left[\frac{-X_o}{c_g}\right]\left(a_g + b_g X_o + d_g X_o^2\right) \tag{131}$$

We assign *c* to be significantly smaller than X_o ; for example, the default values of X_o and c are 0.20 and 0.05 respectively. We may iteratively solve for the remaining four values in $f(X_o)$ and $g(X_o)$ in order to satisfy the boundary conditions in Eqn. (128). Then, we may derive the molar based activity coefficients in the two regions to be Eqn. (132).

$$\ln\gamma_k = \begin{cases} \ln\dfrac{1}{X_o} & X_o > X_o^* \\ -1 - \ln f - \left(\dfrac{n_o}{g}\dfrac{dg}{dX_o} + \sum\dfrac{n_k}{f}\dfrac{df}{dX_o}\right)\left(\dfrac{-X_o}{n^T}\right) & X_o < X_o^* \end{cases} \tag{132}$$

$$\ln\gamma_o = \begin{cases} \ln\dfrac{1}{X_o} - \left(\dfrac{1-X_o}{X_o}\right) & X_o > X_o^* \\ -\ln g - \left(\dfrac{n_o}{g}\dfrac{dg}{dX_o} + \sum\dfrac{n_k}{f}\dfrac{df}{dX_o}\right)\left(\dfrac{1-X_o}{n^T}\right) & X_o < X_o^* \end{cases}$$

Fig. 7 contains a plot of the activity coefficients produced by the default parameters. X_o^* is set to 0.2 in the plot. The activity coefficients are monotonic, continuous and well bounded even in the limit of the solvent disappearing completely. Table 1 contains a listing of the regressed value of Eqns. (130) and (131) that were used in Fig. 7.

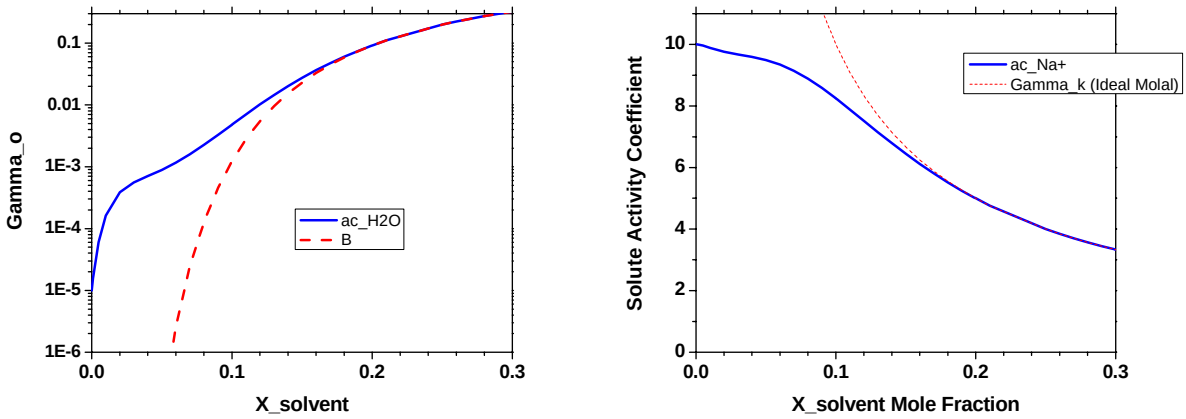

Fig. 7. Solvent and solute activity coefficients for modified Ideal Molal Solution approximation. The red dashed curve is the unmodified Ideal Molal solution model.

Table 1: Parameters for Eqns. (130) and (131), determined via an iterative procedure

	f	g
$\mathbf{a_i}$	3.55663E-2	9.56254E-3
$\mathbf{b_i}$	3.113262E-1	8.08749E-1
$\mathbf{c_i}$	0.05	.05
$\mathbf{d_i}$	-4.11326	5.587491
$\mathbf{e_i}$	1.22163E-3	-1.30613E-3
S_o	0.6	0.0

5.2 Modification of the Pitzer Equations for Cases of High Molalities

Modifications carried out on the Pitzer equations follow the lessons learned in the previous sections. First a common modification is to place a cap on the total ionic strength, *I*. Recall that

$$I = \frac{1}{2}\left(\sum_i m_i z_i^2\right) \quad , \tag{133}$$

where m_i is the molality of ion *i*, and z_i is the charge of ion *i*. To place a cap on the total ionic strength would imply changing Eqn. (133) to:

$$I = \min\left(I_{\max}, \frac{1}{2}\left(\sum_i m_i z_i^2 \right) \right) \tag{134}$$

$I_{\max}$ is an input parameter, whose value is around 20 gmol kg^{-1}. However, such a change would not result in continuous values of the activity coefficients nor would it satisfy the Gibbs-Duhem equations. Alternatively, we may modify the values of all molalities in the global expression, Eqn. (65) for $G_{ex,\Delta}$. The modification of m_i occurs in all terms the extrinsic expression Gibbs free energy expression, $G_{ex,\Delta}$, guaranteeing satisfaction with respect to the Gibbs-Duhem relation, and if the modification is continuous or even C1 or C2, then $G_{ex,\Delta}$ will be continuous or even C1 or C2. Each of the molalities m_i are replaced by the quantity m_i^* where

$$m_i^* = \begin{cases} \dfrac{n_i}{\tilde{M}_o n_o} & X_o > X_o^{\min} \\ \dfrac{X_i}{\tilde{M}_o p\left(X_o\right)} = \dfrac{n_i}{n\tilde{M}_o p\left(\dfrac{n_o}{n}\right)} & X_o < X_o^{\min} \end{cases} \tag{135}$$

$X_o^{\min}$ is an adjustable parameter that we have initially set at 0.20. The expression for $p\left(X_o\right)$, Eqn. (136), is modeled after $f\left(X_o\right)$ and $g\left(X_o\right)$ of the previous section to provide C2 continuity at $X_o^{\min}$.

$$p\left(X_o\right) = X_o + e_p + \exp\left[\frac{-X_o}{c}\right]\left(a_p + b_p X_o + d_p X_o^2\right) \tag{136}$$

Therefore, the modified Gibbs excess free energy, called $G_{ex,\Delta}^{\text{mod}}$, is equal to

$$G_{ex,\Delta}^{\text{mod}} = G_{ex,\Delta}\left(n_o, m_1^*, ..., m_N^*\right)$$

The derivatives of $G_{ex,\Delta}^{\text{mod}}$ are then:

$$\left.\frac{dG_{ex,\Delta}^{\text{mod}}}{dn_k}\right|_{n_l} = \begin{cases} \dfrac{1}{\tilde{M}_o n_o}\dfrac{\partial G_{ex,\Delta}}{\partial m_k} & X_o > X_o^{\min} \\ \displaystyle\sum_{l=1} \left.\frac{\partial\left(\dfrac{G_{ex,\Delta}}{\tilde{M}_o n_o}\right)}{\partial m_l^*}\right|_{n_o, m_k^*} \left(\frac{\delta_{lk}}{n\,\tilde{M}_o p} - \frac{X_l}{n\,\tilde{M}_o p} + \frac{X_l X_o p'}{n\,\tilde{M}_o p^2}\right) & X_o < X_o^{\min} \end{cases} \tag{137}$$

$$\left.\frac{dG_{ex,\vartriangle}^{\mathrm{mod}}}{dn_o}\right|_{n_k} = \begin{cases} \left.\frac{\partial G_{ex,\vartriangle}}{\partial n_o}\right|_{m_k} - \sum_{k=1}^{N}\left(\left.\frac{\partial G_{ex,\vartriangle}}{\partial m_k}\right|_{n_o,m_l}\right)\frac{m_k}{n_o} = -\left(\sum_{k=1}^{N} m_k\right)(\phi-1)\frac{\tilde{M}_o}{RT} & X_o > X_o^{\min} \\ \left.\frac{\partial G_{ex,\vartriangle}}{\partial n_o}\right|_{m_k^*} - \sum_{k=1}^{N}\left(\left.\frac{\partial G_{ex,\vartriangle}}{\partial m_k^*}\right|_{n_o,m_l^*}\right)\left(\frac{m_k^* p + m_k^* p'(1-X_o)}{n\ p}\right) & X_o < X_o^{\min} \end{cases} \tag{138}$$

where

$$p' = \frac{dp}{dX_o} = 1 + \exp\left[\frac{-X_o}{c}\right]\left(-\frac{a_p}{c} + b_p + \left(-\frac{b_p}{c} + 2d_p\right)X_o - \frac{d_p}{c}X_o^2\right)$$

In Eqn. (138), we have written down the relation of the derivative to the osmotic coefficient. Because we only seek numerical stability and do not need rigorous adherence to the Gibbs-Duhem equation in the limit of $X_o \to 0$, we modify the form of Eqn. (138). The modified form of Eqn. (138) is

$$\left.\frac{dG_{ex,\vartriangle}^{\mathrm{mod}}}{dn_k}\right|_{n_l} = \begin{cases} \frac{1}{\tilde{M}_o n_o}\frac{\partial G_{ex,\vartriangle}}{\partial m_k} & X_o > X_o^{\min} \\ \frac{1}{\tilde{M}_o n_o}\frac{\partial G_{ex,\vartriangle}^{\vartriangle}}{\partial m_k^*} & X_o < X_o^{\min} \end{cases} \tag{139}$$

This equation is exactly what one would obtain from Eqn. (81) by just plugging in m_i^* for m_i. Not equivalent to Eqn. (138), Eqn. (139) is computationally inexpensive to implement and maintains the property that the values of the activity coefficients approach a constant non-zero value as $X_o \to 0$. In the same way the following approximation is used to calculate the solvent derivative.

$$\left.\frac{dG_{ex,\vartriangle}^{\mathrm{mod}}}{dn_o}\right|_{n_k} = \begin{cases} f\left(n_o, m_1, ..., m_N\right) & X_o > X_o^{\min} \\ f\left(n_o, m_1^*, ..., m_N^*\right) & X_o < X_o^{\min} \end{cases} \tag{140}$$

In Eqn. (140), $f\left(n_o, m_1, ..., m_N\right)$ is the same function both above and below $X_o^{\min}$, and ϕ is the same function as Eqn. (76) but with m_i^* used instead of m_i.

5.2.1 Application to the Pitzer Equations

The Pitzer equations are expressed in terms of the molal activity coefficients and the osmotic coefficient. The mixture Gibbs free energy change due to mixing, $\Delta G_{mix,\vartriangle}$ the key quantity for thermodynamic calculations, may be divided into two quantities, Eqn. (141). The first, $\Delta G_{mix,\vartriangle}^{id,\vartriangle}$, is the Gibbs free energy change due to mixing of an ideal molality solution. The second is the remainder, $G_{ex,\vartriangle}$.

$$\begin{aligned}\Delta G_{mix,\vartriangle} &= G - \sum_{i\neq 0} n_i\,\bar{\mu}_i^{\vartriangle} - n_o\bar{\mu}_o^{o} = \Delta G_{mix,\vartriangle}^{id,\vartriangle} + G_{ex,\vartriangle} \\ &= RT\left(-\phi\left(\sum_{i\neq 0} n_i\right) + \sum_i n_i\,\ln\left(\frac{m_i\,\gamma_i^{\vartriangle}}{m^{\vartriangle}}\right)\right) = RT\left(\sum_{i\neq 0} n_i\left(\ln\left(\frac{m_i\,\gamma_i^{\vartriangle}}{m^{\vartriangle}}\right) - \phi\right)\right)\end{aligned} \tag{141}$$

The molal ideal solution component to the total $\Delta G_{mix,\vartriangle}$ value is the following

$$\Delta G_{mix,\vartriangle}^{id,\vartriangle} = RT\left(\sum_{i\neq 0} n_i\left(\ln\left(\frac{m_i}{m^{\vartriangle}}\right) - 1\right)\right) \tag{142}$$

We have found a suitable change for $\Delta G_{mix,\vartriangle}^{id,\vartriangle}$ that produces a stable numerical scheme to be the following Eqn. (143).

$$\Delta G_{mix,\vartriangle}^{mod,id,\vartriangle} = RT\left(\sum_{i\neq 0} n_i\left(\ln\left(\frac{m_i}{m^{\vartriangle}}\frac{X_o}{f}\right) - 1\right) + n_o\ln\left(\frac{X_o}{g}\right)\right) \tag{143}$$

Eqn. (143) reduces to Eqn. (6), when $f = g = X_o$. These facts motivate us to start with Eqn. (144) as the basis for a numerically stable formulation of the Pitzer equations.

$$\begin{aligned}\Delta G_{mix,\vartriangle} &= \Delta G_{mix,\vartriangle}^{mod,id,\vartriangle} + G_{ex,\vartriangle}^{\mathrm{mod}} \\ &= RT\left(\sum_{i\neq 0} n_i\left(\ln\left(\frac{m_i}{m^{\vartriangle}}\frac{X_o}{f}\right) - 1\right) + n_o\ln\left(\frac{X_o}{g}\right)\right) + G_{ex,\vartriangle}^{\mathrm{mod}}\end{aligned} \tag{144}$$

$G_{ex,\vartriangle}^{\mathrm{mod}}$ is a modified form of the excess Gibbs free energy on the ideal molality solution basis that we introduced in the previous section. And, we will maintain the following definitions that were originally contained in Eqn. (75) and Eqn. (80).

$$\left.\frac{d\left(\dfrac{G_{ex,\vartriangle}^{\mathrm{mod}}}{RT\tilde{M}_o n_o}\right)}{dm_k}\right|_{T,P,n_{j\neq k}} = RT\ln\left(\gamma_k^{\mathrm{mod},\vartriangle}\right) \qquad \phi^{\mathrm{mod}} - 1 = -\left(\frac{d\left(\dfrac{G_{ex,\vartriangle}^{\mathrm{mod}}}{RT}\right)}{d\left(\tilde{M}_o n_o\right)}\right)\frac{1}{\sum_{k\neq o} m_k} \tag{145}$$

We may then calculate

$$\left.\left(\frac{dG}{dn_k}\right)\right|_{T,P,n_{j\neq k}} = \bar{\mu}_k\left(T,P,\boldsymbol{x}\right) = \bar{\mu}_k^{\vartriangle} + RT\ln\left(\frac{m_k\gamma_k^{\mathrm{mod},\vartriangle}}{m^{\vartriangle}}\right) = \frac{dG^{mod,id,\vartriangle}}{dn_k} + \frac{dG_{ex,\vartriangle}^{\mathrm{mod}}}{dn_k} \tag{146}$$

$$\left(\frac{dG}{dn_o}\right)\Bigg|_{T,P,n_k} = \bar{\mu}_o\left(T,P,\boldsymbol{x}\right) = \bar{\mu}_o^o - RT\phi\left(\sum_{k\neq o}\frac{n_k}{n_o}\right) = \frac{dG^{mod,id,\vartriangle}}{dn_o} + \frac{dG_{ex,\vartriangle}^{\mathrm{mod}}}{dn_o} \tag{147}$$

Starting with Eqn. (114),

$$\frac{dG^{mod,id,\vartriangle}}{dn_k} = \bar{\mu}_k^{\vartriangle} + RT\ln\left(\frac{m_k}{m^{\vartriangle}}\gamma_k^{\vartriangle,\mathrm{mod},id}\right) \quad \text{where } \gamma_k^{\vartriangle,\mathrm{mod},id,\vartriangle} = X_o\gamma_k^{\mathrm{mod},id,\vartriangle} \tag{148}$$

$\gamma_k^{\mathrm{mod},id,\vartriangle}$ is given by the expression in Eqn. (132) after conversion from the molar to the molality-based activity coefficient. Eqn. (139) is then used for the second half of Eqn. (146). Combining everything together, the formula for the complete, numerically stable molal activity coefficient is Eqn. (149).

$$\gamma_k^{\vartriangle} = \left(\gamma_k^{\vartriangle,\mathrm{mod},id}\right)\left(\gamma_k^{\mathrm{mod},\vartriangle}\right) \tag{149}$$

$\gamma_k^{\mathrm{mod},\vartriangle}$ approaches a constant value as $X_o \to 0$. The molar-based value of $\gamma_k^{\mathrm{mod},id}$ approaches a non-zero constant as $X_o \to 0$. Therefore the entire molar based activity approaches a constant value multiplied by X_o, which is the original goal of the stabilization.

We may formulate the expression for the complete osmotic coefficient. Starting with Eqn. (150),

$$\frac{dG^{mod,id,\vartriangle}}{dn_o} = \bar{\mu}_o^o + RT\ln a_o^{\mathrm{mod},id} = \bar{\mu}_o^o + RT\ln X_o\gamma_o^{\mathrm{mod},id} \tag{150}$$

So

$$\begin{aligned}\left(\frac{dG}{dn_o}\right)\Bigg|_{T,P,n_k} &= \bar{\mu}_o\left(T,P,\boldsymbol{x}\right) = \frac{dG^{mod,id,\vartriangle}}{dn_o} + \frac{dG_{ex,\vartriangle}^{\mathrm{mod}}}{dn_o} \\ &= \mu_o^o + RT\ln\left(X_o\gamma_o^{\mathrm{mod},id}\right) - \tilde{M}_o RT\sum_{k\neq o} m_k\left(\phi^{\mathrm{mod}} - 1\right)\end{aligned} \tag{151}$$

The latter term is a constant as $X_o \to 0$, after modifications applied in Eqn. (140), so it poses no concerns in that limit. From Eqn. (132), the value of $\gamma_o^{\mathrm{mod},id}$ approaches a constant as $X_o \to 0$. Note, occurrences wherever, $X_o > X_o^{\min}$ are flagged, so that the numerical conditioning will not normally get in the way of the Gibbs free energy formulation, whenever physically significant conditions are being calculated.

5.2.2 Additional Direct Cropping of Activity Coefficients

In numerical testing it was found that an additional layer of cropping was needed to maintain stability in the equilibrium solver. In general low molar-based activity coefficients in unphysical regions are dangerous, because they may spawn the creation of unphysical phases. The water activity coefficient has a tendency to become extremely low as $X_o \to 0$, despite all of the modifications presented in the

previous sections. This is due in part to the fact that the osmotic coefficient scales with the m^3 power while the solute activity coefficients are scaled with respect to the m^2 power. Therefore, the activity coefficient for water was modified to never fall below nor rise above set values

$$\ln \gamma_o \geq \ln \gamma_o^{\min} \qquad \ln \gamma_o \leq \ln \gamma_o^{\max} \tag{152}$$

$\ln \gamma_o^{\min}$ is currently set at -6.0, and $\ln \gamma_o^{\max}$ is currently set at 3.0. This sets a limit on the reduction of the activity for water. Both $\ln \gamma_o^{\min}$ and $\ln \gamma_o^{\max}$ may be adjusted from the input file.

Additionally, a maximum value was set on the activity for solutes, Eqn. (153) , based on the current value of the solvent mole fraction, X_o .

$$\ln \gamma_k \leq \ln \gamma_k^{\max} - 3.5 \ln X_o \qquad \ln \gamma_k \geq \ln \gamma_k^{\min} - 3.5 \ln X_o \tag{153}$$

All of these modifications are carried out at the end of the activity coefficient calculation. This ensures that all activity coefficients are strictly bounded by these limits. Fig. 8 contains an example of the format for specifying these cropping coefficients.

It should be noted that some of the available Pitzer parameters for very concentrated electrolytes may not extend up to the solubility limits of the salt, particularly at elevated temperatures. For this reason, extrapolated values at very large salt concentrations may not be accurate and could be the source of unphysical results in the computation of activity coefficients. Calculations close to dryness (i.e., $X_o \to 0$) are in computational terms inherently unstable or not feasible. Therefore, these methods are a necessary step to alleviate code run instabilities at conditions where the solvent is nearly absent, even when the modified activity coefficients could be considered fictive. It is then recommended that any result from this cropping approach should be checked against real data (if available) to establish confidence in the code prediction.

The negative coefficient with respect to X_o in Eqn. (153) and the positive or zero coefficient with respect to X_o in Eqn. (152) are motivated by an analysis of the highly nonlinear phase stability subproblem that mathematically describes when and if a multispecies phase becomes stable as a function of temperature, pressure, and composition. These coefficients are chosen from an analysis of that problem in an attempt to avoid multiple solutions to that nonlinear problem in unphysical parameter regimes.

```
<activityCoefficients model="Pitzer" TempModel="complex1">
   <croppingCoefficients>
     <ln_gamma_k_min>
           <pureSolventValue> -5.0 <pureSolventValue>
     <\ln_gamma_k_min>
     <ln_gamma_k_max>
           <pureSolventValue> 15.0 <pureSolventValue>
     <\ln_gamma_k_max>
     <ln_gamma_o_min>
           <pureSolventValue> -6.0 <pureSolventValue>
     <\ln_gamma_o_min>
     <ln_gamma_o_max>
           <pureSolventValue> 3.0 <pureSolventValue>
     <\ln_gamma_o_max>
   </croppingCoefficients>
</activityCoefficients>
```

Fig. 8. The `croppingCoefficients` XML element is a child element of the `activityCoefficients` XML element, for a `HMWThermo` model using the `complex1` temperature model.

5.2.3 Example

Below we demonstrate the theory in this section by carrying out several examples. The example will stretch the NaCl system into unphysical regimes. However, those regimes are regularly queried during

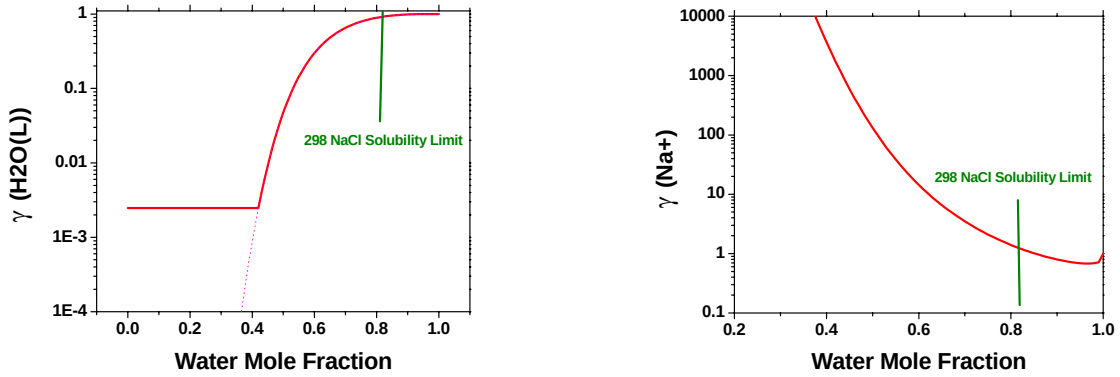

a) b)

Fig. 9. 298 K value for the molar-based activity coefficients of Na^+ and $H_2O(L)$ as a function of the mole fraction of $H_2O(L)$

the execution of the equilibrium solver. The examples are from a later section where we analyse the NaCl system, with only the one salt consisting of Na^+ and Cl^- ionic species having any appreciable concentrations.

Fig. 9 contains a plot at 298 K of the molar-based activity coefficients for water and for Na^+ (note for this particular case Cl^- has the same value for the activity coefficient as Na^+, when presented on the Pitzer pH scale). Also shown on the plot is the solubility limit of NaCl in water (green line) at 298 K. All measurements occur of course on the right side of the green line or below the solubility limit of NaCl solid. The results to the left of the line are due to taking an exponential of the extrapolations of polynomials in the molality outside the range of the fitted values. The results can be widely disparate. Therefore, cropping of their values is a numerical necessity.

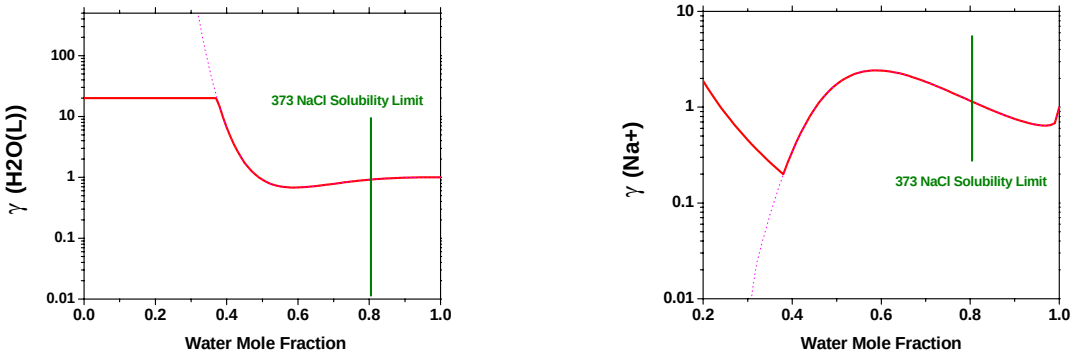

a) b)

Fig. 10. 298 K Value for the molar-based activity coefficients of $H_2O(L)$ (a) and Na^+ (b) as a function of the mole fraction of $H_2O(L)$. Solubility limits are denoted in green. Uncropped activity coefficient values are denoted by dotted magenta lines.

Fig. 10 contains an example of the same system, but at 373 K. The extrapolations of the activity coefficients have different asymptotic values as they approach a zero solvent mole fraction. This particular system can suffer from the existence of multiple solutions in the phase stability problem at these elevated temperatures. This is primarily due to the positive slop of γ_k with respect to X_o exhibited in Fig. 10 (b). Obviously, adjustments in the cropping algorithm could help alleviate these numerical complications. However, it's hard to know a priori and in general how to do this in the general case. Therefore, these parameters are accessible from the input deck.

6 Implementation of Brines within Cantera's ThermoPhase Objects

The base class thermodynamics object within Cantera is called `ThermoPhase`. `ThermoPhase` consists of a multitude of questions about the values of thermodynamics functions, and the values/ properties of the mechanical equation of state. Under `ThermoPhase` are objects that implement mole fractions and species elemental compositions. The `HMWSoln` thermodynamics object, which implements the Pitzer equations, is a derived object of the `ThermoPhase` class.

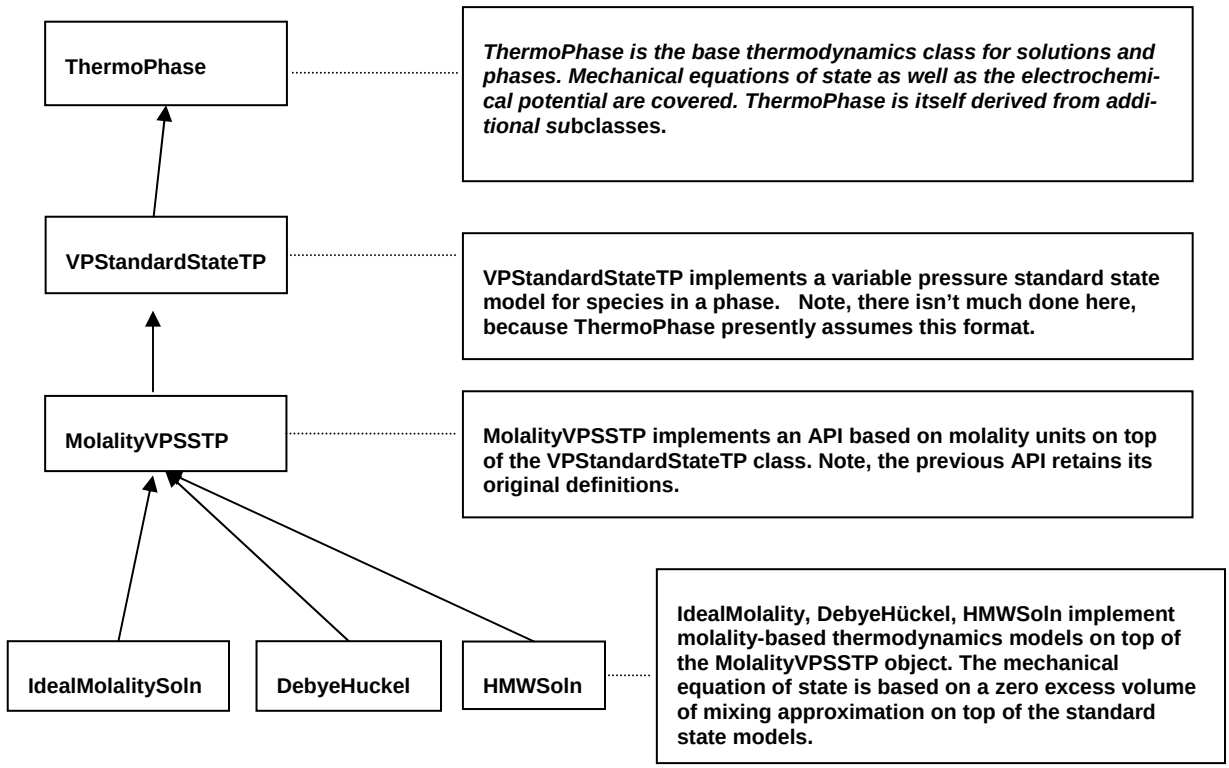

Fig. 11. Layout of Thermodynamic Objects

Fig. 11 describes the inheritance of objects within this architecture. The `HMWSoln` object is derived from the several hierarchal objects which are layered between it and the main `ThermoPhase` object. The first object is the filter, `VPStandardStateTP`. It implements a variable pressure standard state for species on top of base `ThermoPhase` object. There are various ways to implement mixture thermodynamics. However, almost all of the methods for aqueous solutions employ activities. Activities divide the description of the complexity of solution thermodynamics into two levels. The first level is the species standard state, which depends on both temperature and pressure. The second level, the determination of the species activity or species activity coefficient, determines the effects of

mixing the species. For example, Eqn. (154) describes the chemical potential of species *i* in solution:

$$\mu_i\left(T,P,X\right)=\mu_i^o\left(T,P\right)+RT\ln\left(a_i\right)=\mu_i^o\left(T,P\right)+RT\ln\left(\gamma_i X_i\right) \tag{154}$$

is the chemical potential of the standard state for species *i* in solution. It may be a hypothetical state, especially if species *i* is dilute in the solution. It provides a clear break-out of the solution properties based upon whether they involve mixing or not. The standard state properties include specification of how the thermodynamic functions for species *i* change as a function of temperature and pressure at "unit activity". The standard state also includes a description of how the molar volumes behave as a function of temperature and pressure at unity activity. The activities and activity coefficients are clearly based on the values of the standard states. They describe how mixing affects the thermodynamic properties. The activity coefficients are directly tied to specification of the excess thermodynamic functions of solution, i.e., how the mixing process deviates for the ideal solution behavior for mixing.

Note there are other ways to break up the determination of solution properties than a variable pressure standard state. For example, many non-ideal gas based thermodynamics methods use a fixed pressure standard state, and the concept of fugacities instead of Eqn. (154) to break the problem up.

While the `ThermoPhase` object is generally built to handle the variable pressure standard state, the `VPStandardStateTP` object is defined to handle the formulation described in Eqn. (154). Additionally, it answers some of the questions posed by the `ThermoPhase` object where possible.

As part of the Pitzer implementation, a virtual base class called `PDSS` (Pressure Dependent Standard State) has been implemented within Cantera. It serves as a template to hold all of the questions that a pressure dependent standard state has to answer in order to serve its function within `ThermoPhase`. One instantiation of this is for a real equation of state for water, named `WaterPDSS`. This will be described in a later section.

The `MolalityVPSSTP` object implements the molality-based units system. Additionally, it adds to `ThermoPhase` the concept of a molality-based activity coefficient representation, Eqn. (155).

$$\mu_i\left(T,P,X\right)=\mu_i^{\triangle}\left(T,P\right)+RT\ln\left(a_i^{\triangle}\right)=\mu_i^{\triangle}\left(T,P\right)+RT\ln\left(\gamma_i^{\triangle}\frac{m_i}{m^{\triangle}}\right) \tag{155}$$

$\mu_i^{\Delta}\left(T,P\right)$ is the molality-based standard state; it is based on a unit activity coefficient at infinite dilution. $a_i^{\triangle}$ is the molality based activity, which is also defined in Eqn. 155). $\gamma_i^{\triangle}$ is the molality based activity coefficient; m_i is the molality of the i^{th} solute; and $m^{\triangle}$, which usually is left out of the equations, has a value of 1 gmol solute (kg solvent^{-1}) and is needed to make the units work out within the logarithm.

The relationships between the molality-base quantities and molar based quantities are repeated here, having been determined in previous memos:

$$\mu_i^{\Delta}\left(T,P\right) = \mu_i^o\left(T,P\right) + RT\ln\left(m^{\Delta}\tilde{M}_o\right) \qquad \frac{\gamma_i^{\Delta}}{\gamma_i} = x_o \tag{156}$$

`MolalityVPSSTP` implements molality-based units in a way that doesn't override many of the previously defined mole fraction based API for the `ThermoPhase` object. Most of the implementation is under the hood. If mole fractions are input from the API, `MolalityVPSSTP` recalculates an internal molality representation before it goes on to calculate values for thermodynamic functions. `MolalityVPSSTP` implements new functions where it specifically requires molality-based quantities in the API. The API contains an explicit function that returns the molality-based activity coefficients. `MolalityVPSSTP` calculates the molar activity coefficients based on the molality-based activity coefficients using Eqn. (156).

The `HMWSoln` object implements the Pitzer equations within Cantera. It's derived off of the `MolalityVPSSTP` object. The sections below describe details of how the `ThermoPhase` API is implemented within the `HMWSoln` object in terms of broad categories. These categories specify how kinetics expressions are formulated (i.e., activity concentrations), what the mechanical equation of state looks like, and how standard states are implemented.

6.1 Standard State Chemical Potentials

There are two choices for how standard state chemical potentials are handled for molality-based thermodynamics models in the `ThermoPhase` API. The first choice is to maintain the molar-based definition of the return values from `getStandardChemPotentials(double *grt).` This would imply that all standard state chemical potentials remain on a molar basis, and in turn, this would imply that all returned activities by `getActivities(double *a)` be on the molality basis as well. The second choice is to change the API so that `getStandardChemPotentials(double *grt)` returns a molality-based standard chemical potential. This would also imply from Eqn. (155) that the function `getActivities(double *a)` would return molality based activities. wehave chosen the later approach.

In making the choice, it's tempting to stick to the same API, i.e., go with the first option. This option would provide the least amount of work in mixing molality based systems with molarity based systems in thermodynamics codes such as `VCS` (and was the first implementation within `VCS` as well). However, molality based standard states are ubiquitous in the literature. By default, standard state chemical potentials for ions are based on the molality units. For example, the CRC and other reference works give an extensive series of half-cell reactions involving mixed phases involving gases and liquids. It is assumed in the specification of standard EMF's for these cell, which is equivalent to the standard Gibbs free energy of reactions, that gas phase species have standard states on the molar scale, while the liquid phase electrolyte species have standard states on the molality scale. Therefore, in obtaining data from these sources, conversions from $\mu_i^{\Delta}\left(T,P\right)$ to $\mu_i^o\left(T,P\right)$, roughly 2.38 kcal gmol^{-1} at 298 K, would always have to take place before they could be plugged into Cantera's thermodynamics objects. Moreover, comparisons of liquid-phase activities between Cantera and other programs would have to undergo the same filtering process, if choice #1 were made.

The following is a list of changes to the `ThermoPhase` API that are needed to support molality-based standard states activities:

1) Addition to the `ThermoPhase` API of a variable to indicate what standard state basis the current phase adheres to. There are two choices so far: a) molarity-based and b) molality-based. This variable would affect what equation is used, i.e., either Eqn. (154) or Eqn. (155).

2) All standard state properties for molality-based phases are evaluated consistent with the molality scale. This means that the $RT\ln\left(m^{\triangle}\tilde{M}_o\right)$ term adds to the standard state enthalpy. The standard state entropy is not affected by this term.

3) All evaluations of the chemical potential have to take into account the new formulation of the activity for molality-based phases. For example, VCS has to special-case the evaluation of chemical potentials in phases specified by molality-based units, because it relies on the chemical potential equation being specified in terms of mole fractions and molar-based activity coefficients. It can do this by changing the molality-based chemical potentials into the molar form, Eqn. (157).

$$\begin{aligned}\mu_i\left(T,P,X\right) &= \mu_i^{\triangle}\left(T,P\right) + RT\ln\left(a_i^{\triangle}\right) = \mu_i^{\triangle}\left(T,P\right) + RT\ln\left(\gamma_i^{\triangle}\frac{m_i}{m^{\triangle}}\right) \\ &= \mu_i^{\triangle}\left(T,P\right) - RT\ln\left(m^{\triangle}\tilde{M}_o\right) + RT\ln\left(\gamma_i X_i\right)\end{aligned} \tag{157}$$

The extra $RT\ln\left(m^{\triangle}\tilde{M}_o\right)$ can be either subtracted out at the beginning of the nondimensionalization step which is done at the problem setup time, or it can be added in whenever the chemical potential is evaluated.

4) The API for functions providing activity coefficients don't need to be changed. Eqn. (157) is an example of why the evaluation of the molar-based activity coefficient is useful, even in a phase where the activities are based on molalities. Therefore, the `getActivityCoefficient(double ac*)` function always return molarity-based activity coefficients. A new function, `getMolalityActivityCoefficients(double *acMolality)` has been added to the `MolalityVPSSTP` object to return molality-based activity coefficients.

6.2 Water and Solute Standard States

The water standard state used by the `HMWSoln` object employs the full equation of state for water given in the 1995 IAPWS formulation [32]. This formulation, similar to all recent formulations, is based on an accurate specification of the Helmholtz free energy as a function of the independent variables, temperature and density. The formulation therefore covers the liquid, gas, and supercritical regions using a monotonic function.

The pressure is calculated from the first derivative of the Helmholtz free energy. Therefore, specification of the pressure as the independent variable requires that a small nonlinear problem be solved to find the corresponding density. Gas-Water equilibrium is solved from an equation representing the equality of the gas and water chemical potentials at equilibrium.

Within Cantera, the real water equation of state object, named `WaterIAPWS`, is referenced by the object `WaterPDSS`, which inherits from the virtual base class `PDSS` representing a pressure dependent standard state. Because `WaterPDSS` represents the conditions in the liquid state or in some cases the supercritical state, `WaterPDSS` never returns conditions corresponding to the gas state of water. An error occurs whenever `WaterPDSS` is requested to calculate a state point to the gas-side of the water spinodal curve.

Therefore, in contrast to existing treatments in Cantera (i.e., the tpx modules which calculate the equation of state for various two-phase pure fluids such as N_2, O_2, and H_2O), mixed water-gas conditions are not allowed in `WaterPDSS`. Instead the water phase conditions are returned up to the position of the spinodal curve, where the liquid phase ceases to be stable as a phase, i.e., constitutes a minimum in the Gibbs free energy. If conditions beyond the spinodal curve towards the gas state are input to `WaterPDSS`, then a Cantera exception is thrown indicating a fatal error.

No special treatments for the standard states of the solutes have heretofore been implemented within Cantera. There are a range of standard state implementations available to solutes based on various parameterizations of the temperature dependence of the standard state thermodynamic functions. However, these are currently only combined with a constant volume approximation for the mechanical equation of state that yields a constant standard state volume, independent of pressure and temperature. This is inaccurate for most real liquid systems for extended temperature and pressure ranges. In the near future, the HWFT implementation recommended by numerous authors [35] will be implemented for solutes [21, 22, 33, 34]. This implementation contains a complicated temperature and pressure dependence, and most importantly has a range of data available to it for the most common aqueous ions [36].

6.3 Activity Concentrations

In order to use finite kinetics, expressions for reaction rates must be employed that involve the concentrations of species. If the reactions are reversible, in order to be consistent with the thermodynamic limit, reaction rates must include the activities of reactants and products in the forward and reverse directions. However, there is a multiplicative constant (usually having the units of concentrations) that is left unspecified. In Cantera, this multiplicative constant is called the “standard concentration”, and the standard concentration multiplied by the activity is called the “activity concentration”. The standard concentration appears in the equilibrium constant expression for reactions involving unequal moles of reactants and products.

Thus, the activity concentration will appear within the kinetics operator to obtain mass action kinetics rates that are consistent with the thermodynamic limit. Standard concentrations are defined by the requirement that the activity of a species, which appears in thermodynamic equilibrium expressions, be equal to the activity concentration, which appears in kinetics expressions, divided by the standard concentration for that species.

In many cases the proportionality constant between activities and activity concentration, the standard concentration, is independent of species number. In our case of molality-based solution thermodynamics, the most reasonable default is to use the concentration of the pure solvent as the standard

concentration for all species, solutes, and solvents.

For example, let's take the reaction, $1+2\rightarrow 3$. The reaction rate expression for the forward and reverse directions is:

$$R_f = k_f \left[AC_1 \right]\left[AC_2 \right] \quad \text{and} \quad R_r = k_r \left[AC_3 \right] \ , \tag{158}$$

where we have used the expression AC_i as the activity concentration of the i^{th} species. Then, plugging in the expression for the molality-based activity, we obtain:

$$\left[AC_i \right] = C_o^0 a_i^{\triangle} = C_o^0 \left(\gamma_i^{\triangle} \frac{m_i}{m^{\triangle}} \right) .$$

C_o^0 is the concentration of pure water; it's a function of both temperature and pressure. $\gamma_i^{\triangle}$ is the molality-based activity coefficient. $\tilde{M}_o$ is the molecular weight of water divided by 1000. m_i is the molality of the i^{th} solute species. Using this definition means that $\left[AC_i \right]$ has MKS units of kmol m^{-3}, a normal result.

The expression for equilibrium for the reaction $1+2\rightarrow 3$ is given by Eqn. (159).

$$\begin{aligned} &\left(\mu_1^{\triangle}(T,P) + RT\ln\left(\gamma_1^{\triangle} \frac{m_1}{m^{\triangle}} \right) \right) + \left(\mu_2^{\triangle}(T,P) + RT\ln\left(\gamma_2^{\triangle} \frac{m_2}{m^{\triangle}} \right) \right) = \\ &\qquad \left(\mu_3^{\triangle}(T,P) + RT\ln\left(\gamma_3^{\triangle} \frac{m_3}{m^{\triangle}} \right) \right) \end{aligned} \tag{159}$$

Collecting terms:

$$\frac{\dfrac{\gamma_3^{\triangle} m_3}{m^{\triangle}}}{\left(\dfrac{\gamma_1^{\triangle} m_1}{m^{\triangle}} \right)\left(\dfrac{\gamma_2^{\triangle} m_2}{m^{\triangle}} \right)} = \exp\left[\frac{-\Delta\tilde{G}^o}{RT} \right] \quad \text{where } \Delta\tilde{G}^o = \mu_3^{\triangle} - \mu_2^{\triangle} - \mu_1^{\triangle} \tag{160}$$

This can be made consistent with the finite kinetics expression at equilibrium, if we employ the following conventions:

$$\frac{C_o^o \dfrac{\gamma_3^{\triangle} m_3}{m^{\triangle}}}{C_o^o \left(\dfrac{\gamma_1^{\triangle} m_1}{m^{\triangle}} \right) C_o^o \left(\dfrac{\gamma_2^{\triangle} m_2}{m^{\triangle}} \right)} = \left(C_o^o \right)^{\Delta n} \exp\left[\frac{-\Delta\tilde{G}^o}{RT} \right] = K_c(T,P) \tag{161}$$

where Δn is the net change in moles going from the reactants to the products, and the concentration dependent equilibrium constant, K_c, is

$$K_c\left(T,P\right)=\left(C_o^o\right)^{\Delta n}\exp\left[\frac{-\Delta\tilde{G}^o}{RT}\right]=\frac{k_f}{k_r} \tag{162}$$

K_c is potentially dependent on the pressure, because the standard state Gibbs free energies are dependent on the pressure. K_c is independent of the composition of the solution.

Note, kinetics expressions in the liquid phase are very often not based on mass action formulations. A very typical variation from mass action kinetics is to make the reaction rate constant dependent on the pH of solution or to insist on a supersaturation before any reaction takes place (see [17] for an example). Therefore, the kinetics manager for liquid solutions will have to take these additional formulations into account in order to successfully accommodate existing liquid- phase kinetics treatments.

6.4 XML file Format

Extensions to the Cantera XML file format are needed in order to incorporate the complexities of non-ideal solution models. New types of models for the standard state for species must also be added to handle the common formats for liquids. One broad rule will be adhered to when expanding the Cantera XML file format, which involves the general location of new data elements.

A Cantera XML file contains two main parts: the XML elements `phase` and `speciesData`. The first XML element, `phase`, contains a broad description of the phase. The second XML element, `speciesData`, contains subsections for each species in the phase. Cantera has previously stored charge, the elemental composition, and the coefficients for the thermodynamic polynomials that make up the temperature dependent thermodynamic functions within `speciesData`. `speciesData` has also contained the expanded Lennard-Jones coefficients (Stockmayer coefficients) that are used to calculate transport coefficients for gas-phase species.

Therefore, by analogy to what has gone before, the species XML element should generally contain the complete description of the expanded definition of the standard state of the species. Cantera previously has not included pressure dependent data in this part of the XML description. However, it had only dealt with purely ideal gas or ideal surface-solution, or stoichiometric solids previously. Or, it had used real two-phase fluid models that haven't utilized the XML file format.

The species section is now expanded to include everything necessary to calculate the pressure and temperature dependent standard state of a particular species, i.e., $\mu_i^{\Delta}\left(T,P\right)$ in Eqn. (157). The thermodynamics model of the phase itself will still be needed to provide hints as to what particular standard states are appropriate for that phase. In principle, each species may have quite a lot of additional parameters, if, for example, the Helgeson, Kirkham and Flowers (HKF) standard state for aqueous solutes is employed. Additionally, it may involve providing a hook into the real-fluid capability to describe the pressure and temperature dependence of the solvent; the hook will be added to the species section of the `speciesData` XML element.

That leaves the specification of the activity coefficient model to be added to the XML element, `phase`. Everything needed to calculate a_i^{Δ} in Eqn. (157) is to be supplied under the `phase` subelement. This

involves quite a lot of information, as Pitzer coefficient formulations contain two and three-dimensional matrices of coefficients.

With this general approach of separating the a_i^{Δ} and $\mu_i^{\Delta}(T,P)$ implementations in the XML file, different activity coefficient formulations may be readily employed with the same standard state formulations. Let's go through an explicit example of the contents of an XML file.

Fig. 12 contains the `HMW_NaCl.xml` data file. The file contains two main parts, the XML elements, `phase` and `speciesData`. The XML attribute of phase, named `id`, contains the name of the phase, to be used within Cantera, `NaCl_Electrolyte`. The XML-element named `elementArray` contains a list of element names as values. These are the allowable elements to be used in the formula matrix representation for species in that phase. The value of the XML-attribute name `datasrc` contains the file name where the properties (i.e., molecular weights) of these elements are specified. The XML element `speciesArray` contains a description of the species in the phase.

The phase contains 5 species, named `H2O(L), Cl-, H+, Na+,` and `OH-`, whose standard state thermodynamic description is presented in the species data section, identified by the `datasrc` attribute. The thermodynamic model of the phase, `HMW`, is specified as a value of the `model` XML-attribute in the `thermo` XML element. The `speciesData` XML element contains a set of XML subelements named `species`. `Transport` and `kinetics` XML-elements are also included with their model attributes set to `None`. This indicates that no model for transport or kinetics has been specified for this phase. Each species subelement describes the standard state for that species in the phase.

```
<ctml>
  <phase id="NaCl_electrolyte" dim="3">
    <speciesArray datasrc="#species_waterSolution">H2O(L) Cl- H+ Na+ OH-
    </speciesArray>
    <state>
       <temperature units="K">298.15</temperature>
       <pressure units="Pa">101325.0</pressure>
       <soluteMolalities>Na+:6.0954 Cl-:6.0954 H+:2.1628E-9 OH-:1.3977E-6
       </soluteMolalities>
    </state>
    <thermo model="HMW">
      <standardConc model="solvent_volume" />
      <activityCoefficients model="Pitzer" TempModel="complex1">
         <A_Debye model="water" />
         <binarySaltParameters cation="Na+" anion="Cl-">
           <beta0>0.0765, 0.008946, -3.3158E-6, -777.03, -4.4706</beta0>
           <beta1>0.2664, 6.1608E-5, 1.0715E-6</beta1>
           <beta2>0.0</beta2>
           <Cphi>0.00127, -4.655E-5, 0.0, 33.317, 0.09421</Cphi>
           <Alpha1>2.0</Alpha1>
         </binarySaltParameters>
         <binarySaltParameters cation="H+" anion="Cl-">
            <beta0>0.1775, 0.0, 0.0, 0.0, 0.0</beta0>
            <beta1>0.2945, 0.0, 0.0</beta1>
            <beta2>0.0</beta2>
            <Cphi>0.0008, 0.0, 0.0, 0.0, 0.0</Cphi>
            <Alpha1>2.0</Alpha1>
         </binarySaltParameters>
         <binarySaltParameters cation="Na+" anion="OH-">
            <beta0>0.0864, 0.0, 0.0, 0.0, 0.0</beta0>
            <beta1>0.253, 0.0, 0.0</beta1>
            <beta2>0.0</beta2>
            <Cphi>0.0044, 0.0, 0.0, 0.0, 0.0</Cphi>
            <Alpha1>2.0</Alpha1>
         </binarySaltParameters>
         <thetaAnion anion1="Cl-" anion2="OH-">
            <Theta>-0.05</Theta>
         </thetaAnion>
         <psiCommonCation cation="Na+" anion1="Cl-" anion2="OH-">
            <Theta>-0.05</Theta>           <Psi>-0.006</Psi>
         </psiCommonCation>
         <thetaCation cation1="Na+" cation2="H+">
            <Theta>0.036</Theta>
         </thetaCation>
        <psiCommonAnion anion="Cl-" cation1="Na+" cation2="H+">
            <Theta>0.036</Theta> <Psi>-0.004</Psi>
        </psiCommonAnion>
      </activityCoefficients>
      <solvent>H2O(L)</solvent>
    </thermo>
    <elementArray datasrc="elements.xml">O H C Fe Si N Na Cl</elementArray>
    <kinetics model="none" />
  </phase>
```

Fig. 12. Phase XML element for a `HMWThermo` model using the complex1 temperature model.

```
<speciesData id="species_WaterSolution">
  <species name="H2O(L)">
    <atomArray> H:2 O:1 </atomArray>
    <thermo>
      <NASA Tmax="600.0" Tmin="273.14999999999998" P0="100000.0">
        <floatArray name="coeffs" size="7">7.255750050E+01, -6.624454020E-01,
           2.561987460E-03, -4.365919230E-06, 2.781789810E-09, -4.188654990E+04, -
           2.882801370E+02</floatArray>
      </NASA>
    </thermo>
    <standardState model="waterPDSS" />
  </species>

  <species name="Na+">
    <atomArray> Na:1 </atomArray>
    <charge>+1</charge>
    <thermo>
      <Shomate Pref="1 atm" Tmax="623.15" Tmin="298.00">
        <floatArray size="7">12321.25829 , -54984.45383 , 91695.71717 ,
           -54412.15442 , -234.4221295 , -2958.883542 , 26449.31197
        </floatArray>
      </Shomate>
    </thermo>
    <standardState model="constant_incompressible">
      <molarVolume>0.00834</molarVolume>
    </standardState>
  </species>
</speciesData>
```

Fig. 13. Part of the `speciesData` XML element. The solvent `H2O(L)` and electrolyte `Na+` are shown.

Within the `thermo` XML subelement, the thermo model is set to `HMW`. This means that the `ThermoPhase` object is handled by the child `HMWSoln` object (see Figure 1), and it also means that the phase is assumed to have molality-based standard states for its solute species. Within the `thermo` XML element there are three subelements, `standardConc`, `activityCoefficients`, and `solvent`. The `solvent` XML element sets the identity of the solvent species; it must refer to a name contained in the list of species in the `speciesArray` XML element (and currently, it must refer to the first name, as the solvent must be the first species in the mechanism). The `standardConc` XML element contains the default convention for specifying the standard concentration. The value `solvent_volume` in the example triggers the usage of C_o^o, the solvent concentration, as described in the previous section, to be the standard concentration for all species.

The last XML sub-element is `activityCoefficients`. It has two attributes. The first attribute, `model`, with value, `Pitzer`, identifies the activity coefficient formulation as being derived from the Pitzer formulation. The second attribute, `TempModel`, with value, `complex1`, identifies the formulation of the temperature dependence of the Pitzer parameters. `complex1` refers to the formulation in Silvester and Pitzer 1977 [31], where the temperature dependence of the Pitzer parameters, $\beta_{MX}^{(0)}$, $\beta_{MX}^{(1)}$, C_{MX}^{ϕ} are fit to experiment data.

The XML element `binarySaltParameters` contains parameters necessary to specify a single binary cation, anion interaction, i.e., the parameters, $\beta_{MX}^{(0)}$, $\beta_{MX}^{(1)}$, C_{MX}^{ϕ}, $\alpha_{MX}^{(1)}$, and $\alpha_{MX}^{(2)}$. The cation and anion attributes of `binarySaltParameters` identify the particular anion and cation. Each parameter

occupies its own XML subelement: `beta0, beta1, beta2, Cphi, Alpha1, and Alpha2`. The number of parameters for specification of each entry depends on the particular temperature and pressure formulation used. For example, the `complex1` temperature dependence formulation takes 5 parameters to specify the $\beta_{MX}^{(0)}$ temperature dependence. Therefore, there are 5 values in the `beta0` XML subelement.

Anion-anion interaction parameters are specified in the `thetaAnion` XML element, with attributes `anion1` and `anion2`, whose values identify the interaction anions in the mixture. Within this XML element, the XML subelement, `theta`, identifies the value of the parameter $\theta_{aa'}$.

Cation-cation interaction parameters are specified in the `thetaCation` XML element, with attributes `cation1` and `cation2`, whose values identify the interaction anions in the mixture. Within this XML element, the XML subelement `theta` identifies the parameters of the value for the $\theta_{cc'}$ coefficient. `thetaAnion` and `thetaCation` take the same temperature and pressure parameterization as the binary salt parameters. However, if a constant is all that is desired, a single number may always be input into the XML field.

In a similar way, the XML elements `psiCommonCation` and `psiCommonAnion` serve to specify the $\psi_{cc'a}$ and $\psi_{caa'}$ interaction parameters, respectively. `psiCommonCation` and `psiCommonAnion` take the same temperature and pressure parameterization as the binary salt parameters. However, if a constant is all that is desired, a single number may always be input into the XML field.

Another new feature in the phase XML element is the `soluteMolalities` XML subelement of the state description. In the `soluteMolalities` section, the default or initial electrolyte concentration may be specified. Checks to ensure charge neutrality are made in processing this element.

The second part of the XML representation of the `HMW` Pitzer phase is given in the `speciesData` XML element. Fig. 14 contains an example of a charged species `Na+` and the solvent, `H2O(L)`. The solvent water section is very similar to a normal ideal gas species description; the reference thermodynamic functions are given as a NASA polynomial. However, the `standard State` section specifies that the `waterPDSS` model is used. The `waterPDSS` model uses the full IAPWS model for water described in the previous section. The `Thermo` section is only used to specify the initial value for the internal energy and entropy of the liquid at the triple point. As with all steam table-like thermodynamic functions, the IAPWS functions are defined such that the internal energy and entropy of the liquid is equal to zero at the triple point. The `Thermo` section parameters are used to adjust the scale to agree with NIST data tables [24] or any other scale depending on the user's needs.

```
<speciesData id="species_WaterSolution">
  <species name="H2O(L)">
    <atomArray> H:2 O:1 </atomArray>
    <thermo>
      <NASA Tmax="600.0" Tmin="273.14999999999998" P0="100000.0">
        <floatArray name="coeffs" size="7">7.255750050E+01, -6.624454020E-01,
           2.561987460E-03, -4.365919230E-06, 2.781789810E-09, -4.188654990E+04, -
           2.882801370E+02</floatArray>
      </NASA>
    </thermo>
    <standardState model="waterPDSS" />
  </species>

  <species name="Na+">
    <atomArray> Na:1 </atomArray>
    <charge>+1</charge>
    <thermo>
      <Shomate Pref="1 atm" Tmax="623.15" Tmin="298.00">
        <floatArray size="7">12321.25829 , -54984.45383 , 91695.71717 ,
           -54412.15442 , -234.4221295 , -2958.883542 , 26449.31197
        </floatArray>
      </Shomate>
    </thermo>
    <standardState model="constant_incompressible">
      <molarVolume>0.00834</molarVolume>
    </standardState>
  </species>
</speciesData>
```

Fig. 14. Part of the speciesData XML element. The solvent $H_2O(L)$ and electrolyte Na^+ is shown.

The species Na^+ section looks very familiar to gas phase species. The standard state model, `constant_incompressible`, specifies that the standard volume of the ion is constant. This also means that the internal energy doesn't depend on pressure, and that the standard state enthalpy has a simple linear dependence on the pressure. The temperature dependence of the standard state is given by a Shomate polynomial form. The Shomate polynomial is created from the SUPCRT92 J. Phys. Chem. Ref. article [36], and the CODATA recommended values [29]. $\Delta H_f^o\left(298K\right) = -240.34$ kJ gmol^{-1}, $S^o\left(298K\right) = 58.45$ J gmol^{-1} K^{-1}. There is a slight discrepancy between CODATA, SUPCRT92 and Silvester and Pitzer [30], which is resolved in favor of the last authors.

Binary virial-coefficient-like terms may be specified in the λ_{mn} terms that appear in the equations above. Currently these interactions are independent of temperature, pressure, and ionic strength. Also, currently, the neutralities of the species in the λ_{mn} terms are not checked. Therefore, this interaction may involve charged species in the solution as well. The identities of the two species specified by the `species1` and `species2` attributes to the XML `lambdaNeutral` node. These interactions are symmetrical; `species1` and `species2` may be reversed and the interactions are the same. An example of the block is given below.

```
<lambdaNeutral species1="CO2" species2="CH4">
       <lambda> 0.05 </lambda>
</lambdaNeutral>
```

Further discussion about Cantera's XML database structure can be found online and in Cantera's documentation [25, 26].

6.5 `vcs_cantera` Example Problem

As a validation exercise, an explicit calculation of an NaCl equilibrium example problem using Pitzer's activity model is presented, using Cantera's objects and the `vcs` program [28]. The `vcs` program in Cantera computes multiphase-multicomponent chemical equilibria and is based on the Villars-Cruise-Smith (VCS) algorithm described in Smith and Missen [84]. Phases included in the program are the liquid electrolyte containing NaCl, solid NaCl, and a gas phase that includes nitrogen, water, NaCl, H_2, and O_2. The NaCl-H_2O system is chosen given the large amount of thermodynamic data available as function of electrolyte concentration, temperature, and pressure.

The equilibrium solver, `vcs`, not only needs models for the activities and/or activity coefficients of the phases, but it's also necessary to provide the standard state Gibbs free energies at the temperature and pressure of interest (298 K and 1 atm). Following the discussion in ref. [27], we have chosen to set the basis for these to be consistent with the NIST webbook website, chemkin, and the JANAF tables (noted as scheme $\Delta H^o_{f,298}$-B basis), where the absolute values of the standard state Gibbs free energies are set to the following values:

$$\mu_i^o\left(T,P\right) = \left(\mu_i^{o,abs}\left(T,P\right) - H\left(298.15,1\text{ bar}\right)\right) + \Delta H^o_{f,298} \tag{163}$$

$\Delta H^o_{f,298}$ is the standard heat of formation of the species at 298 K from its constitutive elements in their standard state at 298 K and 1 bar. And, the chemical potential, standard state molar volume, standard state entropy and enthalpy of the hydrogen ion in the liquid phase are set to zero. Table 1 provides the standard state Gibbs free energies of the species employed. Standard states for solutes in the liquid phase (whether they are charged or not) are on the molality basis. Standard states for all solids, gas species, and the liquid solvent (`H2O(L)`) are on the molar basis.

With the standard states of all species specified, `vcs` was then used to calculate the equilibrium composition of the system consisting of the Pitzer fluid, the solid NaCl(s), and a gas consisting of N_2, O_2, H_2, and H_2O(g). Pitzer coefficients for the $Na^+ - Cl^-$ interaction, the only important interaction in this example were as follows: $\beta^{(0)} = 0.0765$, $\beta^{(1)} = 0.2664$, $C^{\phi}_{MX} = 0.00127$, and $\alpha^{(1)} = 2.0$.

Table 1 contains the resulting concentrations predicted for the gas, liquid, and solid. For the current input conditions, a solid NaCl phase exists in equilibrium with the solution and the gas phase. The resulting concentrations are within acceptable agreement with the well-known equilibrium solution quoted in Pitzer's paper and in the CRC. Pitzer's paper quotes equilibrium at a molality of 6.146, a value of $\Delta G^0 = -9.042$ kJ gmol^{-1} and an activity coefficient of 1.008.

Table 2: Results from the `vcs_Cantera` NaCl equilibrium calculation at 298K

Species	Molality	Mole Fraction	Activity (Cantera)	μ° (kJ gmol^{-1})	μ (kJ gmol^{-1})
Cl^-	6.1934	.091220	6.2751	-183.974	-179.421
H^+	5.3724E-08	7.913E-10	2.5709E-07	0	-37.6153
Na^+	6.1934	.091220	6.2751	-257.752	-253.199
OH^-	5.3724E-08	7.9128E-10	2.9292E-08	-226.784	-269.784
$H_2O(L)$	55.5084	0.81756	0.74995	-306.686	-307.399
NaCl(S)	NA	1	1	-432.62	-432.62
$N_2(g)$	NA	.97628	0.97628	-57.128	-57.188
$H_2O(g)$	NA	.023718	.023718	-298.904	-307.399
$H_2(g)$	NA	4.5731E-08	4.5731E-08	-38.9624	-80.858

The `vcs` results above are a molality of 6.193, a value of $\Delta G^0 = -9.106$ kJ gmol^{-1} and an activity coefficient of 1.013. Also note at equilibrium the activity of the water is 0.7499. Thus, the relative humidity above an NaCl saturated liquid phase has been reduced from 100% to 75%, by the presence of the salt. The 75% value agrees with the value given in the CRC [37] handbook.

This problem serves as an "admiral's test" to validate the `vcs` program, and the new `HMWSoln` modules. Recently, the equilibrium solver was generalized to handle non-ideal solutions, and to handle charge-neutrality conditions for electrolyte phases. Additions to handle molality formulations for the new liquid electrolyte `ThermoPhase` objects were also added [28]. This test case serves as an example that the new capabilities work.

The next two sections describe submodels that comprise the equilibrium calculation. Section 6.1 describes the evaluation of the species standard states. Section 6.2 describes the evaluation of the solution activities.

7 Examples

7.1 Details of the Binary NaCl Electrolyte Calculation

The most important numbers for an accurate determination of the solubility of NaCl(s) in water are the standard state thermodynamic properties of the solution reaction,

$$\mathrm{NaCl(s)} \rightarrow \mathrm{Na^{+}}(aq) + \mathrm{Cl^{-}}(aq)$$

If the solubility is to be accurately determined over an extended temperature range, then not only $\Delta G_r^o\left(298K\right)$ but both the first derivative, i.e., related to $\Delta H_r^o\left(T\right)$, and the second derivative, i.e., related to $\Delta C_{p,r}^o\left(T\right)$, must be known to be accurately calculated over the extended temperature range. Silvester and Pitzer [31] regressed on the original data for the reaction and found $\Delta G^o\left(298K\right) = -9.042 \pm 0.04$ kJ gmol^{-1} [3], $\Delta H^o\left(298K\right) = 3.843 \pm 0.1$ kJ gmol^{-1}, $\Delta C_p^o\left(298K\right) = -31.25 \pm 0.5$ J gmol^{-1}K^{-1}. How well do the accepted general numbers from general sources come close to the regressed data [31] for this specific NaCl(s) solution reaction?

To answer this question, temperature dependent polynomial representations were obtained for the three species in the reaction from general sources. A Shomate polynomial for the standard state thermodynamic properties of NaCl(s) was obtained from the NIST's online database [24].

Shomate polynomial representations for Na^+ and Cl^- were obtained by fitting data in the SUPCRT92 database [36]. Additionally, the CODATA values [29] for $\Delta H_f^{\triangle}\left(298K\right)$ and $S^{\triangle}\left(298K\right)$ for Na^+ and Cl^- were thrown into the fitting process as well to weight the 298 K limit. Then, the resulting values of $\Delta G_r^o\left(T\right)$, $\Delta H_r^o\left(298K\right)$, and $\Delta C_{p,r}^o\left(298K\right)$ for the NaCl(s) dissolution reaction were compared with Silvester and Pitzer [31] and Pitzer's subsequent papers on the NaCl system [40, 41].

For the Cl^- species case, the CODATA recommended values are $\Delta H_f^{\triangle}\left(298K\right) = -167.08 \pm 0.10$ kJ gmol^{-1} and $S^{\triangle}\left(298K\right) = 56.60 \pm 0.20$ J gmol^{-1} K^{-1}, resulting in a value of $\mu^{\triangle}\left(298K\right) = -183.95 \pm 0.11$ kJ gmol^{-1}. SUPCRT92 quotes an apparent standard partial molar Gibbs free energy of formation, $\Delta G_f^{\triangle}\left(298K\right)$ value of –131.29 kJ gmol^{-1}.

3 Estimate for the uncertainty for $\Delta G^o\left(298K\right)$ came from a general discussion in ref. [31] and Table 4 in ref. [40].

Table 3: Standard State Properties at 298 K (25°C)

Species	$\mu^o(298K)$ (kJ/gmol)	$\Delta H_f^o(298K)$ (kJ/gmol)	$S^o(298K)$ (J/(gmol K))	$C_p^o(298K)$ (J/(gmol K))
H_2O(l)	–306.6858	–285.8287	69.9224	75.3275
Cl^-(shomate)	–183.9736	–167.0967	56.6057	–114.5987
Cl^-(SPEQ06.dat)	–184.0250	–167.1095	56.7350	–118.4659
H^+	0	0	0	0
OH^- (shomate)	–226.7839	–230.0320	–10.8944	–118.1955
OH- (SPEQ06.dat)	–226.8420	–230.0355	–10.7110	–103.3277
NaCl(s)	–432.6201	–411.1207	72.1093	50.5012
N_2(g)	–57.1282	0.0	191.6089	29.1242
H_2O(g)	–298.140	–241.8249	188.8283	33.5876
H_2(g)	–38.9642	0.0	130.6804	28.8362
O_2(g)	–61.1650	0.0	205.1482	29.3782
$Na^+\left(\Delta G_r^o(T)\right)$	–257.6881	–240.1801	58.7218	34.3048
Na^+ (SUPCRT92-shomate)	–257.6911	–240.5765	57.4026	74.3038
Na^+ (SUPCRT92-CODATA-shomate)	–257.7521	–240.3265	58.4456	–0.4415
Na^+ (SPEQ06.dat)	–257.7409	–240.3264	58.4086	39.0321

This may be converted (see previous memos [4, 3, 1]) into a Gibbs free energy of formation on an $\Delta H_f^o(298K)$ elements basis (i.e., the NIST standard that we are using) of $\mu^\triangle(298K) = -184.03$ kJ gmol^{-1}. Therefore, for Cl^-, the SUPCRT92 database is marginally consistent with the CODATA values, at least up to the quoted uncertainty in the CODATA values. Also, the fit to SUPCRT92 produced a Shomate polynomial with $\Delta H_f^\triangle(298K) = -167.10$ kJ gmol^{-1}, in agreement with the CODATA $\Delta H_f^\triangle(298K)$ value.

For the Na^+ species case, the CODATA recommended values are $\Delta H_f^\triangle(298K) = -240.34 \pm 0.06$ kJ gmol^{-1} and $S^\triangle(298K) = 58.45 \pm 0.15$ J gmol^{-1} K^{-1}, resulting in a value of $\mu^\triangle(298K) = -257.78 \pm 0.07$ kJ gmol^{-1}. SUPCRT92 quotes an apparent standard partial molar Gibbs free energy of formation, $\Delta G_f^\triangle(298\,\mathrm{K})$, value of –261.877 kJ gmol^{-1}. This may be converted into a Gibbs free energy of formation on an $\Delta H_f^o(298\,\mathrm{K})$ elements basis of $\mu^\triangle(298K) = -257.69$ kJ gmol^{-1}. Therefore, for Na^+, the SUPCRT92 database is on the edge of consistency with the CODATA values. The fit to SUPCRT92 produced a Shomate polynomial with $\Delta H_f^\triangle(298K) = -240.33$ kJ gmol^{-1}, in agreement

with the CODATA $\Delta H_f^{\triangle}(298K)$ value.

The NaCl(s) thermodynamics was obtained from the NIST website, in the form of a Shomate polynomial. Values of $\mu^o(298K) = -432.62$ kJ gmol^{-1} and $\Delta H_f^o(298K) = -411.12$ kJ gmol^{-1} were obtained from the Shomate polynomial.

CODATA sources, alone, produces $\Delta G_r^o(298K) = -9.110$ kJ gmol^{-1} and SUPCRT92 alone produces $\Delta G_r^o(298K) = -9.100$ kJ gmol^{-1}, compared to Pitzer regressed experimental value of $\Delta G_r^o(298K) = -9.042 \pm 0.04$ kJ gmol^{-1}. CODATA sources, alone, produces $\Delta H_r^o(298K) = 3.700$ kJ gmol^{-1} and SUPCRT92 alone produces $\Delta H_r^o(298K) = 3.698$ kJ gmol^{-1}, compared to Pitzer regressed experimental value of $\Delta H_r^o(298K) = 3.843 \pm 0.15$ kJ gmol^{-1}.

While the agreement is good considering the inherent uncertainties in the data, the predicted $\Delta G_r^o(298K)$ and $\Delta H_r^o(298K)$ values from general sources are either on the edge or nominally out of range of the experimental values determined by Pitzer from the original data. Therefore, for the purposes of studying this one system, the Shomate polynomial for Na^+ was reevaluated to match the $\Delta G_r^o(T)$ values determined by Pitzer and Silvester. The resulting 298 K thermodynamic values, given in Table 3 in the row, $Na^+(\Delta G^o(T))$, match the CODATA values for $S^o(298K)$ and $\Delta H_f^o(298K)$ adequately, and were used throughout the remaining calculations.

Table 3 also contains fits to Na^+ from just the SUPCRT92 database (Na^+(SUPCRT92)), and from fits to Na^+ from SUPCRT92 plus 298 K CODATA values (Na^+(SUP-CODATA)). The resulting $\Delta G^o(T)$ curves from the SUPCRT92-only data are plotted in Fig. 15. Of particular note is the wide disparity in $C_p^{\triangle}(298K)$ values predicted by the three different methods. This demonstrates that forcing fits to the 298 K data may cause large changes in $C_p^o(T)$ to occur that are not physical and thus may be counterproductive. To reinforce this point, the Na+ standard state values produced by the HKFT standard state formulation with parameters from the SPEQ06.dat database [43] are provided in the last row of the table, entitled Na+(SPEQ06.dat). This row clearly demonstrates that the formulation of the HKFT standard state makes a difference in fitting the standard state polynomials, and that the resulting values for $C_p^{\triangle}(T)$ are much smoother with respect to their variation with temperature than the results using Shomate polynomials. Additionally, we have included rows for the standard states for Cl- and OH- calculated from the HKFT standard state using the SPEQ06.dat database within Table 3. The HKFT $\Delta H_f^o(298K)$ and $S^o(298K)$ values are close to the Shomate values for these species. However, the $C_p^o(298K)$ values again demonstrate significant deviations, again demonstrating the dangers and inaccuracies inherit in the fitting process, especially when evaluating quantities obtained from taking derivatives.

The $\Delta G_r^o(T)$ values regressed from SUPCRT92 and from Silvester and Pitzer (1977) are plotted in

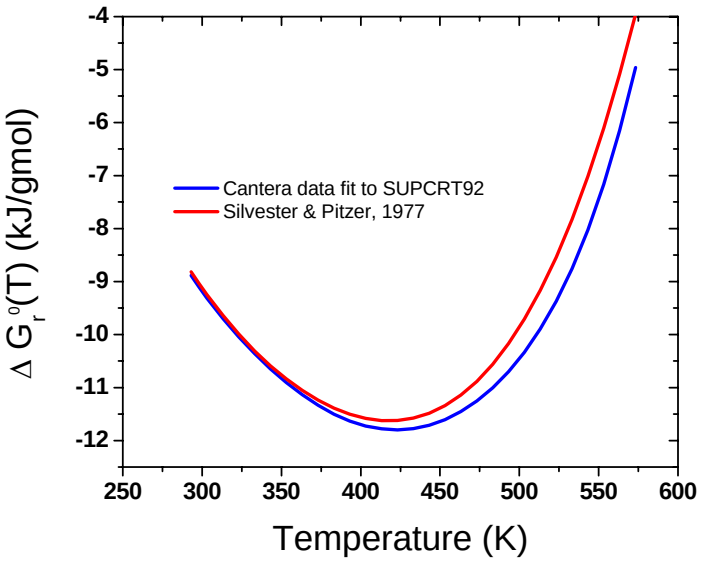

Fig. 15. Plot of $\Delta G_r^o(T)$ for the reaction $\mathrm{NaCl(s)} \rightarrow \mathrm{Na^+}(aq) + \mathrm{Cl^-}(aq)$

Fig. 15. Differences at higher temperature are in the 1 kJ gmol^{-1} range, and can be explained by differences in $\Delta C_{p,r}^o(T)$, which controls the second derivative in $\Delta G_r^o(T)$. With the changes made to the Na^+ standard state, the $\Delta G_r^o(T)$ values used in these calculations follow the Silvester and Pitzer curve in Fig. 15. What is apparent is how sensitive the heat capacity value is when computing it from Gibbs free energy data. The lesson here is to seek out solution heat capacity data whenever possible if accurate thermodynamic data extrapolation to high temperatures is the goal.

The neutral aqueous species `NaCl(aq)` was left out because it's concentration was found not to be appreciable even at high molalities and at high temperatures. Also, the inclusion of ion pairs in the model should be avoided since the Pitzer interaction parameters for this binary electrolyte already captures the effect of ion pairing. Therefore, any explicit use of ion pairs should be avoided unless ion pair constants are part of the Pitzer parameterization for a given electrolyte. This is the case in systems containing weak acids where the non-dissociated aqueous species may have to be included in the calculation. A decision then has to be made whether to include the non-dissociated species with its associated ion pairing constant or to include the effects of the association on the activity of the ions, by adding in a nonzero value to the $\beta_{MX}^{(2)}$ interaction parameter. Pitzer argues that the latter may be more accurate and for practical purposes it behaves like an ion pairing constant. Of course, doing both, i.e., adding in the non-dissociated ion pair while at the same time adding in a nonzero $\beta_{MX}^{(2)}$ interaction, or even adding the ion pairing constant with the 1-1 Pitzer binary interaction parameters would be like "double counting" the effects of ion association and therefore it would lead to a wrong result. It should be noted, however, that some forms of the Pitzer parameterization makes use ion pairing constants along with binary interaction parameters for the ions in the electrolyte of interest. For example, the Pitzer parameterization used in the YMP database, and used here with Cantera, adopts a

form given by Sterner et al. (1998) [66] that includes Pitzer parameters for the complexes $CaCl^+$ and $CaCl_{2(aq)}$ as well as ion pairing constants. That is, the Pitzer parameterization for the $CaCl_2$ electrolyte in this case was regressed consistent with the ion pairing constants as a function of temperature and ionic strength. According to Sterner et al. (1998) [66], the inclusion of these ion pairs resulted in a much better fit to the osmotic coefficient data used to retrieved the ion interaction parameters.

One of the problems with current basis approach is the large negative numbers for the absolute Gibbs free energy. Pertinent differences in the Gibbs free energy are on the order of 0.1 kJ / gmol. However, absolute Gibbs free energies are typically on the order of –300 kJ / gmol. Essentially, 3 significant digits of accuracy are given up with this approach.

This loss of accuracy argues for a reevaluation of the basis used for liquid phase calculations. This is done in many other programs, where an elemental basis is replaced by a species basis. For example, if 1/2 $O_2(g)$, the elemental basis for oxygen were replaced by $H_2O(L)$ as the basis species for oxygen, then formation reactions for all species containing oxygen would exhibit a smaller magnitude. The loss of accuracy would be stemmed. This approach will be considered for adoption in later work.

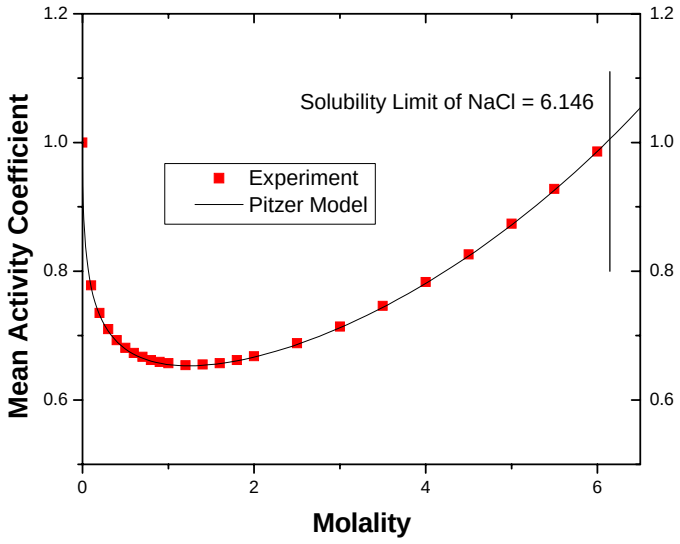

Fig. 16. Dependence of the mean activity coefficient with molality at 25°C. Experimental data from Robinson and Stokes [42].

7.1.1 NaCl Binary System at 25°C

The NaCl-H_2O system has been studied extensively in terms of salt solubilities and/or concentrated electrolytes where the thermodynamic properties of concentrated solutions as function of salt concentration and temperature have been well characterized (Pitzer et al. [41]; Clarke and Glew [69]).

Fig. 16 shows the dependence of the mean activity coefficient on NaCl molality at 25°C. Notice the strong agreement between experiment and prediction using Pitzer parameter data from Greenberg and Møller [72]. These authors retrieved NaCl Pitzer parameters based mainly on the work by Pitzer et al. [41] for temperatures exceeding 200°C along P_{sat}.

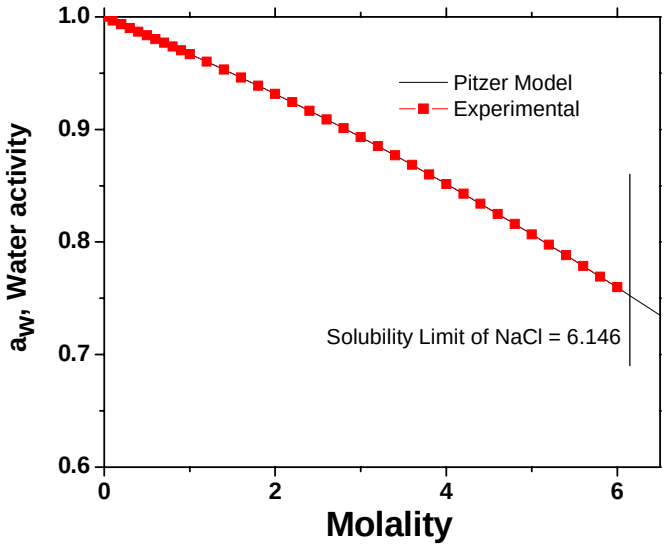

Fig. 17. Dependence of the water activity on the molality of a NaCl solution at 25°C. Experimental data from Robinson and Stokes [42].

Fig. 17 shows the dependence of the water activity on molality at 25°C. The points marked "Experiment" are actually taken from a compilation of the original data in Robinson and Stokes [42].

The Pitzer formulation should be considered a success, due to the fact that it only takes 3 adjustable parameters, $\beta^{(0)}$, $\beta^{(1)}$, and C^{ϕ}, to obtain a very accurate representation of the water activity and the mean activity coefficient over a wide range of concentrations. Other measures of success for the Pitzer formulation are its success in treating multicomponent electrolyte solutions with relatively small-in-size cross terms. Further, the temperature dependency on the thermodynamic properties of various electrolytes has been evaluated successfully using the Pitzer approach. The following sections will provide more examples of the applications of this approach to model thermodynamic properties of electrolyte solutions.

7.1.2 Example Program for Excess Gibbs Free Energy

In order to obtain a unit test for the excess Gibbs free energy calculation, the essential quantity in Pitzer's treatment, weused Silvester and Pitzer's paper [31], which models the binary NaCl system

from 25°C to 300°C. The excess Gibbs free energy is given by the following formula:

$$\frac{G_{ex,\triangle}}{\tilde{M}_o n_o RT} = -\left(\frac{4AI}{3b}\right)\ln\left(1+b\sqrt{I}\right) + m^2\left(2\nu_M\nu_X B_{MX}\right) + m^3\left(\left(\nu_M\nu_X\right)^{3/2} C^{\phi}_{MX}\right) \qquad (164)$$
$$= \nu m\left(1-\phi+\ln\gamma_{\pm}\right)$$

A key feature is the temperature dependence of the Pitzer coefficient. What coefficients need to be dependent on the temperature and what functional formalism will be used to describe that temperature dependence. Silvester and Pitzer [31] described one set of numerical fitting data where he fit much of the experimental data for NaCl over an extensive data range, below the critical temperature. He found a temperature functional form, Eqn. (165), for fitting the 3 coefficients that describe the Pitzer parameterization for a single salt that can adequately describe how those three coefficients change with respect to temperature. Additionally, there are temperature dependencies involved with specification of the standard states. The Pitzer coefficients only describe the evolving concentration effects.

$$\beta^{(0)} = q_1 + q_2\left(\frac{1}{T}-\frac{1}{T_r}\right) + q_3\ln\left(\frac{T}{T_r}\right) + q_4\left(T-T_r\right) + q_5\left(T^2-T_r^2\right) \qquad (165)$$

$$\beta^{(1)} = q_6 + q_9\left(T-T_r\right) + q_{10}\left(T^2-T_r^2\right)$$

$$C^{\phi} = q_{11} + q_{12}\left(\frac{1}{T}-\frac{1}{T_r}\right) + q_{13}\ln\left(\frac{T}{T_r}\right) + q_{14}\left(T-T_r\right)$$

In Pitzer's cumulative paper [18], he presents tables of derivatives of these three quantities at the reference temperature of 25°C for a range of binary salt systems. Therefore, it seems prudent to generate functional dependencies which parameterize the temperature dependence of the three Pitzer coefficients, $\beta^{(0)}$, $\beta^{(1)}$, C^{ϕ}, as a way to handle the general case.

Also, in later papers, Pitzer has added additional temperature dependencies to all of the other remaining second and third order virial coefficients. Some of these dependences are justified and motivated by theory. Therefore, a formalism wherein all of the coefficients in the base theory have temperature dependences associated with them. We will denote the temperature derivative of these coefficients with a superscript "*L*".

A small program was written to directly calculate G^{ex}, $\gamma_{\pm}$, and ϕ at 50°C and 200°C, and was then used to validate the results from `HMWSoln`'s implementation. The small program produced these values for a fixed molality of 6.146.

50°C (323.15 K): $G^{ex} = -8.930005$ kJ / kg Water, $\ln\gamma_{\pm} = 0.004969$, and $\phi = 1.2753$

200°C (473.15 K): $G^{ex} = -35.9022$ kJ / kg Water, $\ln\gamma_{\pm} = 0.71353$, and $\phi = 1.0289$

Table 4 Excess Gibbs Free Energy as a function of temperature for the NaCl-H_2O System

Temperature	**Pressure**	**A_ϕ**	**$\Delta G°$**	**ΔG**	**G_{ex}**	**mean activity**	**ϕ - 1**
Kelvin	(bars)	sqrt(kg/gmol)	(kJ/gmol)	(kJ/gmol)	kJ/kgWater	dimensionless	dimensionless
293.15	1.01325	0.388193	-8.81994	0.0278395	-8.55678	0.999211	0.28481472
298.15	1.01325	0.391469	-9.04161	-0.0048679	-8.48944	1.006910	0.28549018
303.15	1.01325	0.394908	-9.2523	-0.040418	-8.47584	1.011634	0.2851374
313.15	1.01325	0.402277	-9.64279	-0.120008	-8.60387	1.012999	0.2817495
323.15	1.01325	0.4103	-9.99482	-0.210642	-8.93001	1.004982	0.275359
333.15	1.01325	0.41898	-10.311	-0.311754	-9.44534	0.989198	0.2665432
343.15	1.01325	0.428325	-10.593	-0.422564	-10.1429	0.967101	0.2557636
353.15	1.01325	0.438348	-10.8421	-0.542127	-11.0177	0.940003	0.2433916
363.15	1.01325	0.449067	-11.0585	-0.669359	-12.0665	0.909013	0.2297206
373.15	1.01418	0.460504	-11.2422	-0.803071	-13.2879	0.875070	0.2149790
383.15	1.43379	0.472673	-11.3928	-0.942158	-14.6808	0.838989	0.1993502
393.15	1.98674	0.485612	-11.5087	-1.08514	-16.248	0.801381	0.1829576
403.15	2.7028	0.499358	-11.5883	-1.23069	-17.993	0.762764	0.1658911
413.15	3.61539	0.513953	-11.6294	-1.3775	-19.9212	0.723550	0.1482070
423.15	4.76165	0.529446	-11.6295	-1.52436	-22.0399	0.684065	0.129932
433.15	6.18235	0.545895	-11.5858	-1.67018	-24.3584	0.644568	0.111067
443.15	7.92187	0.563366	-11.4949	-1.81407	-26.8882	0.605261	0.091588
453.15	10.0281	0.581938	-11.3534	-1.9554	-29.6436	0.566304	0.071452
463.15	12.5524	0.601705	-11.1573	-2.09391	-32.6414	0.527821	0.0505913
473.15	15.5493	0.622777	-10.9025	-2.22983	-35.9022	0.489913	0.0289190
483.15	19.0767	0.645286	-10.5846	-2.36401	-39.4503	0.452662	0.0063259
493.15	23.1959	0.669394	-10.199	-2.49814	-43.3151	0.416138	-0.017321
503.15	27.9709	0.695296	-9.74073	-2.63502	-47.5323	0.380399	-0.042186
513.15	33.4693	0.723235	-9.20474	-2.77892	-52.1456	0.345501	-0.0684628
523.15	39.7617	0.753518	-8.58571	-2.93612	-57.2088	0.31149	-0.0963907
533.15	46.9226	0.786537	-7.87817	-3.11562	-62.7901	0.278422	-0.126265
543.15	55.0299	0.822801	-7.07643	-3.33028	-68.9765	0.246341	-0.158457
553.15	64.1658	0.862992	-6.17465	-3.59848	-75.8829	0.215298	-0.193448
563.15	74.4178	0.908045	-5.16684	3.9468	-83.664	0.185348	-0.231878
573.15	85.879	0.959282	-4.04685	-4.41438	-92.5358	0.156552	-0.274627

`HMWSoln`'s implementation used a pressure of 1 atm, until the vapor pressure curve advanced past 1 atm at 100°C. Above 100°C, the pressure was set equal to the pure water vapor pressure. **Table 4** contains the results for a fixed molality of 6.146. **Table 4** also contains results for the calculation of A_ϕ, the Debye-Hückel parameter for the osmotic coefficient. This result closely agrees with Silvester and Pitzer's numbers over the entire temperature range.

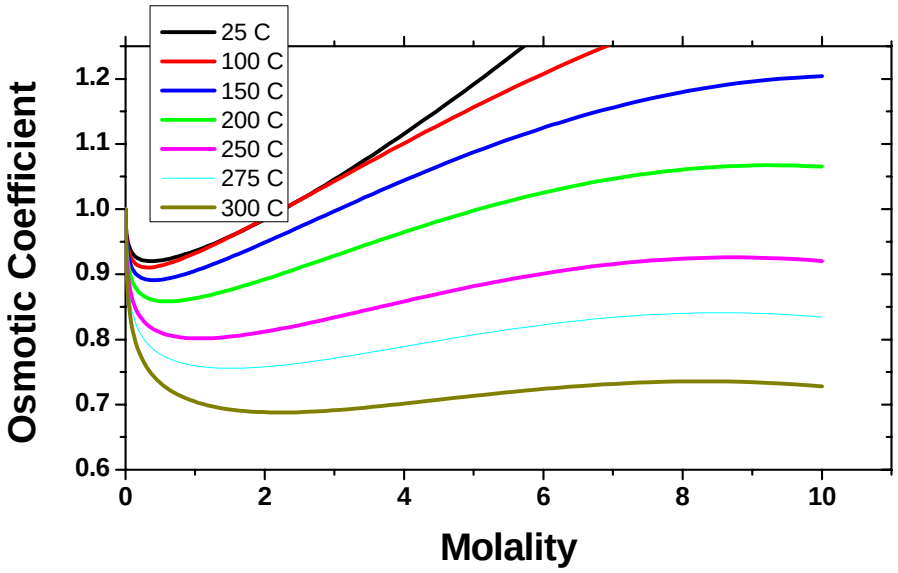

Fig. 18. Osmotic coefficient of NaCl solutions as a function of molality at various temperatures.

Fig. 18 depicts the dependency of osmotic coefficient on solution molality for a wide range of temperature. These values closely agree with those given in Figure 7 in ref. [31].

7.1.3 Expressions for the Mixture Enthalpy

Partial molar enthalpies, $\bar{H}_i$, are related to the derivative of the Gibbs free energy by the following Eqn. (166). μ_i is the partial molar Gibbs free energy for the i^{th} species. $\bar{S}_i$ is the partial molar entropy of the i^{th} species. n is the total number of moles in solution, and n_i is the number of moles of species i in the solution.

$$\bar{H}_i = \mu_i + T\bar{S}_i = \mu_i - T\left(\frac{d\mu_i}{dT}\right)_{P,n_k} = -T^2\left(\frac{d\left(\frac{\mu_i}{T}\right)}{dT}\right)_{P,n_k} \quad \text{where } \bar{H}_i = \left(\frac{dnH}{dn_i}\right)_{P,n_k} \qquad (166)$$

The total enthalpy of the system may be related also to the total Gibbs free energy via the following similar formula:

$$\left(n\tilde{H}\right)=\left(n\tilde{G}\right)+\left(n\tilde{S}\right)T=\left(n\tilde{G}\right)-T\left(\frac{dn\tilde{G}}{dT}\right)_{P,n_k}=T^2\left(\frac{d\left(\frac{n\tilde{G}}{T}\right)}{dT}\right)_{P,n_k} \tag{167}$$

The change in enthalpy due to the non-ideality of the mixing is encapsulated in the definition of the relative enthalpy of mixing, *L*, Eqn. (168). X_i is the mole fraction of species *i* in solution.

$$\tilde{L}=\tilde{H}-\tilde{H}^o \tag{168}$$

where $\tilde{H}^o=\sum_{i=o}^{N}X_i\,\tilde{H}_i^o$ and $\tilde{H}=\sum_{i=o}^{N}X_i\,\bar{H}_i$

$\tilde{L}$ is on a "per mole of solution" basis. A more useful expression is to put the enthalpy of mixing expression on a "per mole of salt" basis. The resulting expression is called the apparent relative molal enthalpy of mixing, ${}^{\phi}L$, Eqn. (169).

$${}^{\phi}L=\frac{\left(n\tilde{L}\right)}{n_{salt}}=\frac{\left(n\tilde{H}-n\tilde{H}^o\right)}{n_{salt}} \tag{169}$$

Because the ideal component of the mixing Gibbs free energy doesn't contribute to the total enthalpy, formulas for expressing the relative enthalpy of mixing, $\tilde{L}=\tilde{H}-\tilde{H}^o$, may be directly related to the excess Gibbs free energy.

$$\left(n\tilde{G}\right)=\sum n_i\,G_i^o-RT\sum n_i\left(1-\ln\left(m_i\right)\right)+\left(n\tilde{G}_{ex,\triangle}\right) \tag{170}$$

Therefore,

$$n\tilde{L}=-T^2\left(\frac{d\left(\frac{n\tilde{G}_{ex,\triangle}}{T}\right)}{dT}\right)_{P,n_k} \tag{171}$$

The expressions for partial molar enthalpy of species *i* may all be related to the derivatives of the molality-based activity coefficients added to the standard state enthalpy by the following Eqns. (172) and (173).

$$\bar{H}_i = H_i^{\triangle} + \left(-RT^2\right)\left(\frac{d\ln\gamma_i^{\triangle}}{dT}\right)_{P,n_k} \tag{172}$$

Since,

$$\phi = \left(-\frac{1}{\tilde{M}_o}\right)\frac{\ln a_o}{\sum_i m_i}$$

and

$$\frac{n\tilde{G}_{ex,\triangle}}{RT} = \sum_i n_i\left(\ln\gamma_i^{\triangle} + (1-\phi)\right)$$

$$n\tilde{L} = \left(-RT^2\right)\left(\sum_i n_i\left(\left.\frac{d\ln\gamma_i^{\triangle}}{dT}\right|_{P,m_k} - \left.\frac{d\phi}{dT}\right|_{P,m_k}\right)\right) \tag{173}$$

The general expression for the temperature derivative of the log of the activity coefficient is not given in Pitzer's papers. It is presented below. Note the *L* superscript refers to a partial derivative with respect to temperature.

$$\begin{aligned}\frac{d\ln\left(\gamma_M^{\triangle}\right)}{dT} &= z_M^2\left(\frac{dF}{dT}\right) + \sum_a m_a\left(2B_{Ma}^L + ZC_{Ma}^L\right) + z_M\left(\sum_c\sum_a m_c m_a C_{Ma}^L\right) \\ &+ \sum_c m_c\left[\Phi_{Mc}^L + \sum_a m_a\psi_{Mca}^L\right] + \sum_{a<a'}\sum m_a m_{a'}\psi_{Maa'}^L + 2\sum_n m_n\lambda_{nM}^L\end{aligned} \tag{174}$$

$$\begin{aligned}\frac{d\ln\left(\gamma_X^{\triangle}\right)}{dT} &= z_X^2\left(\frac{dF}{dT}\right) + \sum_c m_c\left(2B_{cX}^L + ZC_{cX}^L\right) + \left|z_X\right|\left(\sum_a\sum_c m_a m_c C_{ca}^L\right) \\ &+ \sum_a m_a\left[\Phi_{Xa}^L + \sum_c m_c\psi_{cXa}^L\right] + \sum_{c<c'}\sum m_c m_{c'}\psi_{cc'X}^L + 2\sum_n m_n\lambda_{nX}^L\end{aligned} \tag{175}$$

where

$$\begin{aligned}\frac{dF}{dT} &= -\frac{A_L}{4RT^2}\left[\frac{\sqrt{I}}{1+b\sqrt{I}} + \frac{2}{b}\ln\left(1+b\sqrt{I}\right)\right] + \sum_a\sum_c m_c m_a\left(\frac{\beta_{ca}^{(1)L}h\left(\alpha\sqrt{I}\right)}{I}\right) \\ &+ \sum_{c<c'}\sum m_c m_{c'}\left(\Phi_{cc'}^{'L}\right) + \sum_{a<a'}\sum m_a m_{a'}\left(\Phi_{aa'}^{'L}\right)\end{aligned}$$

$$\frac{d\phi}{dT}=\frac{2}{\sum_{k\neq o}m_k}\Bigg[-\frac{A_L}{4RT^2}\left(\frac{I^{3/2}}{1+b\sqrt{I}}\right)+\sum_c\sum_a m_c m_a\left(B_{ca}^{\phi L}+ZC_{ca}^{L}\right)$$
$$+\sum_{c<c'}\sum m_c m_{c'}\left[\Phi_{cc'}^{\phi L}+\sum_a m_a\psi_{cc'a}^{L}\right]+\sum_{a<a'}\sum m_a m_{a'}\left[\Phi_{aa'}^{\phi L}+\sum_c m_c\psi_{aa'c}^{L}\right] \quad (176)$$
$$+\sum_n\sum_c m_n m_c\lambda_{nc}^{L}+\sum_n\sum_a m_n m_a\lambda_{na}^{L}+\sum_{n<n'}\sum m_n m_{n'}\lambda_{nn'}^{L}+\frac{1}{2}\left(\sum_n m_n^2\lambda_{nn}^{L}\right)\Bigg]$$

The following definition for the enthalpy Debye-Hückel coefficient, A_L,

$$A_L=4RT^2\frac{d\left(\frac{A}{3}\right)}{dT}=4RT^2\frac{d\left(A_\phi\right)}{dT}=\left(-6RT\ A_\phi\right)\left(1+T\frac{d\ln\varepsilon}{dT}+T\frac{\alpha_w}{3}\right), \quad (177)$$

Was made in the previous equations. Eqn. (176) may be combined with the following equation,

$$\left(\frac{d\phi}{dT}\right)\left(\sum_{k\neq o}m_k\right)\tilde{M}_o=-\frac{d\ln a_o}{dT}=-\frac{d\ln\left(x_o\gamma_o\right)}{dT}=-\frac{d\ln\left(\gamma_o\right)}{dT}, \quad (178)$$

to create an expression for the temperature derivative of the water activity coefficient. This may be plugged into the expression for the partial molar enthalpy expression to yield an expression for the partial molar enthalpy for water in terms of the derivative of the osmotic coefficient, Eqn. (179).

$$\bar{H}_o=H_o^o-RT^2\frac{d\ln\left(\gamma_o\right)}{dT}=H_o^o+RT^2\left(\sum_{k\neq o}m_k\right)\tilde{M}_o\left(\frac{d\phi}{dT}\right) \quad (179)$$

The mixture excess Enthalpy, which Pitzer calls the relative enthalpy, *L*, may be obtained by taking the derivative with respect to the temperature (Eqn. (171) at constant *p* and *n*) applied to Eqn. (65) to yield Eqn. (180).

$$\frac{L}{\tilde{M}_o n_o R}=-\left(\frac{A_L I}{RT^2 b}\right)\ln\left(1+b\sqrt{I}\right)+2\sum_c\sum_a m_c m_a B_{ca}^{L}+\sum_c\sum_a m_c m_a ZC_{ca}^{L}$$
$$+\sum_{c<c'}\sum m_c m_{c'}\left[2\Phi_{cc'}^{L}+\sum_a m_a\psi_{cc'a}^{L}\right]+\sum_{a<a'}\sum m_a m_{a'}\left[2\Phi_{aa'}^{L}+\sum_c m_c\psi_{aa'c}^{L}\right] \quad (180)$$
$$+2\sum_n\sum_c m_n m_c\lambda_{nc}^{L}+2\sum_n\sum_a m_n m_a\lambda_{na}^{L}+2\sum_{n<n'}\sum m_n m_{n'}\lambda_{nn'}^{L}+\sum_n m_n^2\lambda_{nn}^{L}\Bigg]$$

This expression may be used directly to calculate the relative enthalpy contribution, and may further be used as an alternative calculation to check the consistency of the calculations of the partial molar enthalpies if the total enthalpy is calculated via two routes:

$$\tilde{H} = \sum_i X_i \bar{H}_i \quad \text{and} \quad \tilde{H} = \tilde{H}^o + \tilde{L} \tag{181}$$

7.1.4 Relative Enthalpy for a Binary Electrolyte

We may use the definition of L directly in Eqn. (173) to obtain the relative enthalpy of a binary electrolyte solution. For the single electrolyte case, G_{ex} is given by Eqn. (94). We will make the following definition for the enthalpy Debye-Hückel coefficient, A_L:

$$A_L = 4RT^2 \frac{d\left(\frac{A}{3}\right)}{dT} = 4RT^2 \frac{d\left(A_\phi\right)}{dT} = \left(-6RT\ A_\phi\right)\left(1 + T\frac{d\ln\varepsilon}{dT} + T\frac{\alpha_o}{3}\right) \tag{182}$$

where $\alpha_o = d\ln V / dT$ is the coefficient of thermal expansion of water. Then,

$$\frac{G_{ex,\Delta}}{\tilde{M}_o n_o RT} = -\left(\frac{4AI}{3b}\right)\ln\left(1 + b\sqrt{I}\right) + 2m_M m_X B_{MX} + m_M m_X \left(ZC_{MX}\right),$$

and

$$n\tilde{L} = \left(\frac{A_L \tilde{M}_o n_o I}{b}\right)\ln\left(1 + b\sqrt{I}\right) - 2\tilde{M}_o n_o RT^2 m_M m_X B^L_{MX} - \tilde{M}_o n_o RT^2 m_M m_X \left(ZC^L_{MX}\right) \tag{183}$$

where

$$B^L_{MX} = \frac{dB_{MX}}{dT} \quad \text{and} \quad C^L_{MX} = \frac{dC_{MX}}{dT}$$

An expression for the apparent relative molal enthalpy, ${}^\phi L$, Eqn. (169), may be obtained using the relation, $2I = \nu m z_M z_X$:

$${}^\phi L = \left(\frac{\nu z_m \left|z_X\right| A_L}{2b}\right)\ln\left(1 + b\sqrt{I}\right) - 2RT^2 \frac{m_M m_X}{m} B^L_{MX} - RT^2 \frac{m_M m_X}{m}\left(ZC^L_{MX}\right) \tag{184}$$

This last equation agrees with Pitzer, Eqn. (81), p. 95, ref [18], after using $Z = \sum m_i \left|z_i\right|$ and after substitution into Eqn. (184) to yield Eqn. (185).

$${}^\phi L = \left(\frac{\nu_{MX} z_m \left|z_X\right| A_L}{2b}\right)\ln\left(1 + b\sqrt{I}\right) - 2\nu_M \nu_X \left(RT^2\right)\left(mB^L_{MX} + m^2 \nu_M \left|z_M\right| C^L_{MX}\right) \tag{185}$$

${}^\phi L$ is directly related to the concentration effects of the heat of solution of a salt. ${}^\phi L$ decreases to zero as the salt concentration decreases to zero.

Table 5 Excess Enthalpy for the NaCl system at a fixed 6.146 molality

Temperature	**Pressure**	**A_L/RT**	**ΔH°**	**ΔH_s**	**$^{\phi}L$**
(Kelvin)	bar	sqrt(kg/gmol)	(kJ/gmolSalt)	(kJ/gmolSalt)	(kJ/gmolSalt)
273.15	1.01325	0.553549	7.43878	2.95801	-4.48077
298.15	1.01325	0.80117	3.84389	2.07339	-1.77051
323.15	1.01325	1.0806	0.789801	1.5597	0.769897
348.15	1.01325	1.39756	-2.05146	1.1928	3.24426
373.15	1.01418	1.76347	-5.00826	0.77393	5.78219
398.15	2.32238	2.19377	-8.41039	0.129084	8.53947
423.15	4.76165	2.71154	-12.5861	-0.868498	11.7176
448.15	8.92602	3.35214	-17.8642	-2.2714	15.5928
473.15	15.5493	4.17423	-24.5734	-3.99291	20.5805
498.15	25.4972	5.28282	-33.0422	-5.6694	27.3728
523.15	39.7617	6.88318	-43.599	-6.33484	37.2642
548.15	59.4639	9.42389	-56.5718	-3.55165	53.0202
573.15	85.879	14.0453	-72.2884	9.33798	81.6264
598.15	120.51	24.3899	-91.0764	54.3933	145.47
623.15	165.294	57.1522	-113.263	234.925	348.189

7.1.5 Mixture Enthalpy Sample Problem

To check the implementation of the enthalpy functions within the `HMWSoln` object, the NaCl binary electrolyte problem was solved as a function of temperature, for a fixed molality of 6.146. Table 5 contains a sample of the results. The value of A_L is also presented in the table. It closely agrees with the results given in ref. [31].

A small program was written to directly calculate $^{\phi}L$ at 50°C and 200°C, and was then used to validate the results from `HMWSoln`'s implementation. The small program produced these values for a fixed molality of 6.146.

50°C (323.15 K): $^{\phi}L = 0.76990$ kJ / gmolSalt,

200°C (473.15 K): $^{\phi}L = 20.581$ kJ / gmolSalt

These numbers agree with the more elaborate calculation presented in the table.

The validity of Eqn. (185) was checked 2 ways in order to ensure internal consistency at 323.15 K.

The following values resulted from the first method: H_o – 269.556 kJ gmolSoln^{-1}, $L = 0.6979$ kJ gmolSoln^{-1}, $H = -269486$ kJ gmolSoln^{-1}.

The partial molar enthalpies were -284.104 kJ gmol^{-1}, -238.453 kJ gmol^{-1}, and -168.502 kJ gmol^{-1} for `H2O(L)`, `Na+`, and `Cl-`. Their mole fractions are 0.818703, 0.090648, and 0.090648. When summed up the molar solution enthalpy again produces $H = -269.486$ kJ gmolSoln^{-1}, passing the check for internal consistency.

An even more encompassing test for the calculation of excess enthalpy was carried out as a function of temperature and NaCl molality. The result of these code runs were compared to the extensive tabulations for the thermodynamic properties NaCl solution given by Pitzer et al. (1984), and Clarke and Glew (1985). Fig. 19 shows the excellent agreement obtained from the Cantera predictions and the tabulated excess enthalpies given by the above-mentioned authors. There is a slight deviation from the tabulated data at NaCl concentrations of 3 and 6 molal at T > 280°C but these are considered to be relatively small within the bounds of the overall standard error given by Clarke and Glew (1985) tabulations. Moreover, the Pitzer parameters used in this calculation have an upper limit of 250°C so any computed value beyond this temperature limit is an extrapolation. Still, these extrapolated values beyond this temperature are in very good agreement with the tabulated data.

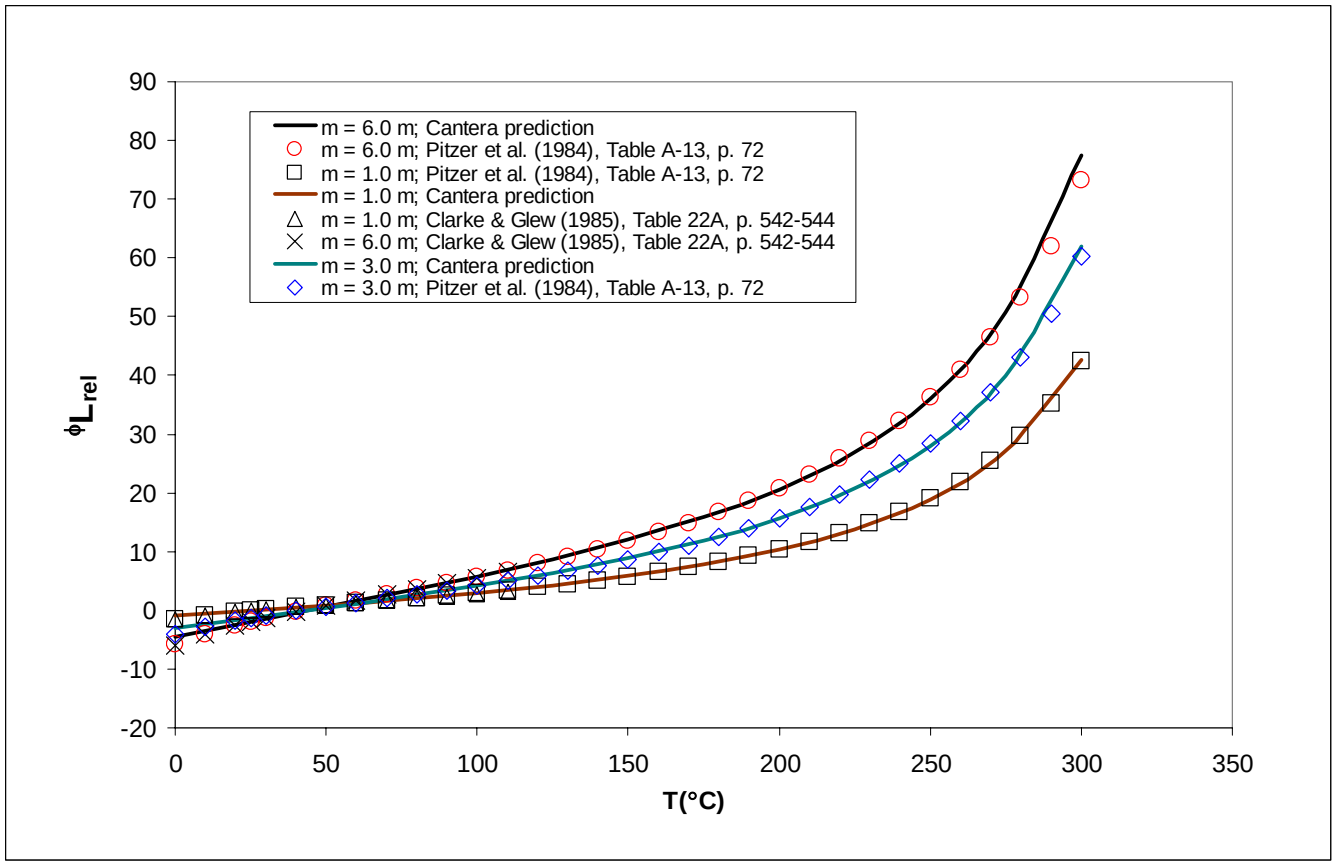

Fig. 19. Plot of excess Enthalpy as a function of temperature (along P_{sat}) and NaCl molality. Data from the tabulations of Pitzer et al.[68], and Clarke and Glew [69].

7.1.6 Expressions for the Mixture Heat Capacity

The total heat capacity at constant pressure is given by

$$\left(n\tilde{C}_p\right) = \left.\frac{d\left(n\tilde{H}\right)}{dT}\right|_p \tag{186}$$

The partial molar heat capacity for species *i* is given by the following equation:

$$\bar{C}_{p,i} = \left.\frac{d\bar{H}_i}{dT}\right|_p = C^{\triangle}_{p,i} + \frac{d}{dT}\left(-RT^2 \left.\frac{d\ln\gamma_i^{\triangle}}{dT}\right|_{p,m_k}\right) \tag{187}$$

Plugging the expression into Eqn. (172) results in

$$\bar{C}_{p,i} = C^{\triangle}_{p,i} - 2RT \left.\frac{d\ln\gamma_i^{\triangle}}{dT}\right|_{p,m_k} - 2RT^2 \left.\frac{d^2\ln\gamma_i^{\triangle}}{dT^2}\right|_{p,m_k} \tag{188}$$

The total relative heat capacity, $\tilde{J}$ an analog to the total relative enthalpy, is given by

$$\tilde{J} = \tilde{C}_p - \tilde{C}_p^o \tag{189}$$

And, it is related to the total relative enthalpy by

$$\tilde{J} = \left.\frac{d\tilde{L}}{dT}\right|_{p,m_k} \tag{190}$$

An apparent molal heat capacity, ${}^{\phi}C_p$, may also be defined in Eqn. (191).

$${}^{\phi}C_p = \frac{\left(n\tilde{J}\right)}{n_{salt}} \tag{191}$$

The derivations of the previous section mostly go through unchanged. The Debye-Hückel constant used for the expression for heat capacity is named A_J, and it is defined as

$$A_J = \frac{dA_L}{dT} \tag{192}$$

Also note that:

$$\frac{d}{dT}\left(\frac{A_L}{4RT^2}\right)=\frac{d^2A_\phi}{dT^2} \tag{193}$$

To evaluate the heat capacity by Eqn. (188), the second derivative in the activity coefficient and osmotic coefficients with respect to temperature must be evaluated. The general expression for this is given below. Second derivatives with respect to temperature for the Pitzer parameters are denoted by a superscript *LL*.

$$\begin{aligned}\frac{d^2\ln\left(\gamma_M^{\triangle}\right)}{dT^2}&=z_M^2\left(\frac{d^2F}{dT^2}\right)+\sum_a m_a\left(2B_{Ma}^{LL}+ZC_{Ma}^{LL}\right)+z_M\left(\sum_c\sum_a m_c m_a C_{Ma}^{LL}\right)\\&+\sum_c m_c\left[2\Phi_{Mc}^{LL}+\sum_a m_a\psi_{Mca}^{LL}\right]+\sum_{a<a'}\sum m_a m_{a'}\psi_{Maa'}^{LL}+2\sum_n m_n\lambda_{nM}^{LL}\end{aligned} \tag{194}$$

$$\begin{aligned}\frac{d^2\ln\left(\gamma_X^{\triangle}\right)}{dT^2}&=z_X^2\left(\frac{d^2F}{dT^2}\right)+\sum_c m_c\left(2B_{cX}^{LL}+ZC_{cX}^{LL}\right)+\left|z_X\right|\left(\sum_a\sum_c m_a m_c C_{ca}^{LL}\right)\\&+\sum_a m_a\left[2\Phi_{Xa}^{LL}+\sum_c m_c\psi_{cXa}^{LL}\right]+\sum_{c<c'}\sum m_c m_{c'}\psi_{cc'X}^{LL}+2\sum_n m_n\lambda_{nX}^{LL}\end{aligned} \tag{195}$$

$$\begin{aligned}\frac{d^2\phi}{dT^2}&=\frac{2}{\sum_i m_i}\left[-\left(\frac{d^2A_\phi}{dT^2}\right)\frac{I^{3/2}}{1+b\sqrt{I}}+\sum_c\sum_a m_c m_a\left(B_{ca}^{\phi LL}+ZC_{ca}^{\phi LL}\right)\right.\\&+\sum_{c<c'}\sum m_c m_{c'}\left[\Phi_{cc'}^{\phi LL}+\sum_a m_a\psi_{cc'a}^{LL}\right]+\sum_{a<a'}\sum m_a m_{a'}\left[\Phi_{aa'}^{\phi LL}+\sum_c m_c\psi_{aa'c}^{LL}\right]\\&\left.+\sum_n\sum_c m_n m_c\lambda_{nc}^{LL}+\sum_n\sum_a m_n m_a\lambda_{na}^{LL}+\sum_{n<n'}\sum m_n m_{n'}\lambda_{nn'}^{LL}+\frac{1}{2}\left(\sum_n m_n^2\lambda_{nn}^{LL}\right)\right]\end{aligned} \tag{196}$$

where

$$\begin{aligned}\frac{d^2F}{dT^2}&=-\frac{d^2A_\phi}{dT^2}\left[\frac{\sqrt{I}}{1+b\sqrt{I}}+\frac{2}{b}\ln\left(1+b\sqrt{I}\right)\right]+\sum_a\sum_c m_c m_a\left(\frac{\beta_{ca}^{(1)LL}h\left(\alpha\sqrt{I}\right)}{I}\right)\\&+\sum_{c<c'}\sum m_c m_{c'}\left(\Phi_{cc'}^{'LL}\right)+\sum_{a<a'}\sum m_a m_{a'}\left(\Phi_{aa'}^{'LL}\right)\end{aligned} \tag{197}$$

7.1.7 Excess Heat Capacity for a Binary Electrolyte

Starting from the expression for $\tilde{L}$ for a binary electrolyte, Eqn. (183), and then taking another temperature derivative, the following expression may be derived for the apparent molal heat capacity for a

binary electrolyte:

$$^{\phi}J = \left(\frac{\nu z_M \left| z_X \right| A_J}{2b} \right) \ln\left(1 + b\sqrt{I}\right) - 2\nu_M \nu_X RT^2 \left(mB_{MX}^J + m^2 \nu_M \left| z_m \right| C_{MX}^J \right) , \quad (198)$$

where

$$B_{MX}^J = \frac{d^2 B_{MX}}{dT^2} + \frac{2}{T}\frac{dB_{MX}}{dT} = B_{MX}^{LL} + \frac{2}{T} B_{MX}^L \quad (199)$$

$$B_{MX}^J = \frac{d^2 B_{MX}}{dT^2} + \frac{2}{T}\frac{dB_{MX}}{dT} = B_{MX}^{LL} + \frac{2}{T} B_{MX}^L \quad (200)$$

$$C_{MX}^J = \frac{d^2 C_{MX}}{dT^2} + \frac{2}{T}\frac{dC_{MX}}{dT} = C_{MX}^{LL} + \frac{2}{T} C_{MX}^L \quad (201)$$

Table 6 Mixture Heat Capacities Evaluated for the NaCl-H_2O System at a fixed 6.146 NaCl Molality

Temperature	**Pressure**	**A_J/(RT)**	**ΔCp°**	**ΔCp_s**	**J**	**$^{\phi}J$**
Kelvin	bar	sqrt(kg/gmol)	kJ/gmolSal	kJ/gmolSalt	kJ/gmolSoln	kJ/gmolSalt
273.15	1.01325	4.08571	-0.158977	-0.0364738	0.0111047	0.122503
298.15	1.01325	4.61251	-0.130795	-0.0199542	0.0100476	0.110841
323.15	1.01325	5.50274	-0.115719	-0.0105879	0.00952996	0.105131
348.15	1.01325	6.72519	-0.113771	-0.00869599	0.00952492	0.105075
373.15	1.01418	8.35345	-0.124962	-0.0135842	0.0100962	0.111378
398.15	2.32238	10.5422	-0.14929	-0.0237735	0.0113779	0.125517
423.15	4.76165	13.5794	-0.186752	-0.0365059	0.0136196	0.150246
448.15	8.92602	17.9948	-0.237338	-0.0467077	0.0172803	0.19063
473.15	15.5493	24.8263	-0.301036	-0.0444412	0.0232599	0.256595
498.15	25.4972	36.2771	-0.377833	-0.00862773	0.0334679	0.369205
523.15	39.7617	57.5281	-0.467713	0.110286	0.0523947	0.578
548.15	59.4639	102.55	-0.570661	0.445904	0.09215	1.01657
573.15	85.879	217.096	-0.68666	1.43571	0.192389	2.12237
598.15	120.51	603.91	-0.815692	5.01831	0.528843	5.834
623.15	165.294	2810.91	-0.957741	25.9944	2.44317	26.9522

Table 6 contains the results for evaluating $^{\phi}J$ for the NaCl binary electrolyte problem. In that calculation, J was evaluated from $J = C_p - C_p^o$ and C_p was obtained from $C_p = \sum X_i C_{p,i}$. The table also contains calculated A_J values. In contrast to the previous results, there was a discrepancy with Pitzer values of A_J on the order of about 12%. My values were consistently higher. No resolution has yet been found.

A small program directly calculates $^{\phi}J$ from Eqn. (198) at two temperatures for a fixed molality of 6.146. The following results are obtained.

50°C (323.15 K): $^{\phi}J = 0.10513$ kJ / gmol Salt,

200°C (473.15 K): $^{\phi}J = 0.25659$ kJ / gmol Salt

The results from the small program agree with the more elaborate calculations presented in the table.

7.1.8 Expressions for the Excess Volume of Mixing

The change in volume due to mixing is also affected by the pressure derivatives of the Pitzer coef-

ficient for the activity coefficients as well as the pressure dependence of the Debye-Hückel constant. The partial molar volume of species *i* in solution is given by the following relation:

$$\bar{V}_i = \left.\frac{d\bar{G}_i}{dP}\right|_T = V_i^o + RT^2 \left.\frac{d\ln\gamma_i^{\triangle}}{dP}\right|_{T,m_k} \tag{202}$$

Also, the net excess volume due to mixing, $\tilde{V}_{ex,\triangle}$, is given by Eqn. (203).

$$\tilde{V}_{ex,\triangle} = \tilde{V} - \tilde{V}^o = \left.\frac{d\tilde{G}_{ex,\triangle}}{dP}\right|_{T,m_{k=0,N}} \quad \text{where } \tilde{V}^o = \sum_{i=0}^{N} X_i \tilde{V}_i^o \tag{203}$$

The apparent molal volume, ${}^{\phi}V$, can then be defined via Eqn. (204) as the excess volume per mole of added salt.

$${}^{\phi}V = \frac{n\tilde{V}_{ex,\triangle}}{n_{salt}} \tag{204}$$

The derivations of the previous sections having to do with the temperature derivative of the activity coefficient mostly go through unchanged for pressure derivatives. The Debye-Hückel constant used for the expression for the excess liquid volume is named A_V and is defined by Eqn. (205).

$$A_V = \left(-4RT\right)\left.\frac{dA_{\phi}}{dP}\right|_T = 2A_{\phi}RT\left(3\left.\frac{d\ln\varepsilon}{dP}\right|_T + \left.\frac{d\ln V_w}{dP}\right|_T\right) \tag{205}$$

The first derivative involves the dependence of the dielectric constant on pressure, which is nonzero, while the second derivative is the isothermal compressibility of water. To evaluate the excess volume, the first derivative of the activity coefficient and osmotic coefficients with respect to pressure must be evaluated. The general expression for this is given below. Derivatives with respect to pressure are denoted by a superscript *V*.

$$\begin{aligned}\frac{d\ln\left(\gamma_M^{\triangle}\right)}{dP} &= z_M^2\left(\frac{dF}{dP}\right) + \sum_a m_a\left(2B_{Ma}^V + ZC_{Ma}^V\right) + z_M\left(\sum_c\sum_a m_c m_a C_{Ma}^V\right) \\ &\quad + \sum_c m_c\left[2\Phi_{Mc}^V + \sum_a m_a\psi_{Mca}^V\right] + \sum_{a<a'}\sum m_a m_{a'}\psi_{Maa'}^V + 2\sum_n m_n\lambda_{nM}^V\end{aligned} \tag{206}$$

$$\begin{aligned}\frac{d\ln\left(\gamma_X^{\triangle}\right)}{dP} &= z_X^2\left(\frac{dF}{dP}\right) + \sum_c m_c\left(2B_{cX}^V + ZC_{cX}^V\right) + \left|z_X\right|\left(\sum_a\sum_c m_a m_c C_{ca}^V\right) \\ &\quad + \sum_a m_a\left[2\Phi_{Xa}^V + \sum_c m_c\psi_{cXa}^V\right] + \sum_{c<c'}\sum m_c m_{c'}\psi_{cc'X}^V + 2\sum_n m_n\lambda_{nX}^V\end{aligned} \tag{207}$$

$$\frac{d\phi}{dP} = \frac{2}{\sum_{k\neq o} m_k}\left[\left(\frac{A_V}{4RT^2}\right)\left(\frac{I^{3/2}}{1+b\sqrt{I}}\right) + \sum_c\sum_a m_c m_a\left(B_{ca}^{\phi V} + ZC_{ca}^V\right)\right.$$
$$+\sum_{c<c'}\sum m_c m_{c'}\left[\Phi_{cc'}^{\phi V} + \sum_a m_a \psi_{cc'a}^V\right] + \sum_{a<a'}\sum m_a m_{a'}\left[\Phi_{aa'}^{\phi V} + \sum_c m_c \psi_{aa'c}^V\right] \qquad (208)$$
$$\left.+\sum_n\sum_c m_n m_c \lambda_{nc}^V + \sum_n\sum_a m_n m_a \lambda_{na}^V + \sum_{n<n'}\sum m_n m_{n'}\lambda_{nn'}^V + \frac{1}{2}\left(\sum_n m_n^2 \lambda_{nn}^V\right)\right]$$

where

$$\frac{dF}{dP} = \frac{A_V}{4RT^2}\left[\frac{\sqrt{I}}{1+b\sqrt{I}} + \frac{2}{b}\ln\left(1+b\sqrt{I}\right)\right] + \sum_a\sum_c m_c m_a\left(\frac{\beta_{ca}^{(1)V} h\left(\alpha\sqrt{I}\right)}{I}\right)$$
$$+\sum_{c<c'}\sum m_c m_{c'}\left(\Phi_{cc'}^{'V}\right) + \sum_{a<a'}\sum m_a m_{a'}\left(\Phi_{aa'}^{'V}\right)$$

7.1.9 Excess Volume of Mixing for a Binary Electrolyte

Eqn. (209) may be derived for the apparent molal volume for a binary electrolyte by starting with Eqn. (94) and then using Eqn. (203) and Eqn. (204). Eqn.'s (99) and Eqn. (95) are also needed.

$${}^{\phi}V = \left(\frac{\nu z_M |z_X| A_V}{2b}\right)\ln\left(1+b\sqrt{I}\right) + 2\nu_M\nu_X RT\left(mB_{MX}^V + m^2\nu_M |z_m| C_{MX}^V\right) \qquad (209)$$

where

$$B_{MX}^V = \frac{dB_{MX}}{dP} \text{ and } C_{MX}^V = \frac{dC_{MX}}{dP}$$

Under the current implementation, $B_{MX}^V = C_{MX}^V = 0$. Therefore, the only pressure dependence exhibited by the excess volume of mixing is due to the pressure dependence of the dielectric constant and the water density. Pitzer has gone on to add the pressure dependence into the Pitzer parameters for the NaCl system in a later series of papers [40, 41]. We have not implemented the pressure parameterizations for B_{MX} and C_{MX} used in those papers at this time. It should be noted, however, that some Pitzer parameters have been retrieved for several electrolytes at 25°C (see the work of Monnin [88] and references therein) to calculate partial molal volume of solutes at elevated concentrations. Moreover, the work of Monnin [89] extended this approach to evaluate the effect of pressure on the activity coefficients of a mixed solute system at temperatures up to 200°C and a pressure of one kilobar. Implementation of these pressure-dependent parameters is left as a topic of future work.

Table 7 Excess Volume Properties for NaCl Solutions at a fixed molality of 6.146 as a function of Temperature

T (Kelvin)	Pres (bar)	A_V $cm^3kg^{1/2}gmol^{-3/2}$	V_{ex} m^3/gmolSoln	$^{\phi}V$ cm^3/gmol Salt	MolarV kg/gmolSoln	MolarV0 kg/gmolSoln
273.15	1.01325	1.50618	0.157014	1.73212	16.4205	16.2635
298.15	1.01325	1.87445	0.195404	2.15563	16.5003	16.3049
323.15	1.01325	2.37356	0.247435	2.72961	16.6872	16.4398
348.15	1.01325	3.06967	0.320001	3.53014	16.9618	16.6418
373.15	1.01418	4.05119	0.422321	4.65889	17.3245	16.9022
398.15	2.32238	5.4505	0.568194	6.26811	17.7871	17.2189
423.15	4.76165	7.48	0.779762	8.60205	18.3758	17.596
448.15	8.92602	10.4881	1.09335	12.0614	19.1351	18.0417
473.15	15.5493	15.0766	1.57168	17.3382	20.1415	18.5698
498.15	25.4972	22.3411	2.32898	25.6925	21.5312	19.2022
523.15	39.7617	34.437	3.58993	39.6028	23.5639	19.974
548.15	59.4639	56.041	5.84206	64.4475	26.7863	20.9443
573.15	85.879	98.8083	10.3004	113.63	32.5236	22.2232
598.15	120.51	198.394	20.6818	228.155	44.7348	24.053
623.15	165.294	494.718	51.5725	568.929	78.7484	27.1758

Table 7 presents $^{\phi}V$ calculations for the binary NaCl system as a function of temperature. In these calculations, the standard state volume for both Na^+ and Cl^- was set equal to one half the standard state volume at 25°C for NaCl(aq) quoted in ref. [41], 17.49 cm^3 $gmol^{-1}$. No attempt was made to adjust for the large temperature and pressure dependence of V^{o}_{Na+} and/or V^{o}_{Cl-}. A_V is also printed out in Table 6. It agrees well with the values presented in pg. 99, ref [18]. A small program directly calculates $^{\phi}V$ from Eqn. (209) at two temperatures for a fixed molality of 6.146. The following results are obtained.

50°C (323.15 K): $^{\phi}V = 2.7296$ cm^3 / gmolSalt,

200°C (473.15 K): $^{\phi}V = 17.3382$ cm^3 / gmolSalt

These values from the small program agree with the more elaborate calculations presented in Table 6.

7.2 Analysis of a 2-2 Electrolyte

Predicted values of osmotic coefficients by Cantera for a $MgSO_4$(aq) 2-2 electrolyte were compared to those reported by Rard and Miller [73], Holmes and Mesmer [74], and Archer and Rard [75]. Selected results from the Cantera code runs at 298 K are listed in Table 8. The comparisons between code predictions and literature values are depicted in Fig. 20 and they indicate good agreement with experimental data and values from other models. The values reported by Archer and Rard [75] are the result of a variant of the Pitzer model that modifies the binary parameter C_{MX}^{ϕ} to have an ionic strength dependency and therefore is not consistent with the standard Pitzer formalism. The model presented by these authors is parameterized by a comprehensive evaluation of existing thermodynamic data for $MgSO_4$(aq) plus isopiestic measurements at 298 K conducted in that study.

Table 8 Selected Properties of $MgSO_4$(aq) at 298 K computed using Cantera.

Ionic Strength (m)	Activity of Water	Osmotic Coefficient
0	1.0	1.0
0.0010203	0.999967	0.893758
0.0255076	0.999375	0.679756
0.10203	0.997812	0.595962
0.539741	0.989789	0.527751
1.04479	0.980095	0.534094
2.06612	0.950818	0.677467
2.55076	0.929929	0.79046
3.08642	0.900617	0.941276
3.55168	0.869646	1.09143
4.04959	0.830883	1.26974

The source of Pitzer parameters adopted in Cantera for these code runs are retrieved from the model presented by Pabalan and Pitzer [77]. These authors retrieved Pitzer parameter mainly by evaluating excess Gibbs energy of aqueous electrolytes and experimental solubility data for solids. The Cantera predictions are compared to the ion-interaction model results listed in Table VI of Rard and Miller [73], Table 3 of Holmes and Mesmer [74], and Table 7 of Archer and Rard [75]. The agreement of these results as depicted in Fig. 20 is very good considering that we are comparing different sets of data and also different models. There is a slight deviation with the reported values of Holmes and Mesmer [74], particularly within the $MgSO_4$(aq) molal concentration between 0.5 to 1.5 molal and above ~2.5 molal. Somewhat similar deviations where found by Archer and Rard [75] between their

model and some osmotic coefficient data from Holmes and Mesmer [74]. Overall, the resulting good correspondence can be extended to reported measurements and model results of up to 5 molal $MgSO_4$(aq) and temperatures of up to 423.15 K.

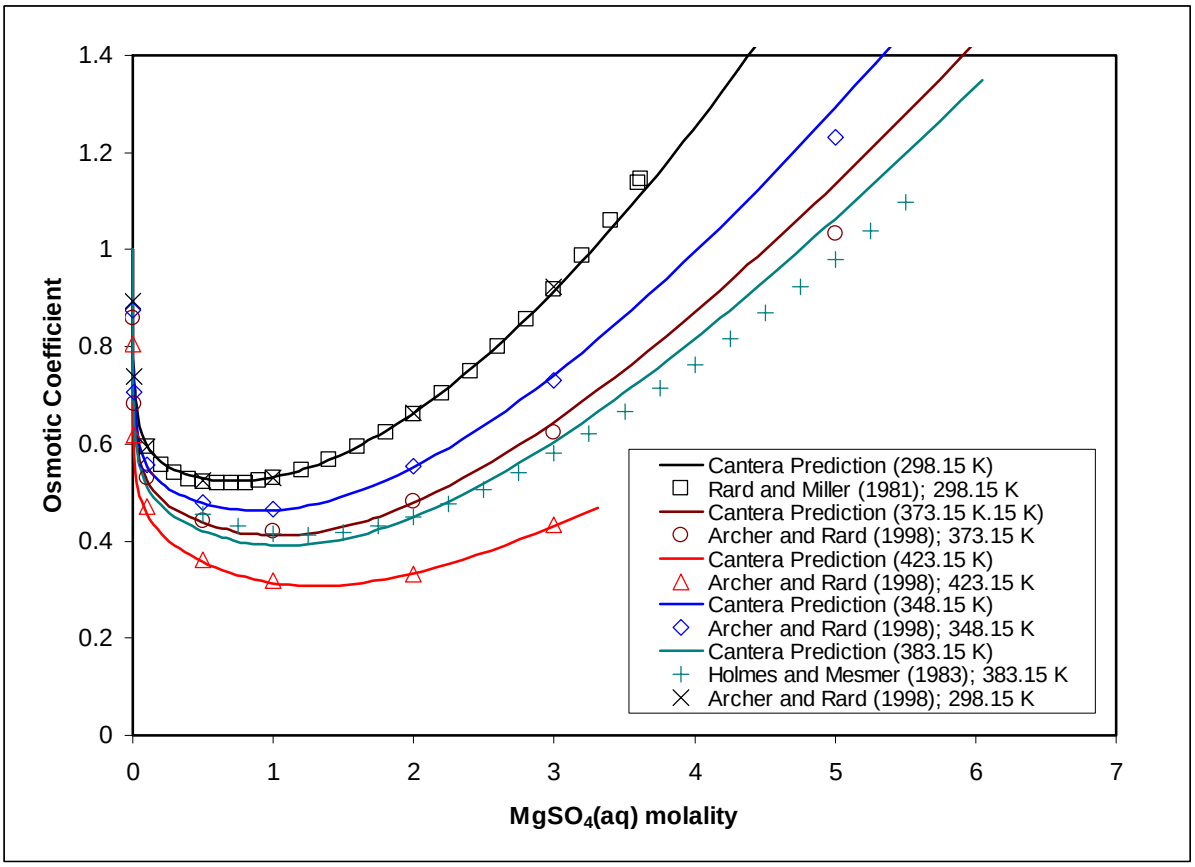

Fig. 20. Plot of osmotic coefficient versus $MgSO_4$(aq) molality for various temperatures. Solid lines are the Cantera predictions whereas symbols represent data from either experiments or models given in the literature..

7.3 Analysis of a 2-1 Electrolyte

All the examples presented so far are for symmetrical electrolytes of the type 1-1 or 2-2. The following example is for the 2-1 electrolyte Na_2SO_4(aq). We compare the Cantera code predictions to the work of Rard et al. [76] which is a comprehensive evaluation of thermodynamic data for Na_2SO_4(aq) and provides a robust model to represent the thermodynamic properties of this electrolyte as a function of temperature. Selected results from the Cantera code runs at 298 K are listed in Table 9.

Table 9 Selected Properties of Na_2SO_4(aq) at 298 K Computed Using Cantera.

Ionic Strength (m)	Activity of Water	Osmotic Coefficient
0	1.0	1.0
0.0010203	0.999947	0.960757
0.0255076	0.998816	0.859637
0.10203	0.995644	0.791635
0.539741	0.980329	0.681046
1.04479	0.964955	0.631762
2.06612	0.933271	0.618453
2.55076	0.916149	0.635267
3.08642	0.894861	0.665953

Fig. 21 depicts the behavior of this salt as a function salt concentration at 298 K and 373.15 K. The Pitzer parameters adopted for the Cantera code runs are based on the work by Greenberg and Møller [72].

Similar to the comparison presented in Section 7.2, there is a very good agreement between the osmotic coefficient values predicted by Cantera and those given by the extended Pitzer model reported in Rard et al. [76]. Again, this comparison not only indicates the consistency with more recent critical evaluations and their associated models but also the validity of Pitzer parameters obtained from earlier studies.

7.4 Analysis of the Calcite Equilibria

Carbonate equilibria in natural systems is inherently important to carbon mass fluxes that are to a large extent controlled by biogeochemical cycles. In particular, calcite ($CaCO_3$) formation plays an important role on natural processes as well as in others of industrial interest where, for example, scale formation in geothermal wells can be deleterious to the efficiency of geothermal energy exploitation (Møller et al. [85]). Also, a better understanding of CO_2 solubility in brines is needed in the accurate modeling and application of subsurface carbon sequestration in geological formations (Kervévan et al. [86]). This example involves the prediction of calcite solubility as a function of NaCl concentration at 298 K at a given P_{CO2}. Calcite equilibrium is sensitive to P_{CO2}, temperature, and ionic strength so this problem is a good test of multiphase-multicomponent equilibria in the system Ca-CO_3-CO_2-Na-Cl-H_2O. The experimental data used in this comparison is from Wolf et al. [87] where calcite solubility experiments were conducted at three different temperatures (10, 25, and 60 °C) at a P_{CO2} of ~1 kPa.

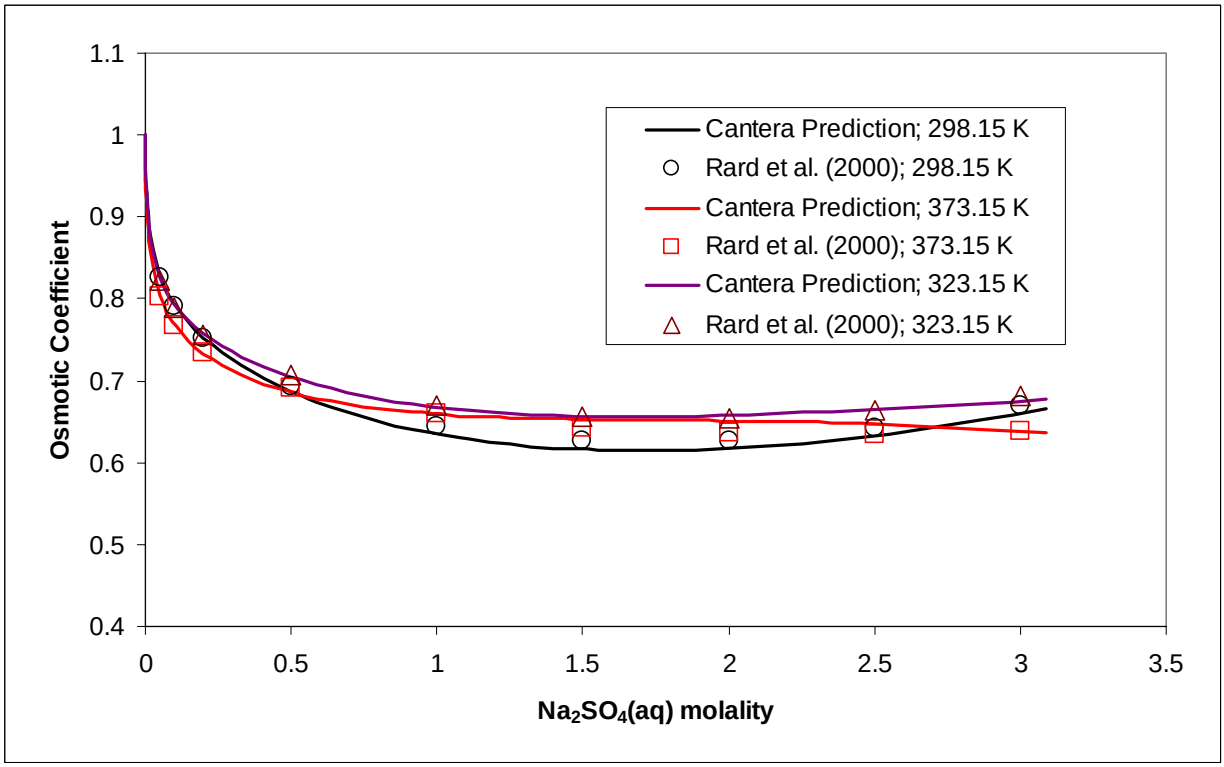

Fig. 21. Plot of osmotic coefficient versus Na_2SO_4(aq) molality for 298 K and 373.15 K. Solid lines are the Cantera predictions whereas symbols represent data reported by Rard et al. [76].

The YMP Pitzer database developed in [43] is used in these simulations. The gas mole fractions between N_2(g) and CO_2(g) were set in the code to be consistent with the P_{CO2} reported in Wolf et al. [87] experiments. The mole fractions of N_2(g) and CO_2(g) used in these runs are 0.99 and 0.0091, respectively, assuming a total pressure of 101325 Pa or one atm. The selected experimental data at 298 K were obtained at a P_{CO2} of ~0.92 kPa according to Table I of Wolf et al. [87]. The results shown in Fig. 22 indicate a very good agreement with the experimental data from the dilute concentration range up to 6 molal NaCl. The thermodynamic data for calcite used in this example is from the YMP Pitzer thermodynamic database. These data is to a large extent consistent with recent calcite solubility data and, the Pitzer parameters and aqueous species therein for a wide range of temperatures. The log K values calculated from the calcite solubility reaction (i.e., $CaCO_3 + H^+ = Ca^{++} + HCO_3^-$) at 298 K using thermodynamic data consistent with SPEQ06 or the YMP Pitzer databases would yield almost identical values at this temperature. The only observable differences in log K values from the two databases would be at temperatures above 100°C. The activity coefficients calculated by Cantera for Ca^{++} and CO_3^{--} are in excellent agreement with those reported in Table IV of Wolf et al. [87]. The only significant discrepancy in the computed activity coefficient values is for Ca^{++} at 6.14 molal NaCl. The difference exceeds about 20% and the reason for such discrepancy, which is restricted to the maximum ionic strength of the experiments, cannot be resolved at this point. However, it was noted in

a sensitivity analysis of Pitzer parameter for $CaCl_2$ that data this 2-1 binary could play an important role in the computation of activity coefficients of Ca^{++} at 298 K. It should also be noted that the Pitzer parameter data adopted by Wolf et al. [87] for $CaCl_2$ and carbonate species are from different sources compared to those in the YMP Pitzer thermodynamic database, so minor discrepancies should be expected. Overall, the agreement between solubility and activity coefficient predictions can be considered excellent within the uncertainties in the experimental data and the different sources of Pitzer parameter data used in this test relative to those adopted in the source [87].

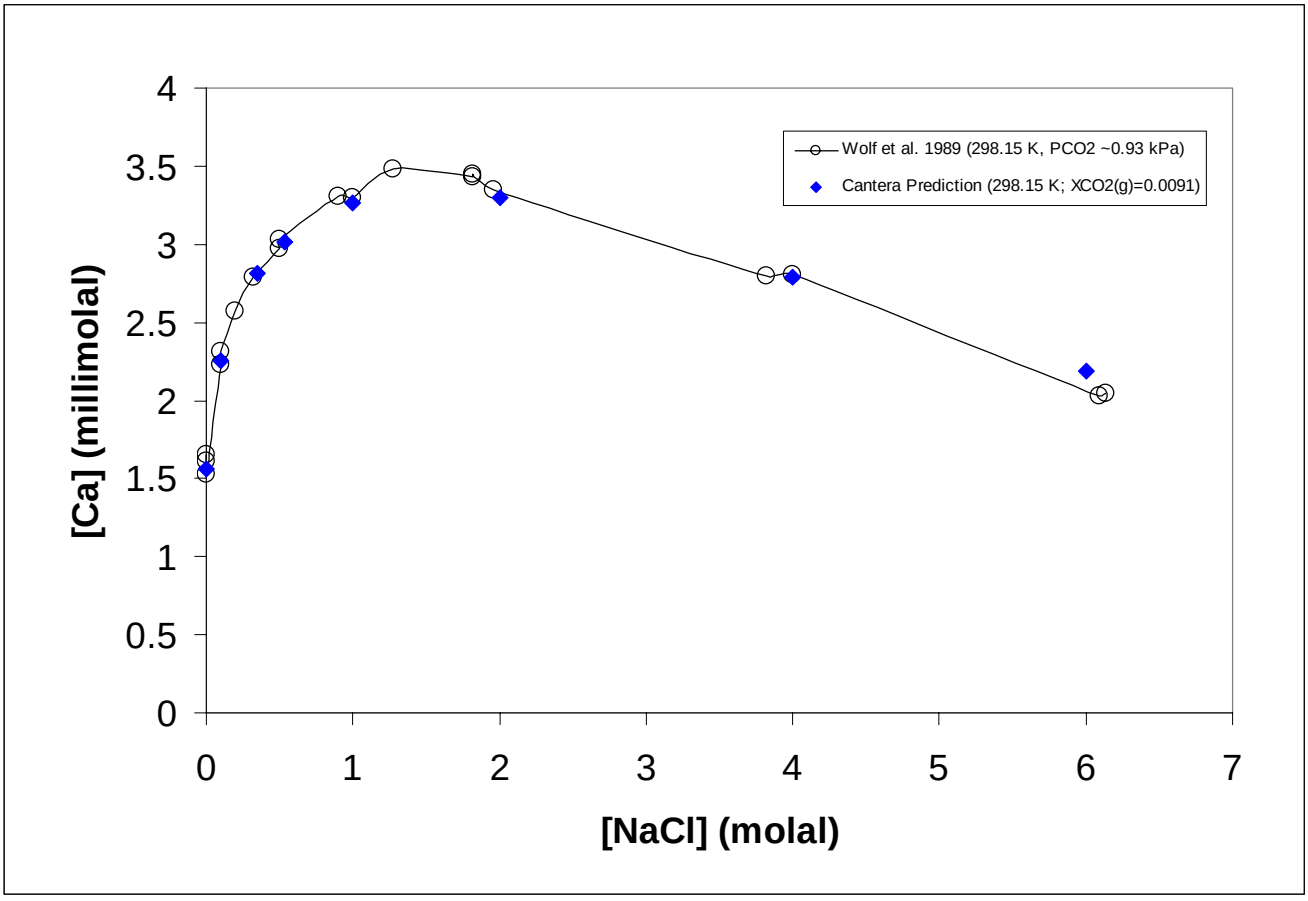

Fig. 22. Plot of calcite ($CaCO_3$) solubility as a function of NaCl concentration at 298 K and P_{CO2} fixed at 0.92 kPa or at the equivalent X_{CO2} of 0.0091. The solid line connecting the data points of Wolf et al. [87] is just a guide for the eye.

7.5 Verification of the HKFT Standard State

Agreement of Cantera's calculation of ΔG_f^o, the Gibbs free energy of formation reaction for ions and aqueous species with respect to the SUPCRT92 formulation is displayed in Fig. 23 (a) to (d). The formulas are from Eqn. (39) and Eqn. (29). The Gibbs free energies of formation reactions for these reactions are listed below.

$$\mathrm{Na(s)} + \mathrm{H^+} \rightarrow \mathrm{Na^+} + \frac{1}{2}\mathrm{H_2}(g) \tag{210}$$

$$\frac{1}{2}\mathrm{Cl_2(g)} + \frac{1}{2}\mathrm{H_2}(g) \rightarrow \mathrm{Cl^-} + \mathrm{H^+}$$

$$4\mathrm{C(s)} + 5\frac{1}{2}\mathrm{H_2}(g) + \frac{1}{2}\mathrm{N_2}(g) \rightarrow \mathrm{C_4H_9NH_2(aq)}$$

$$4\mathrm{C(s)} + 5\mathrm{H_2}(g) + \frac{1}{2}\mathrm{O_2}(g) \rightarrow \mathrm{C_4H_9OH(aq)}$$

Eqn. (29) must be used to evaluate the Gibbs free energy of formation reported in Fig. 23 (a) to (d). Cantera's element database has been modified to include the entropy at 298 K and 1 bar for each element in its standard state. That allows for the easy conversion between $\Delta\bar{G}^{\triangle}_{f,j}\left(T_r, P_r\right)$ and $\tilde{G}^{\triangle}_{j}\left(T_r, P_r\right)$ within the code. The following entropies are used within Fig. 23 (a) to (d).

$$\frac{1}{2}S^{o}_{H_2(g)}\left(T_r, P_r\right) = 65.34 \text{ J gmol}^{-1}\text{ K}^{-1} \qquad S^{o}_{Na(s)}\left(T_r, P_r\right) = 51.455 \text{ J gmol}^{-1}\text{ K}^{-1}$$

$$\frac{1}{2}S^{o}_{Cl_2(g)}\left(T_r, P_r\right) = 111.535 \text{ J gmol}^{-1}\text{ K}^{-1} \qquad \frac{1}{2}S^{o}_{N_2(g)}\left(T_r, P_r\right) = 95.8045 \text{ J gmol}^{-1}\text{ K}^{-1}$$

$$S^{o}_{C(s)}\left(T_r, P_r\right) = 5.74 \text{ J gmol}^{-1}\text{ K}^{-1} \qquad \frac{1}{2}S^{o}_{O_2(g)}\left(T_r, P_r\right) = 102.573 \text{ J gmol}^{-1}\text{ K}^{-1}$$

a)

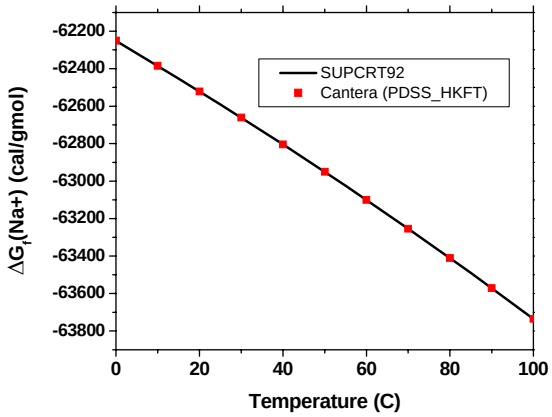

b)

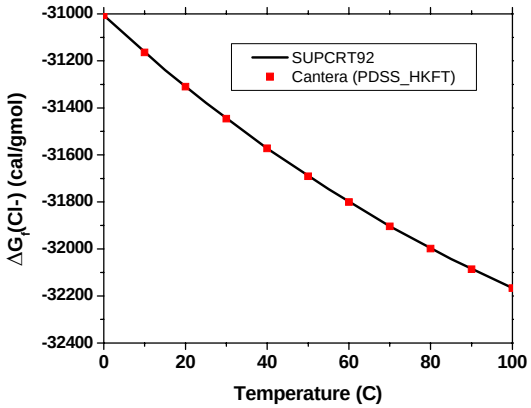

c)

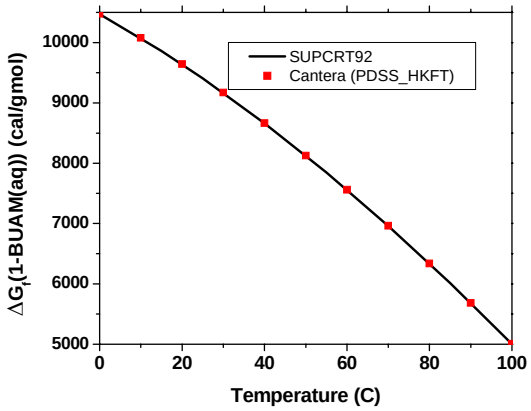

d)

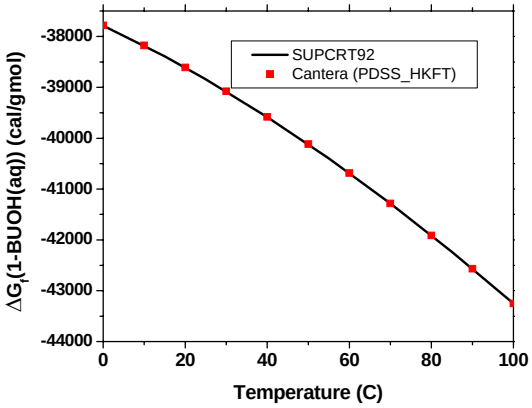

Fig. 23. Agreement of ΔG_f^o for various ions and aqueous species between Cantera and other formulations.

7.6 Multicomponent Salt System – an Example

The NaCl-KCl system has been studied extensively [71, 72, 79, 80, 81, 82]. We present detailed comparisons of Cantera's results on this system at 100°C compared with both EQ3NR code results and experimental data to validate Cantera's implementation of the multicomponent Pitzer equations. In these comparisons, "EQ3/Pitzer" in Tables Table 10 and Table 11 refers to EQ3NR code runs with

data from the YMP Pitzer database developed in [43]. Eqn. (211) provides the two solution reactions within the system. The solubility of the two salts is mainly driven by the standard state values of Gibbs free energies of solution of these reactions, ΔG_r°.

$$\mathrm{KCl(s)} \rightarrow \mathrm{K^+ + Cl^-} \qquad \Delta G_r^o = \mu^{\triangle}\left(\mathrm{K^+}\right) + \mu^{\triangle}\left(\mathrm{Cl^-}\right) - \mu^o\left(\mathrm{KCl(s)}\right) \qquad (211)$$

$$\mathrm{NaCl(s)} \rightarrow \mathrm{Na^+ + Cl^-} \qquad \Delta G_r^o = \mu^{\triangle}\left(\mathrm{Na^+}\right) + \mu^{\triangle}\left(\mathrm{Cl^-}\right) - \mu^o\left(\mathrm{NaCl(s)}\right)$$

The value of $\log_{10} K$ quoted in the table is from the following equation, Eqn. (212).

$$\log_{10} K = \frac{-\Delta G_r^o}{RT \ln 10} \qquad (212)$$

Table 10 Breakdown of the Calculation of the KCl Equilibrium Constant at the Stationary Point

(kJ gmol^{-1})	EQ3/Pitzer	Cantera/SPEQ06	Cantera/NIST
$\Delta H_{f,298}^{\triangle}\left(\mathrm{K^+}\right)$	-252.1359	-252.1359	-252.1359
$\mu^{\triangle}\left(\mathrm{K^+}, 25°C\right)$	-282.262	-282.2621	-282.2621
$\mu^{\triangle}\left(\mathrm{K^+}, 100°C\right)$	-289.9583	-289.9583	-289.9583
$\Delta H_{f,298}^{\triangle}\left(\mathrm{Cl^-}\right)$	-167.1095	-167.1095	-167.1095
$\mu^{\triangle}\left(\mathrm{Cl^-}, 25°C\right)$	-184.0250	-184.0250	-184.0250
$\mu^{\triangle}\left(\mathrm{Cl^-}, 100°C\right)$	-187.321	-187.321	-187.321
$\Delta H_{f,298}^{\circ}\left(\mathrm{KCl(s)}\right)$	NA	-436.8464	-436.6819
$\mu^{\circ}\left(\mathrm{KCl(s)}, 25°C\right)$	NA	-461.4588	-461.2969
$\mu^{\circ}\left(\mathrm{KCl(s)}, 100°C\right)$ (1)	-467.6936	-468.0997	-467.9404
$\Delta G_r^{\circ}\left(\mathrm{KCl}, 25°\mathrm{C}\right)$ (2)	-5.2216	-4.8283	-4.9902
$\log_{10} K\left(\mathrm{KCl}, 25°\mathrm{C}\right)$ (2)	0.9148	0.8459	0.8742
$\Delta G_r^{\circ}\left(\mathrm{KCl}, 100°\mathrm{C}\right)$ (2)	-9.5856	-9.1800	-9.3393
$\log_{10} K(\mathrm{KCl}, 100°C)$ (2)	1.3418	1.2850	1.3073

(1) Calculated from the EQ3NR computed ion activities for the equilibrium at the stationary point using thermodynamic from [43].

(2) Log K and ΔG_r° values calculated from the tabulated parameters for standard chemical potentials in Greenberg and Møller [72] and adopted in the YMP Pitzer database developed in [43].

The PDSS_HKFT pressure dependent standard state was used for the aqueous phase in this section. All data for aqueous phase species are consistent with the YMP Pitzer database developed in [43]. There is consistency in the thermodynamic data for the relevant aqueous species between the considered databases. However, there are some discrepancies with the thermodynamic data for the solids and the effects of this on the computed solubilities are discussed below.

We have used various sources for the solid salt, NaCl and KCl, phases to show the relative effects of variations in thermodynamic properties on the agreement with solubility data. Table 10 contains a breakdown of the calculation of $\Delta G_r^{\circ}(\mathrm{KCl})$ from the various sources of data. The stationary or invariant point refers to the condition where the brine is coexistent with as many solid phases as is thermodynamically possible; in this case halite and sylvite. The $\log_{10} K(\mathrm{KCl},100^{\circ}\mathrm{C})$ value used in the EQ3NR code run is 1.3418. For EQ3NR, the thermodynamics of salts are actually specified in the form of $\log_{10} K$ values in a dabase file with respect to dissolution reactions with aqueous brine and not in terms of their Gibbs free energies of formation. For the specific purpose of matching experimental data on solubilities, this is a superior representation, as the $\log_{10} K$ values determine solubilities directly. However, it's not very general. The values for $\Delta G_r^{\circ}(\mathrm{KCl},\ 100°\mathrm{C})$, $\mu^{\circ}(\mathrm{KCl},100°\mathrm{C})$, and $\Delta H_{f,298}^{\circ}(\mathrm{KCl(s)})$ reported in Table 10 are backcalculated from the value of $\log_{10} K(\mathrm{KCl},100°\mathrm{C})$. The Cantera/NIST column is calculated assuming the NIST shomate polynomial formulation for the KCl(s) salt from NIST"s web page [24]. The Cantera/SPEQ06 column is calculated using the MineraEQ3 standard state assuming species data from the SPEQ06 database [67]. The differences in $\log_{10} K(\mathrm{KCl},100°\mathrm{C})$ create a demonstrable difference in the solubility of KCl in the mixed brine solution (see Fig. 24). Calculations indicate that the majority of the difference in the calculated saturation molality in a pure KCl solution between EQ3NR and Cantera lies in the calculated values for $\log_{10} K$. These differences stem from taking different sources of data that may not be entirely internal consistent, as input to Cantera. Of particular note is the disagreement between the EQ3/Pitzer column, which is expressed as log K values at a set of temperatures, and the Cantera/SPEQ06 column, which is calculated from the PDSS_HKFT standard state object, with inputs from the SPEQ06 thermodynamic database. It is clear that the EQ3NR calculations using the YMP Pitzer data fits the experimental data best. However, the SPEQ06 inputs are widely used. Resolution of the discrepancy lies in the need for refitting the SPEQ06 parameters used in the HKFT equation of state to the solubility data. Indeed, the $\log_{10} K$ values adopted in the YMP Pitzer database developed in [43] are consistent with the source of Pitzer parameters for the Na-Cl-KCl-H_2O system by Greenberg and Møller [72]. These authors fitted solubility data for various salt systems as a function of temperature using the Pitzer equations.

Table 11 Breakdown of the Calculation of the NaCl Equilibrium Constant at the Stationary Point

(kJ gmol^{-1})	EQ3/Pitzer	Cantera/SPEQ06	Cantera/ NIST
$\Delta H^{\triangle}_{f,298}\left(\mathrm{Na^+}\right)$	-240.3264	-240.3264	-240.3264
$\mu^{\triangle}\left(\mathrm{Na^+}, 25°C\right)$	-257.7409	-257.7409	-257.7409
$\mu^{\triangle}\left(\mathrm{Na^+}, 100°C\right)$	-262.5284	-262.5284	-262.5284
$\Delta H^{\triangle}_{f,298}\left(\mathrm{Cl^-}\right)$	-167.1095	-167.1095	-167.1095
$\mu^{\triangle}\left(\mathrm{Cl\text{-}}, 25°C\right)$	-184.0250	-184.0250	-184.0250
$\mu^{\triangle}\left(\mathrm{Cl^-}, 100°C\right)$	-187.321	-187.3214	-187.321
$\Delta H^{o}_{f,298}\left(\mathrm{NaCl(s)}\right)$	NA	-411.2097	-411.1207
$\mu^{o}\left(\mathrm{NaCl(s)}, 25°C\right)$	NA	-432.7159	-432.6201
$\mu^{o}\left(\mathrm{NaCl(s)}, 100°C\right)$ (1)	-438.5614	-438.5728	-438.4735
$\Delta G^{o}_{r}\left(\mathrm{NaCl}, 25°\mathrm{C}\right)$ (2)	-9.0511	-9.0500	-9.1458
$\log_{10} K\left(\mathrm{NaCl}, 25°\mathrm{C}\right)$ (2)	1.5857	1.5855	1.6023
$\Delta G^{o}_{r}\left(\mathrm{NaCl}, 100°\mathrm{C}\right)$ (2)	-11.2086	-11.1974	-11.2966
$\log_{10} K\left(\mathrm{NaCl}, 100°\mathrm{C}\right)$ (2)	1.5690	1.5674	1.5813

(1) Calculated from the EQ3NR computed ion activities for the equilibrium at the stationary point using thermodynamic from [43].

(2) Log K and ΔG^{o}_{r} values calculated from the tabulated parameters for the standard chemical potentials in Greenberg and Møller [72] and adopted in the YMP Pitzer database developed in [43].

Table 11 contains a breakdown of the calculation of $\Delta G^{o}_{r}\left(\mathrm{NaCl}\right)$ at the stationary point from the various sources of data considered in these code runs. The value of $\log_{10} K\left(\mathrm{NaCl}, 100°\mathrm{C}\right)$ used by EQ3NR is 1.5690, in much closer agreement with the SPEQ06 database. The NIST database is in surprisingly good agreement for NaCl as well.

In Fig. 24 we display the agreement between Cantera, EQ3NR, and various experimental data on the system from de Lima and Pizter (1983). The blue curve represents Cantera's calculations of the solubility curve when the SPEQ06 database is used for the NaCl(s) and KCl(s) phases, respectively. It's observed that there is a noticeable deviation from agreement with experiment due to the lack of agreement with the $\log_{10} K\left(\mathrm{KCl}, 100°\mathrm{C}\right)$ value, previously mentioned.

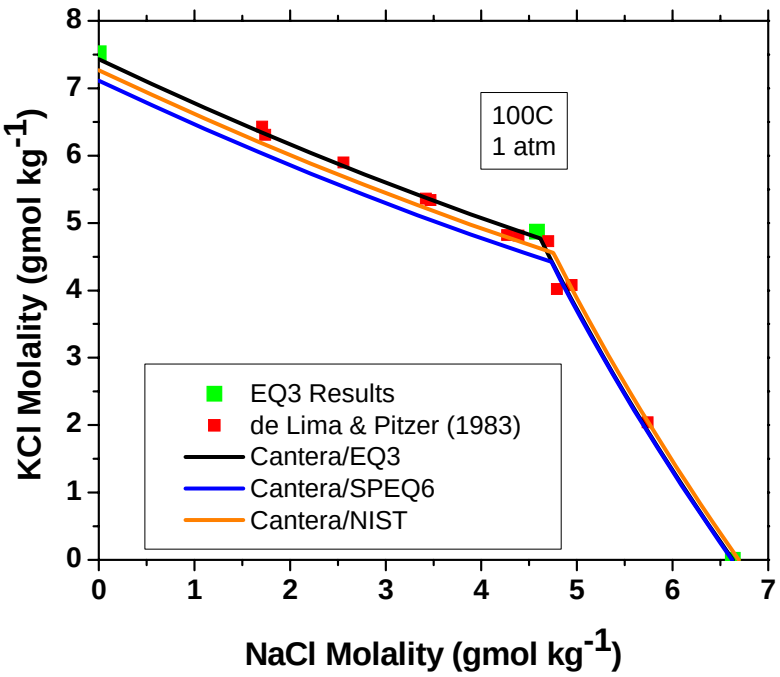

Fig. 24. Agreement between Cantera, EQ3NR, and various experimental data from de Lima and Pitzer (1983). The Cantera/EQ3 runs were conducted using log K values consistent with those in YMP Pitzer database developed in [43]. See text for explanation.

Pointwise comparisons were also made between EQ3NR outputs, Table 13, and Cantera outputs, Table 12. These results are the predicted equilibrium concentrations and single-ion activity coefficients at the stationary point in the system. In order to carry out the comparisons, we have matched the log K values for NaCl and KCl exactly before carrying out the calculation by adjusting the 298 K heats of formation of NaCl(s) and KCl(s). We have also had to add small amounts of HCl to the mixture in order to match the H^+ molality used by EQ3NR. H^+ concentrations (or equivalently the pH) are specified by an input option to EQ3NR, while they are calculated from equilibrium principles within Cantera. By adding small amounts of HCl, we can iterate until we have matched a desired pH within Cantera. All results are given on the NBS pH scale. Note, the pH scale matters a great deal in this nondilute solution case.

Table 12 Pointwise Comparison of molality and activity coefficient data at the Stationary point (NBS pH Scale): Cantera Results

Species	olality	Activity Coefficient
$H_2O(l)$	X=0.7459	0.897586
Cl-	9.4535	0.469079
Na+	4.5835	1.82376
K+	4.8701	1.01725
OH-	9.794E-8	0.4859
H+	8.856E-7	8.956

Table 13 Pointwise Comparison of molality and activity coefficient data at the Stationary point (NBS pH Scale): EQ3NR Results using the YMP Pitzer database.

Species	Molality	Activity Coefficient
$H_2O(l)$	X=0.7460	0.8856
Cl^-	9.4522	0.46914
Na^+	4.5829	1.8239
K^+	4.8693	1.0174
OH^-	8.093E-8	0.4536
H^+	8.856E-7	11.293

Comparison between EQ3NR code results and Cantera demonstrates that Cantera exhibits about 3 significant digits of agreement with EQ3NR on the major ions. However, the activity coefficient for H^+ remains about 25% underpredicted by Cantera, and the molar activity coefficient is 1% overpredicted by Cantera. The number in the molalities column for $H_2O(l)$ is the predicted mole fraction of $H_2O(l)$ in the brine. Reasons for these discrepancies have yet to be found.

7.7 The Standard Hydrogen Electrode (SHE)

In order to fully understand the intricacies of implementing electrode reactions within Cantera, there's no substitute for actually carrying the process out on a sample reaction.

The standard hydrogen electrode is the reference electrode used for electrode reaction. Therefore, it's the obvious choice. However, as will be shown in the discussion below, the implementation of the

electrode reaction is by no means a simple task, and the actually kinetic parameters to be used in the elementary steps that comprise the reaction are not generally agreed upon, possibly due to their severe dependence on surface preparation issues.

Cantera, however, is demonstrated to have all of the tools necessary to successfully implement what's known about the elementary steps of the reaction and to produce a global reaction rate in the Butler-Volmer format (where it's the appropriate form) that may be used for comparison against experiment. Additionally, with its emphasis/reliance on elementary steps, Cantera is a good vehicle for providing robust and reproducible links between experimental data and models attempting to reproduce experiment (see ref. [55] for a good example of this).

Below the thermodynamic treatment of the various phases needed to provide a treatment of electrode reactions within Cantera is reviewed. wethen present the three reversible elementary reactions which are thought to comprise the Standard Hydrogen Electrode (SHE) electrode kinetics, populate the model with reasonable data, and present the resulting Butler-Volmer global reaction and polarization curves for the reaction.

How this is all implemented within the Cantera framework [44] is the emphasis of this section. Nothing necessarily new has been developed within Cantera to handle electrode reactions. This capability to model Butler-Volmer electrode reactions has previously been used extensively within Cantera to model solid oxide fuel cells [45]. An explaination for how this functionality is used within liquid water electrolyte systems is provided, however.

7.7.1 SHE Electrode Reaction

The half-cell reaction for the standard hydrogen electrode reaction, written in the cathodic direction as required by recent conventions, is defined to be

$$2\mathrm{H}^+(aq) + 2\mathrm{e}^- \rightarrow \mathrm{H}_2(g) \qquad E^o = 0 \text{ volts (SHE)} \qquad (213)$$

E^o, the standard electrode potential to be defined below, is set to zero by convention at all temperature and pressures for this reaction. The potential difference between two phases cannot be readily measured. This is because the measurement always introduces other interfaces which have their own potential difference. Therefore, the (SHE) convention mitigates this problem by creating a relative interphase potential standard against which to compare other electrodes against. Eqn. (213) involves a single-ion activity coefficient. Therefore, the specification of the SHE electrode reaction rate involves the specification of a the correct pH scale given by the NBS standard, Eqn. (113).

The hydrogen evolution reaction occurs on various electrode materials at greatly varying rates of progress. The fastest and therefore most non-polarizable surfaces on which this reaction occurs are platinum surfaces. One of the slowest surfaces on which this reaction occurs (and therefore most polarizable) is Hg.

The reaction is thought to occur via the following reversible intermediate steps, each of which only involves the transfer of at most one electron. An intermediate of adsorbed hydrogen atoms (on platinum surface sites) is assumed, and calculation of the overall reaction), involves solving for the adsorbed hydrogen atom concentration assuming a pseudo-steady state.

The Volmer reaction,

$$\mathrm{H}^+(aq) + \mathrm{e}^- + \mathrm{Pt}^*(s) \rightarrow \mathrm{H}(s) \ , \tag{214}$$

involves the transfer of a proton across the electric double layer to an adsorbed position on the platinum surface, where it combines with an electron. It is considered to be the rate limiting elementary step on platinum-like surfaces.

The Tafel reaction,

$$2\mathrm{Pt}^*(s) + \mathrm{H}_2(g) \rightarrow \mathrm{H}(s) + \mathrm{H}(s) \ , \tag{215}$$

involves the reversible recombination of adsorbed hydrogen to form molecular gas-phase Hydrogen. The Heyrovsky reaction, Eqn. (216), is a competitor to the Tafel reaction, and involves the direct transfer of

$$\mathrm{H}^+(aq) + \mathrm{e}^- + \mathrm{H}(s) = \mathrm{Pt}^*(s) + \mathrm{H}_2(g) \tag{216}$$

a proton across the electric double layer where it reacts with a previously adsorbed hydrogen adatom and an electron from the metal to form molecular hydrogen. It's considered to be the rate limiting step for the hydrogen evolution reaction on some other metals such as Hg. There is an extensive discussion of these reactions in Chapter 8 of Newman's book [23]. Depending upon the identity and construction of the electrode, Newman states that different elementary reactions will be rate limiting. Reaction rate constants for the elementary steps and thermodynamic properties of absorbates are not given, however.

7.7.2 General Formulation for Equilibrium

Let's say we have an electrode reaction that produces electrons. We will write this in the cathodic direction as Eqn. (217).

$$\sum_{i=1}^{N_s} \nu_i^r \mathrm{M}_i + ne^- = \sum_{i=1}^{N_s} \nu_i^p \mathrm{M}_i \tag{217}$$

ν_i^p and ν_i^r (both defined to be always positive) are the stoichiometric coefficients for the products and reactants. The overall stoichiometric coefficient for species *i* in the reaction is equal to $\nu_i = \nu_i^p - \nu_i^r$. M_i is the chemical symbol for species *i*.

The condition for chemical equilibrium is given by the equilibration of the electrochemical potentials, which we denote by the symbol, ζ_i :

$$\sum_{i=1}^{N_s} \nu_i^r \zeta_i + ne^- = \sum_{i=1}^{N_s} \nu_i^p \zeta_i \tag{218}$$

For uncharged species, ζ_i reduces to the value of the chemical potential, $\mu_i\left(T,P\right)$. If all species participating in the reaction are in the same phase, then the equation above reduces to the standard chemical potential equation, due to charge conservation within the phase. However, if the reaction involves net charge transfer across the interface, then the equation above will also include the potential difference across the interface in its equilibrium expression.

The chemical potential of an electron in a metal, ζ_{e^-} (actually any metal), is equal to

$$\zeta_{e^-} = \mu_{e^-}^o + z_{e^-} F \Phi_{\text{electrode}} \ , \qquad \text{where} \quad z_{e^-} = -1 \tag{219}$$

In this equation, $\mu_{e^-}^o$ is nonzero, and because of the SHE potential convention of $E^o = 0$ at standard state conditions, it must be equal to one half the hydrogen gas standard state chemical potential, a point that is discussed in a very convoluted way in Newman's Chap 2, ref.[23]. Note, this implies that the electron chemical potential is equal to one-half the hydrogen gas chemical potential at arbitrary temperature and one bar pressure in order to be consistent with the SHE reference electrode convention.

$$\mu_{e^-}^o\left(T,P\right) = \frac{1}{2}\mu_{\text{H2(g)}}^o\left(T,1\,\text{bar}\right) \tag{220}$$

Also, the electron chemical potential $\mu_{e^-}^o\left(T,P\right)$ for electrons in metals is the same for all metals and electrodes, despite the fact that work functions for electrons have values that vary with the identity of the metal, due to the SHE reference electrode convention which encompasses these effects. A key reason for the necessity of Eqn. (220) is that the standard state chemical potential of the hydrogen ion is defined by convention to be equal to zero at all temperatures and pressures,

$$\mu_{\text{H+}}^{\triangle}\left(T,P\right) = 0 \ , \tag{221}$$

due the charge neutrality constraint creating an essential immeasurable degree of freedom in liquid phase electrochemistry. The Eqn. (221) convention is sometimes called Latimer's convention. This degree of freedom is satisfied by arbitrarily assigning the hydrogen ion to have a zero standard state chemical potential, where the standard state is defined to be the unit molality condition, assuming an ideal molal solution. Therefore, writing down the standard state Gibbs free energy change of reaction for the reaction Eqn. (213),

$$\Delta G_1 = \mu_{\text{H2(g)}}^o - 2\mu_{\text{H+}}^{\triangle} - 2\mu_{e^-}^o \quad , \tag{222}$$

and applying the relationship between the standard electrode potential and the Gibbs free energy of reaction,

$$\Delta\zeta_1^o = \Delta G_1^o + nFE^o = 0 \quad \rightarrow \quad nFE_{\rm SHE}^o = -\Delta G_1^o = 0\,, \tag{223}$$

Eqn. (220) is derived. The electron is assumed to be in its own "electron electrode phase" within Cantera, because of the form of Eqn. (220).

```
<phase dim="3" id="electronPhase">
  <elementArray datasrc="elements.xml"> E </elementArray>
  <speciesArray datasrc="#species_PtH2electrode"> Pt_electron </speciesArray>
  <thermo model="electrodeElectron">
    <referenceInterface> SHE </referenceInterface>
  </thermo>
  <transport model="None" />
  <kinetics model="none" />
</phase>
<!--  species definitions    -->
<speciesData id="species_PtH2electrode">
  <species name="Pt_electron">
    <atomArray> E:1 </atomArray>
    <charge> -1 </charge>
    <thermo>
      <NASA Tmax="1000.0" Tmin="200.0" P0="100000.0">
        <floatArray name="coeffs" size="7">1.172165560E+00, 3.990260375E-03, -9.739075500E-06,
          1.007860470E-08, -3.688058805E-12, -4.589675865E+02, 3.415051190E-01</floatArray>
      </NASA>
      <NASA Tmax="6000.0" Tmin="1000.0" P0="100000.0">
        <floatArray name="coeffs" size="7">1.466432895E+00, 4.133039835E-04, -7.320116750E-08,
          7.705017950E-12, -3.444022160E-16, -4.065327985E+02, -5.121644350E-01</floatArray>
      </NASA>
    </thermo>
  </species>
</speciesData>
```

Fig. 25. XML format for the electron phase within Cantera

Fig. 25 provides the Cantera implementation of this electron phase within a metal relative to the SHE interface. The phase itself is named `electronPhase`, and is defined as a stoichiometric phase, meaning that it consists of one species. It contains one species named `Pt_electron`, with the nontrivial NASA polynomial form necessary to duplicate the one half of the standard state of the hydrogen gas chemical potential, defined using the "zero enthalpy of elements in their natural state" basis (H^o(298 K, $H_2(g)$, 1 bar) = 0.0) used by NIST [24], CODATA [29], Chemkin [56] and the JANAF [57] tables. See previous memos for a more complete explanation of the specification of consistent bases [3] for presentation of the chemical potentials of species in gas and electrolyte phases and for an explanation of how to convert between the NIST convention and other conventions such as those used in SUPCRT92 [36].

The chemical potential of species *i* in phase *a*, where *a* may be the electrode, the solution, or the interface between the two, is equal to

$$\zeta_i = \mu_i\left(T, P, x_i\right) + z_i F\Phi_a \tag{224}$$

$\mu_i\left(T,P,x_i\right)$ may have multiple formats. For example it may be a stoichiometric phase, such as an oxide, it may be an ideal solution on the mole fraction basis, or it may be an electrolyte solution, whose activities are defined on the molality scale [53] and whose solute standard states are defined at unit molality assuming an ideal molal solution:

$$\mu_i = \mu_i^{\triangle}\left(T,P\right) + RT\ln\left(\frac{m_i\gamma_i^{\triangle}}{m^{\triangle}}\right), \text{ where } m_i = \frac{n_i}{\tilde{M}_o n_o} \text{ and } \tilde{M}_o = \frac{M_o}{1000} \tag{225}$$

$m^{\triangle} = 1\,\text{gmol (kg solvent)}^{-1}$. The $^{\triangle}$ symbol signifies that the standard state and the activity coefficients are on the molality scale.

```
<phase dim="3" id="h2gas">
  <elementArray datasrc="elements.xml">H</elementArray>
  <speciesArray datasrc="#species_data">H2</speciesArray>
  <state>
    <temperature units="K">300.0</temperature>
    <pressure units="Pa">101325.0</pressure>
  </state>
  <thermo model="IdealGas" />
  <kinetics model="none" />
  <transport model="Mix" />
</phase>
<speciesData id="species_data">
  <species name="H2">
    <atomArray>H:2</atomArray>
    <thermo>
      <NASA Tmax="1000.0" Tmin="200.0" P0="100000.0">
        <floatArray name="coeffs" size="7">2.344331120E+00, 7.980520750E-03, -1.947815100E-05,
          2.015720940E-08, -7.376117610E-12, -9.179351730E+02, 6.830102380E-01</floatArray>
      </NASA>
      <NASA Tmax="6000.0" Tmin="1000.0" P0="100000.0">
        <floatArray name="coeffs" size="7">2.932865790E+00, 8.266079670E-04, -1.464023350E-07,
         1.541003590E-11, -6.888044320E-16, -8.130655970E+02, -1.024328870E+00</floatArray>
      </NASA>
    </thermo>
  </species>
</speciesData>
```

Fig. 26. XML description of the Hydrogen Gas Phase

The hydrogen gas phase is given by Fig. 26. It's a pure ideal gas with one species. Let's expand the electrochemical potentials in Eqn. (224) using Eqn. (218) to develop an expression for equilibrium of the electrode reaction.

$$\sum_{i=1}^{N_s}\nu_i^r\mu_i + \sum_{i=1}^{N_s}\nu_i^r z_i F\Phi_i + n\mu_{e^-}^o - nF\Phi_{\text{electrode}} = \sum_{i=1}^{N_s}\nu_i^p\mu_i + \sum_{i=1}^{N_s}\nu_i^p z_i F\Phi_i \tag{226}$$

Collecting terms results in

$$\sum_{i=1}^{N_s}\nu_i^r z_i F\Phi_i - \sum_{i=1}^{N_s}\nu_i^p z_i F\Phi_i + -nF\Phi_{\text{electrode}} = \sum_{i=1}^{N_s}\nu_i^p\mu_i - \sum_{i=1}^{N_s}\nu_i^r\mu_i - n\mu_{e^-}^o \tag{227}$$

The rhs of Eqn. (227) is ΔG, the Gibbs free energy of reaction. Φ_i is the potential of the phase in which species *i* belongs. However, to simplify the lhs of Eqn. (227), we will may the assumption that all charged species are reactants are located in the electrolyte solution phase. Therefore, $\sum_{i=1}^{N_s} \nu_i^r z_i = n$. And, we may define the potential difference between the electrode and solution phase as E:

$$E = \Phi_{\text{electrode}} - \Phi_{\text{soln}} \tag{228}$$

Then, Eqn. (227) simplifies to

$$-nFE = \sum_{i=1}^{N_s} \nu_i^p \mu_i - \sum_{i=1}^{N_s} \nu_i^r \mu_i - n\mu_{e^-}^o = \Delta G \tag{229}$$

We may separate the Gibbs free energy of reaction out into it's standard state contribution, ΔG^o, defining an equivalent standard potential, E^o, based on ΔG^o,

$$-nFE^o = \sum_{i=1}^{N_s} \nu_i^p \mu_i^o - \sum_{i=1}^{N_s} \nu_i^r \mu_i^o - n\mu_{e^-}^o = \Delta G^o, \tag{230}$$

and the deviation from the standard state contribution,:

$$-nF\left(E - E^o\right) = \Delta G - \Delta G^o \tag{231}$$

The later may be rewritten as Eqn. (232).

$$E = E^o - \frac{\Delta G - \Delta G^o}{nF} \quad , \tag{232}$$

Eqn. (232) is recognized as the Nernst equation for the reaction, after $\Delta G - \Delta G^o$ is written out in terms of the logs of the activity coefficients. For the SHE, the Nernst equation reduces to

$$E = E^o - \frac{\Delta G - \Delta G^o}{nF} = \frac{RT}{F} \ln a_{H+}^{\triangle} - \frac{RT}{2F} \ln\left(\frac{p_{H2(g)}}{1\,\text{bar}}\right) \tag{233}$$

E^o for aqueous electrodes is ubiquitously tabulated in standard references such as the CRC. There are several issues to note, in using these tabulations. $\mu_{e^-}^o$ must be appropriately recognized as being equal to 1/2 $\mu_{H2(g)}^o\left(T, 1\,\text{bar}\right)$. Also, the standard state for species in the aqueous electrolytes is defined to be one at which the species is at unit molality in an ideal molal solution state. E^o is used as an alternative tabulation of the standard-state Gibbs free energy of formation for ionic species, albeit at only one temperature and pressure.

E^o may be thought of as the barrier in voltage that must be built up in order for a reaction, which would normally want to go forwards spontaneously, i.e., $\Delta G < 0$, to instead be at equilibrium. For

example, the noble metals have very high values of E^o. Eqn. (234) is an example of a noble metal standard electrode potential reaction.

$$\mathrm{Pt}^{2+} + 2e^- \rightarrow \mathrm{Pt} \qquad E^o = 1.118 \text{ volts (SHE)} \qquad (234)$$

In the reaction, there is a very strong driving force in the cathodic reaction, i.e., the direction involving the reduction of the metal and the consumption of the electron. Therefore, in order for the reaction to be at equilibrium a very high compensating potential *E* must be built up in the metal, which tends to drive the creation of electrons in metals, because it makes the chemical potential of electrons lower - see Eqn. (219).

Typically, E^o values are tabulated in terms of the overall global reaction stoichiometry, which may hide the fact that there are intermediate elementary reaction steps and intermediate species that must be defined. The hydrogen electrode reaction is found to occur via an adsorbed intermediate, which forms a Langmuir-Hinshelwood adsorbate on the platinum catalyst. The Cantera implementation of this surface phase is given in Fig. 27.

The phase is called `platinum_surface`, and consists of two species, `pt_site`, and `H*_site`. The thermodynamics model is named `Surface`, which implements an ideal solution model for the adsorbate phase. This surface model is similar to models which have been used in Cantera to treat surface site compositions for solid oxide fuel cells and diamond growth in CVD systems. The surface site density must be specified. Here, we use a typical value used in the analyses above, 3×10^{-9} gmol cm^{-2}, to fill in this number, not having an actual estimated number to go by. The thermodynamics of the absorbates must also be specified. Again, we must guess at the numbers. We use the `const_cp` formulation for the standard states of the adsorbate species, because it is the simplest.

With this formulation we only need to specify $H^o\left(T_o\right)$, $S^o\left(T_o\right)$, and $C_p^o\left(T_o\right)$ at a single temperature T_o. Because we don't know the thermodynamics of these adsorbate species, using the simplest formulation is prudent. The thermodynamics of adsorbate species will affect the Gibbs free energies of reaction of the reactions in the mechanisms, and thus the reverse rate constants of these reactions. The relative values between the `H*_site` species, a single hydrogen adatom adsorbed onto a base site, and the `pt_site` species, a bare site, will determine the degree of binding energy of hydrogen adsorbed onto the bare platinum metal. An early literature value of 10 kcal gmol^{-1} for the hydrogen molecular adsorption on Hg motivates the magnitude of the relative differences in enthalpies between the `pt_site` and `H*_site` values [65]. The binding energy has a large effect on the observed Tafel slope when the `H*_site` surface site fractions become significant. The numbers, however, should be considered to be speculative without a thorough investigation.

```
<phase dim="2" id="platinum_surface">
  <elementArray datasrc="elements.xml">H E</elementArray>
  <speciesArray datasrc="#species_PtH2electrode">pt_site H*_site</speciesArray>
  <state>
    <temperature units="K">300.0</temperature>
    <coverages>pt_site:0.9 H*_site:0.1</coverages>
  </state>
  <thermo model="Surface">
    <site_density units="mol/cm2"> 3e-09 </site_density>
  </thermo>
  <kinetics model="Interface" />
  <reactionArray datasrc="#reaction_data" />
  <transport model="None" />
  <phaseArray>Pt_H2electrons NaCl_electrolyte h2gas</phaseArray>
</phase>

<speciesData id="species_PtH2electrode">

<!--  species pt_site -->
  <species name="pt_site">
    <atomArray />
    <thermo>
      <const_cp Tmax="5000.0" Tmin="100.0">
        <t0 units="K">298.15</t0>
        <h0 units="kJ/mol">0.0</h0>
        <s0 units="J/mol/K">0.0</s0>
        <cp0 units="J/mol/K">0.0</cp0>
      </const_cp>
    </thermo>
  </species>

<!--  species H*_site   -->
  <species name="H*_site">
    <atomArray>H:1</atomArray>
    <thermo>
      <const_cp Tmax="5000.0" Tmin="100.0">
        <t0 units="K">298.15</t0>
        <h0 units="kJ/mol">-21.0</h0>
        <s0 units="J/mol/K">63.0</s0>
        <cp0 units="J/mol/K">10.0</cp0>
      </const_cp>
    </thermo>
  </species>
</speciesData>
```

Fig. 27. Data for the `platinum_surface` phase, the location for the interfacial reaction

7.7.3 Cantera's Implementation of Interfacial Kinetics

The interfacial kinetics object is initiated in the XML element called `phase` by the addition of the `kinetics` XML element (see Fig. 27). The attribute model id of `Interface` indicates that the object `InterfaceKinetics` should be constructed to handle the calculation of the rates of progress of reactions defined on the interface and the species source terms for species in bulk and surface phases at or adjacent to the interface. The object automatically includes the interface species in its list of

species that may be reactants and products of reactions defined in it, as all reactions may be considered to be located on the interface. In addition, the XML element called `phaseArray` defines other phases which are present at the interface (or on either side of it) and whose species may also be reactants and/or products in reactions. For the particular case of Hydrogen evolution on a platinum electrode, three additional bulk phases are needed to be present at the electrode and defined within the `InterfaceKinetics` object: `Pt_H2electrons` which are electrons in the platinum metal, `NaCl_electrolyte` which is the name of the liquid water electrolyte obeying the Pitzer formulation for specification of the molality-based activities, and `H2gas` which corresponds to pure Hydrogen gas bubbles injected over the platinum metal. The species in these phases are all added into the species vector within the `InterfaceKinetics` object. The actual platinum metal isn't involved in the reaction.

In Fig. 27, the `reactionArray` XML object defines where to look in the XML file for the reactions defined at the interface. The attribute `datasrc` defines the id of the `reactionData` XML element to look for the reactions.

```
<reactionData id="reaction_data">
 <!--  reaction 0001  Volmer reaction - rate limiting -->
  <reaction reversible="yes" type="surface" id="0001">
    <equation>H+ + Pt_electron + pt_site [=] H*_site</equation>
    <rateCoeff>
      <electrochem beta="0.5" />
      <Arrhenius>
        <A>1.1180000E+5</A>
        <b>0.0</b>
        <E units="kJ/mol">40.000000</E>
      </Arrhenius>
    </rateCoeff>
    <reactants>H+:1.0 Pt_electron:1.0 pt_site:1.0</reactants>
    <products>H*_site:1.0</products>
  </reaction>
 <!--  Tafel reaction - fast -->
  <reaction reversible="yes" type="surface" id="0002">
    <equation>2 pt_side + H2 [=] 2 H*_site</equation>
    <rateCoeff>
    <Arrhenius>
      <A>1.900000E+13</A>
      <b>0.0</b>
      <E units="kJ/mol">10.000000</E>
    </Arrhenius>
    </rateCoeff>
    <reactants>pt_site:2.0 H2:1.0</reactants>
    <products>H*_site:2.0</products>
  </reaction>
<!--  Heyrovsky reaction - set to slow here -->
  <reaction reversible="yes" type="surface" id="0003">
    <equation> pt_side + H2 [=] H*_site + H+ + Pt_electron</equation>
    <rateCoeff>
      <Arrhenius>
        <A>6.000000E-5</A>
        <b>0.0</b>
        <E units="kJ/mol">30.000000</E>
      </Arrhenius>
    </rateCoeff>
    <reactants>pt_site:1.0 H2:1.0</reactants>
    <products>H*_site:1.0 H+:1.0 Pt_electron:1.0</products>
  </reaction>
</reactionData>
```

Fig. 28. Cantera's XML description of the rate constants for the Hydrogen electrode reaction

Fig. 28 contains the `reactionData` XML element with the matching id of `reaction_data`, where the three Hydrogen electrode reactions are listed. The reactions are in standard Cantera format (see http://www.cantera.org). One addition is the `electrochem` XML element with the attribute `beta`. The next section will describe how this β^e changes the reaction rates.

7.7.4 Formulation of the Kinetics in Terms of Elementary Steps

Cantera's implementation of kinetics involving charge transfer reaction is based on the following equation for the forward and reverse reaction rate coefficients for the reaction) given by Eqn. (235).

$$k_f = A_f \beta^f \exp\left[\frac{-E_f}{RT}\right] \exp\left[\frac{-\beta^e F\left(\sum_k \nu_k z_k \Phi_k\right)}{RT}\right] = k_f^c \exp\left[\frac{-\beta^e F\left(\sum_k \nu_k z_k \Phi_k\right)}{RT}\right] \qquad (235)$$

k_f^c is the "chemical part of the rate coefficient. $\beta^e F\left(\sum_k \nu_k z_k \Phi_k\right)$, which includes the electron term, may be thought of as the change in the activation energy barrier (or the relative transition state energy level) due to the potential energy difference between the products and reactants in the reaction. The motivation for the form is based on transition state theory applied to electron transfer reactions and is supplied in several standard electrochemistry books (see ref.64,62). β^e is the symmetry factor for the transition state, and is an additional input parameter for electron transfer reactions.

Let's take a look at this term for the case of the Volmer Reaction, Eqn. (214). In this case

$$\sum \nu_k z_k \Phi_k = n\left(\Phi_{\text{metal}} - \Phi_{\text{soln}}\right) = nE \qquad (236)$$

The forward reaction, which is the cathodic direction, is reduced for positive values of *E*, and enhanced for negative values of *E*. This makes sense, because high values of Φ_{metal} stabilize the presence of electrons in the metal by reducing the chemical potential of electrons.

The reverse reaction rate may be calculated from the electrochemical equilibrium constant, which includes the electrical potential energy term in Eqn. (236):

$$\sum \nu_k \zeta_k = 0\,. \qquad (237)$$

$$\Delta G_R^o + RT \ln\left[\frac{\prod_k^p a_k^{\nu_k^p}}{\prod_k^r a_k^{\nu_k^r}}\right] + F\sum_k \nu_k z_k \Phi_k^{eq} = 0\,, \qquad (238)$$

Expanding the terms in Eqn. (238),

$$\Delta G_R^o + RT \ln\left[\frac{\prod_k^p a_k^{\nu_k^p}}{\prod_k^r a_k^{\nu_k^r}}\right] + F\sum_k \nu_k z_k \Phi_k^{eq} = 0\,, \tag{239}$$

where ΔG_R^o is the standard Gibbs free energy of the reaction, the last term on the rhs may be solved for *E*, the equilibrium value of the potential drop across the interface that would induce an equilibrium condition for the elementary reaction. Eqn. (239) can be rewritten as

$$\frac{\prod_k^p a_k^{\nu_k^p}}{\prod_k^r a_k^{\nu_k^r}} = \exp\left[\frac{\Delta G_R^o - F\sum_k \nu_k z_k \Phi_k^{eq}}{RT}\right] = \exp\left[\frac{\Delta G_R^o - FnE}{RT}\right] \tag{240}$$

where $E = \Phi_{\text{metal}}^{eq} - \Phi_{\text{soln}}^{eq}$

The numerator in Eqn. (240) is a multiplication over the products of the reaction, while the denominator is a multiplication over the reactants of the reaction. We may formulate the reverse rate constant by considering Cantera's treatment of the forward rate of progress of the reaction as

$$ROP_f = k_f\left(\prod_k^r \left(c_k^a\right)^{\nu_k^r}\right), \tag{241}$$

where c_k^a are the activity concentrations of the reactant species *k*, ($c_k^a = c_k^s a_k$, where c_k^s is the standard concentration and a_k is the activity of species *k*), with the expression for the reverse rate of progress of the reaction based on mass action kinetics,

$$ROP_r = k_r\left(\prod_k^p \left(c_k^a\right)^{\nu_k^p}\right), \tag{242}$$

$$ROP_r = k_r^c\left(\frac{\prod_k^r \left(c_k^s\right)^{\nu_k^r}}{\prod_k^p \left(c_k^s\right)^{\nu_k^p}}\right)\exp\left[\frac{\Delta G_r^o + \left(1-\beta^e\right)F\sum_k \nu_k z_k \Phi_k}{RT}\right]\prod_k^p \left(c_k^a\right)^{\nu_k^p} \tag{243}$$

to generate an expression for k_r that is consistent with electrochemical equilibrium, Eqn. (240).

$$ROP_r = k_r^c \left(\frac{\prod_k^r \left(c_k^s\right)^{\nu_k^r}}{\prod_k^p \left(c_k^s\right)^{\nu_k^p}} \right) \exp\left[\frac{\Delta G_r^o + \left(1-\beta^e\right) F \sum_k \nu_k z_k \Phi_k}{RT} \right] \prod_k^p \left(c_k^a\right)^{\nu_k^p} \tag{244}$$

When the electric potential drop across the interface is at the equilibrium value, $nE = \sum \nu_k z_k \Phi_k^{eq}$, the forward rate of progress and reverse rate of progress are equal. However, the potential drop across the interface may not be at equilibrium and will not be for finite currents crossing the interface electrode. Define this difference as the surface overpotential η_s

$$n\left(\Phi_{\text{metal}} - \Phi_{\text{soln}}\right) = n\left(E + \eta_s\right) = \sum \nu_k z_k \Phi_k \tag{245}$$

The surface overpotential η_s represents the departure from the equilibrium potential at the specific conditions of the electrode (including the calculation of the activities) and it is also given by the expression:

$$Fn\eta_s = -n\zeta_{e^-} + \sum_i^p \nu_i^p \zeta_i - \sum_i^r \nu_i^r \zeta_i \tag{246}.$$

Note, we have defined η_s away from the standard state conditions where all unity activities are assumed, and even irrespective of equilibrium conditions. Therefore it's valid under any circumstance, especially one in which there is a net current flowing across the interface.

The forward and reverse rates of progress may be reorganized so that the Butler-Volmer form of the equation is generated. Following the derivation in [55], the forward rate of progress is expressed as:

$$\begin{aligned} ROP_f &= k_f^c \exp\left[\frac{-\beta^e Fn\left(E + \eta_s\right)}{RT} \right] \prod_k^r \left(c_k^a\right)^{\nu_k^r} \\ &= k_f^c \exp\left[\frac{-\beta^e FnE}{RT} \right] \prod_k^r \left(c_k^a\right)^{\nu_k^r} \exp\left[\frac{-\beta^e Fn\eta_s}{RT} \right] \end{aligned} \tag{247}$$

Then,

$$
\begin{aligned}
ROP_r &= k_r^c \left(\frac{\prod_k^r \left(c_k^s\right)^{\nu_k^r}}{\prod_k^p \left(c_k^s\right)^{\nu_k^p}} \right) \exp\left[\frac{\Delta G_r^o + \left(1-\beta^e\right) F \sum_k \nu_k z_k \Phi_k}{RT} \right] \prod_k^p \left(c_k^a\right)^{\nu_k^p} \\
&= k_r^c \left(\frac{\prod_k^r \left(c_k^s\right)^{\nu_k^r}}{\prod_k^p \left(c_k^s\right)^{\nu_k^p}} \right) \left(\frac{\prod_k^r a_k{}^{\nu_k^r}}{\prod_k^p a_k{}^{\nu_k^p}} \right) \exp\left[\frac{\left(1-\beta^e\right) Fn\eta_s - \beta^e FnE}{RT} \right] \prod_k^p \left(c_k^a\right)^{\nu_k^p} \qquad (248) \\
&= k_r^c \exp\left[\frac{-\beta^e FnE}{RT} \right] \prod_k^r \left(c_k^a\right)^{\nu_k^r} \exp\left[\frac{\left(1-\beta^e\right) Fn\eta_s}{RT} \right]
\end{aligned}
$$

Then, the net rate of progress for the reaction may be written as

$$
ROP_{net} = k_r^c \exp\left[\frac{-\beta^e FnE}{RT} \right] \left(\prod_k^r \left(c_k^a\right)^{\nu_k^r} \right) \left(\exp\left[\frac{-\beta^e Fn\eta_s}{RT} \right] - \exp\left[\frac{\left(1-\beta^e\right) Fn\eta_s}{RT} \right] \right) \qquad (249)
$$

may be used to eliminate *E* from the Eqn. (250).

$$
\exp\left[\frac{-\beta^e FnE}{RT} \right] = \left(\frac{\prod_k^p \left(c_k^a\right)^{\nu_k^p \beta^e}}{\prod_k^r \left(c_k^a\right)^{\nu_k^r \beta^e}} \right) \left(\frac{\prod_k^r \left(c_k^s\right)^{\nu_k^r \beta^e}}{\prod_k^p \left(c_k^s\right)^{\nu_k^p \beta^e}} \right) \exp\left[\frac{\beta^e \Delta G_R^o}{RT} \right] \qquad (250)
$$

Eqn. (240) may be used to eliminate *E* from the Eqn. (250).

$$
\exp\left[\frac{-\beta^e FnE}{RT} \right] = \left(\frac{\prod_k^p \left(c_k^a\right)^{\nu_k^p \beta^e}}{\prod_k^r \left(c_k^a\right)^{\nu_k^r \beta^e}} \right) \left(\frac{\prod_k^r \left(c_k^s\right)^{\nu_k^r \beta^e}}{\prod_k^p \left(c_k^s\right)^{\nu_k^p \beta^e}} \right) \exp\left[\frac{\beta^e \Delta G_R^o}{RT} \right] \qquad (251)
$$

to yield

$$
\begin{aligned}
ROP_{net} &= k_r^c \left(\frac{\prod_k^p \left(c_k^a\right)^{\nu_k^p \beta^e}}{\prod_k^r \left(c_k^a\right)^{\nu_k^r \beta^e}} \right) \left(\frac{\prod_k^r \left(c_k^s\right)^{\nu_k^r \beta^e}}{\prod_k^p \left(c_k^s\right)^{\nu_k^p \beta^e}} \right) \exp\left[\frac{\beta^e \Delta G_R^o}{RT} \right] \left(\prod_k^r \left(c_k^a\right)^{\nu_k^r} \right) \\
&\qquad \left(\exp\left[\frac{-\beta^e F n \eta_s}{RT} \right] - \exp\left[\frac{\left(1-\beta^e\right) F n \eta_s}{RT} \right] \right) \\
&= k_r^c \left(\prod_k^p \left(c_k^a\right)^{\nu_k^p \beta^e} \right) \left(\frac{\prod_k^r \left(c_k^s\right)^{\nu_k^r \beta^e}}{\prod_k^p \left(c_k^s\right)^{\nu_k^p \beta^e}} \right) \exp\left[\frac{\beta^e \Delta G_R^o}{RT} \right] \left(\prod_k^r \left(c_k^a\right)^{\nu_k^r \left(1-\beta^e\right)} \right) \\
&\qquad \left(\exp\left[\frac{-\beta^e F n \eta_s}{RT} \right] - \exp\left[\frac{\left(1-\beta^e\right) F n \eta_s}{RT} \right] \right)
\end{aligned}
\tag{252}
$$

Now the net rate of electron generation may be calculated from ROP_{net}:

$$
\frac{d\left[e^-\right]}{dt} = \left(-n\right) ROP_{net} \tag{253}
$$

and the current through the electrode and into the solution may be defined in terms of the electron generation rate as

$$
I = F \frac{d\left[e^-\right]}{dt} \tag{254}
$$

Then, the rate of progress for elementary electrode reactions may be defined in terms of the current density, *i*, in the traditional Butler-Volmer form as

$$
i = i_o \left(\exp\left[\frac{\left(1-\beta^e\right) F \eta_s}{RT} \right] - \exp\left[\frac{-\beta^e F \eta_s}{RT} \right] \right) \tag{255}
$$

where i_o, the exchange current density, is given by:

$$
i_o = nFk_r^c \left(\prod_k^r \left(c_k^a\right)^{\nu_k^r \left(1-\beta^e\right)} \right) \left(\prod_k^p \left(c_k^a\right)^{\nu_k^p \beta^e} \right) \left(\frac{\prod_k^r \left(c_k^s\right)^{\nu_k^r \beta^e}}{\prod_k^p \left(c_k^s\right)^{\nu_k^p \beta^e}} \right) \exp\left[\frac{\beta^e \Delta G_R^o}{RT} \right]. \tag{256}
$$

Therefore, for elementary kinetics steps, Cantera's implementation leads to the Butler-Volmer format given by Eqn. (255) and (256), a point that has already been made in ref. [55]. However, for sets of interfacial electrode reactions, especially when they are intermixed with non-electrode reactions, the resulting global current density may or may not be reducible to Butler-Volmer form. A more general approach is needed.

7.7.5 Formulation of the Global Reaction Rates

There are few elementary steps in Electrodics that involve the transfer of more than a single electron. The hydrogen evolution reaction is not one of those. It is a combination of steps.

While each individual elementary electron-transfer reaction step obeys the Butler-Volmer, the overall reaction mechanism on a surface may not obey the Butler-Volmer formulation, Eqn. (257).

$$i_n = i_o \left(\exp\left[\frac{\left(1-\beta^e\right) F \eta_s}{RT} \right] - \exp\left[\frac{-\beta^e F \eta_s}{RT} \right] \right) \tag{257}$$

In this equation, i_o is the exchange current density and has units of A cm^{-2}. i_n is the current density of electrons stemming from the electrode reaction.

Yet, a lot of the electrochemical reaction rate data is presented in a Butler-Volmer format representing a global result. How are these issues reconciled?

They are reconciled by introducing the concept of a Global Overall Reaction, that may be defined to calculate the net rate of progress of a single reactant or product. The stoichiometry of the Global reactions are further defined via a linear combination of elementary reaction steps, such that intermediates drop out of the formulation, in order to make sure that global reactions conserve elements. However, global reaction rates are calculated using the entire reaction network and assuming intermediate quantities are at their pseudo steady-state values.

For example, below is the half-cell reaction for the standard hydrogen cell.

$$2\mathrm{H}^+(aq) + 2\mathrm{e}^- \rightarrow \mathrm{H}_2(g) \tag{258}$$

This may be considered to be a linear combination of two times the Volmer reaction:

$$\mathrm{H}^+(aq) + \mathrm{e}^- + \mathrm{Pt}^*(s) \rightarrow \mathrm{H}(s)$$

added to -1 times the Tafel reaction:

$$2\mathrm{Pt}^*(s) + \mathrm{H}_2(g) \rightarrow \mathrm{H}(s) + \mathrm{H}(s)$$

Together with the specification of a special species, in this case, `Pt_electron`, the speciation allows us to calculate a specific rate of progress for the global reaction. The concept of global reaction rates

has been introduced into the program `cttables`. Fig. 29 contains a sample input deck for the SHE system.

For a given global reaction the product and reactant stoichiometry are uniquely specified. Therefore, the potential complication of having separate values for η_s defined for each elementary reaction in a complicated mechanism goes away. The equilibrium value of *E* is distinctly defined in terms of reaction products and reactants for that global reaction. The fact that there may be multiple pathways for getting to the products from the reactants is irrelevant to the value of *E*.

Newman [23] has an extensive section on the SHE kinetics. However, what's revealing is that nowhere are the rate constants or energetics of the Langmuir-Hinshelwood adsorption system that comprises the inner workings actually provided. This is true for all of the other secondary sources that we have found that discuss electrode reactions [23, 61, 62, 63, 64]. It may be, as is discussed in many of these texts, that variations due to the surface preparation of the electrode make this reaction (and many other electrode reactions) inherently irreproducible, and therefore, these sources have found it difficult to provide consistent numbers. It also may be the case that the lack of a sufficient rigorousness in the analysis, especially in earlier work before the widespread use of numerical modeling, may have hampered the derivation of the rate constants and energetics in these elementary steps.

While it may be possible to go back to the more primary literature [65] and analyze the reaction system, in putting together this sample problem, weonly resorted to grossly fitting the reaction rates so that the global reaction as calculated by `cttables` fit one of Newman's Tafel plot curves for the reaction on a platinum electrode.

```
Number of Cantera Files = 3
Cantera File Name = Pt_electrode.xml
Cantera File Name = HMW_NaCl_sp1977_alt.xml
Cantera File Name = h2gas.xml
Bath Temperature = 300.
Bath Pressure =  1 atm
Add Chemical Potential Column = true
START BLOCK Temperature Table Format
  Number of Points = 8
  Delta Temperature = 20.
  Low Temperature = 300.
  Added Temperatures = 333.15 273.15 373.15
 END BLOCK Temperature Table Format
 start block Bath Specification for Phase H2gas
       Bath Species ID = H2
       start block Bath Species Mole Fraction
        H2 =  1.0
       End block Bath Species Mole Fraction
end block Bath Specification for Phase H2gas
start block Bath Specification for Phase NaCl_Electrolyte
       Bath Species ID = H2O(L)
       start block Bath Species Molalities
       Na+ = 1.0
       Cl- = 1.8
       H+ =  0.8
       End block Bath Species Molalities
end block Bath Specification for Phase NaCl_Electrolyte

Start block Extra Global Reaction
   Special Species = Pt_electron
   Start block Elementary Reaction Specification
     Reaction Index = 0
     Reaction multiplier = 2.0
   End block Elementary Reaction Specification
   Start block Elementary Reaction Specification
     Reaction Index = 1
     Reaction multiplier = -1.0
   End block Elementary Reaction Specification
End block Extra Global Reaction
```

Fig. 29. Sample input deck for the cttables program

An additional problem was that Newman's Fig. 8.6 p. 220 did not fully specify the electrolyte concentrations, which the value of the exchange current density depends on. Fig. 29 specifies the composition of the solution that weused in the `cttables` calculation. The equilibrium electric potential for the reaction for this particular bath gas conditions turned out to be equal to $E = -0.00494$ volts, as the solution pH calculated from the Pitzer-based activity coefficients was 0.0839.

Over most of the curve voltages surveyed, except for extremely cathodic conditions, the surface remains dominated by free sites. This is observed in experiments. This puts a requirement on the upper bound on the heat of adsorption of hydrogen molecules on the surface. For cathodic conditions, the Tafel slope is reduced below the 0.5 limit produced by the Volmer reaction, whenever there are significant concentrations of adsorbed hydrogen; this curvature shows up a little bit in Fig. 30 at the lowest voltages. The fact the reduction in the Tafel slope is not readily seen (at least up to the voltage value of -0.6 on Pt - see p., 220 [23]) indicates, from the model, that the binding energy of Hydrogen on the surface is below a certain value. For the numbers we have used this value is 15 kJ/gmol, not a terribly large number.

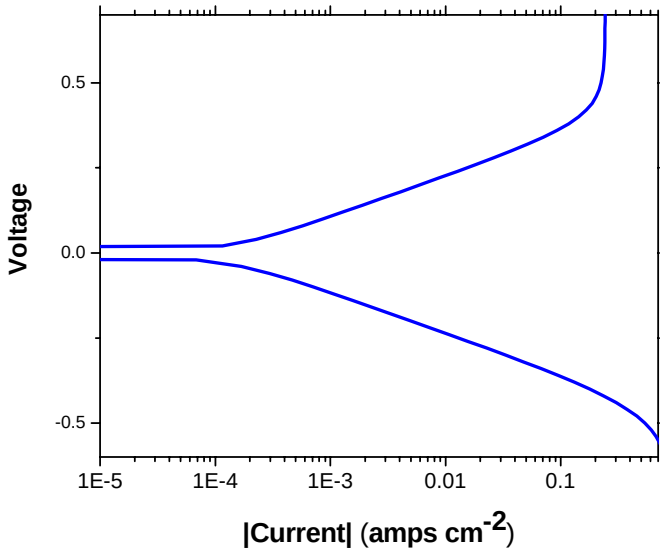

Fig. 30. Polarization Plot for the Hydrogen electrode reaction The current, which represents the charge flowing into the electrolyte from the electrode, is positive for voltages > E (anodic conditions) and negative for voltages < E (cathodic conditions)

Fig. 30 contains the net polarization plot for the hydrogen reaction network discussed above and calculated by `cttables`. Cathodic voltages, i.e., negative voltages, produce negative values of the current, i.e., there is a net current from the electrolyte into the electrode, which in turn means that electrons are consumed at the interface. The cathodic and the anodic side of the polarization curve are not symmetric, reflecting the fact that the reaction network even for this seemingly simple reaction, is not an elementary single-step reaction. In particular, on the anodic side (high voltage where electrons are created at the interface), the reaction eventually becomes independent of the voltage. The is because the reaction becomes rate limited by adsorption rate of H_2(g) onto the bare platinum surface. In other words, the branching ratio between the reverse reaction where H_2(g) is reformed from adsorbed hydrogen and the forward step where it dissociates into H+ and an electron in the metal is skewed towards heavily towards the later, the electrodic reaction step.

The Butler-Volmer form of this equation is calculated by `cttables` to be equal to

$$i = 1.1157\times10^{-4}\left(\exp\left[\frac{0.5F\eta_s}{RT}\right]-\exp\left[\frac{-0.5F\eta_s}{RT}\right]\right) \tag{259}$$

At the equilibrium potential of E = -0.00494 Volts, the parameters have been adjusted so that a simple Butler-Volmer (BV) form is generated at low overpotentials, as is observed in experiment. In particular the value of the BV form agrees on the cathodic side with one of Pt-metal curves in

Newman's Fig. 8.6 on p.220 of ref. [23]. However, setting different parameters in the elementary reaction mechanism may lead to significantly different behavior. In particular, asymmetric Butler-Volmer behavior, where $\alpha_a \neq \alpha_c \neq 0.5$, may be generated when there is significant hydrogen adsorption on the Platinum.

All of this behavior can be captured by Cantera's reaction mechanism framework. However, the most important take-home point should be that the level of experimental data that is required to fully take advantage of Cantera's framework may or may not be available.

8 Nomenclature

8.1 Subscripts

l	Represents aqueous electrolytes in solution (e.g., NaCl)
j	Represents individual ions in solution
i, e	Represents elements

8.2 Superscripts

^{o}	Refers to the molar scale
$^\vartriangle$	Refers to the molality scale
$\widehat{G}$	Intrinsic partial molal quantities (i.e., derivatives with respect to m_j)
~ or -	Intrinsic partial molar quantities
$\wedge$	Intrinsic specific quantities (i.e., derivatives with respect to kg of species)

8.3 Regular

α_o	Coefficient of thermal expansion of water, $d\ln V / dT$
γ_k	Molar based activity coefficient for species *k*
$\gamma_k^\vartriangle$	Molality based activity coefficient for species *k*
$\gamma_M^\vartriangle$	Molality based activity coefficient for the cation M
$\gamma_X^\vartriangle$	Molality based activity coefficient for the anion X
$\gamma_\pm^\vartriangle$	Mean activity coefficient on the molality scale
η_s	Surface overpotential
ϕ	Osmotic coefficient

Φ_p	Electric potential of phase *p*
ν_i^r	Reactant stoichiometric coefficient for species *i*
$\mu_o^o(T,P)$	Standard state of the solvent (J per kmol)
$\mu_k^o(T,P)$	Standard state for the solute *k* (J per kmol)
$\mu_k^{\triangle}(T,P)$	Molality based standard state for the solute *k* (J per kmol)
ζ_k	Electrochemical potential of species *k*
a_o	Molar based activity of the solvent
A_L	Debye-Huckel coefficient for the Mixture Enthalpy (Eqn. (177))
b	Coefficient in the extended Pitzer parameterization of the long range Debye-Huckel term
B_{MX}	Pitzer binary activity coefficient between cation *M* and anion *X*
B_{MX}^L	Derivative with respect to temperature of the Pitzer binary activity coefficient between cation *M* and anion *X*
F	Faraday's constant
$\bar{C}_{p,k}^{\triangle}$	Partial molar heat capacity for species *k*
$\tilde{C}_{p,k}^{\triangle}$	Standard state molar heat capacity for species *k* on the molality scale
${}^{\phi}C_p$	Apparent molal heat capacity
$\Delta\widehat{G}_k^{\triangle,abs}(T,P)$	Absolute standard partial molal Gibbs free energies of species *k*. Units of (J (kg solvent) gmol^{-1}).
$\Delta\widehat{G}_k^{\triangle}(T,P)$	Apparent standard partial molal Gibbs free energies of formation for species k. Species *k* is assumed to have a standard state on the molality scale. Units of (J (kg solvent) gmol^{-1}).
$\Delta\widehat{G}_{f,k}^{\triangle}(T,P)$	Apparent standard partial molar Gibbs free energies of formation for species *k* from its elements in their stable forms at the reference pressure (P_r) and temperature T_r of 1 bar and 298 K. Species *k* is assumed to have a standard state on the molality scale. Units of (J kmol^{-1}).
$\Delta\bar{G}_{f,k}^{\triangle}(T_r,P_r)$	Standard partial molar Gibbs free energies of formation of species k from its elements in their stable forms at the reference pressure (P_r) and temperature T_r of 1 bar and 298 K. Species *k* is assumed to have a standard state on the molality scale. Units of (J kmol^{-1}).

$\Delta\bar{G}^{o}_{f,k}\left(T_r, P_r\right)$ Standard partial molar Gibbs free energies of formation of species *k* from its elements in their stable forms at the reference pressure (P_r) and temperature T_r of 1 bar and 298 K. Species *k* is assumed to have a standard state on the molar scale. Units of (J kmol^{-1}).

$\tilde{G}^{o}_{k}\left(T,P\right)$ Molar standard state Gibbs free energies based on $\Delta\tilde{H}^{o}_{f,e,298}\left(T_r, P_r\right)=0$ standard. That standard, followed by NIST and the JANAF tables, sets the Enthalpy of formation of the elements, *e*, at T_r and P_r to zero. Standard state is assumed to be on the molar scale.

$\tilde{G}^{\triangle}_{k}\left(T,P\right)$ Molar standard state Gibbs free energies based on $\Delta\tilde{H}^{o}_{f,e,298}\left(T_r, P_r\right)=0$ standard. That standard, followed by NIST and the JANAF tables, sets the Enthalpy of formation of the elements, *e*, at T_r and P_r to zero. Standard state is assumed to be on the molality scale.

G Total Gibbs free energies of the solution. Extensive quantity. *nG* denotes the same quantity.

$\tilde{G}$ Total Gibbs free energies of the solution (J kmol^{-1}). Extensive quantity but presented on a per kmol basis.

$G_{ex,\triangle}$ Excess Gibbs free energy of a solution based on the deviation from the ideal molality solution approximation (J)

$G^{\mathrm{mod}}_{ex,\triangle}$ Excess Gibbs free energy of a solution based on the deviation from the ideal molality solution approximation (J), modified to remove the singularity that occurs as the solvent mole fraction goes to zero.

$\tilde{G}_{ex,\triangle}$ Excess Gibbs free energy of a solution based on the deviation from the ideal molality solution approximation on a per kmol basis (J kmol^{-1}).

$G^{id,\triangle}_{ex}$ Excess Gibbs free energy of a solution based on the "normal" ideal solution approximation for a solution which obeys the ideal molality solution approximation. Note, this is not zero, and actually exhibits a singularity as the solvent concentration goes to zero.

$G^{\mathrm{mod},id,\triangle}_{ex}$ Excess Gibbs free energy of a solution based on the "normal" ideal solution approximation for a solution which obeys a modified ideal molality solution approximation. Note, this is not zero, and the modification is introduced to remove the singularity that occurs in the limit of the solvent concentration going to zero.

$\Delta G^{id,\triangle}_{mix,\triangle}$ Ideal Gibbs free energy of mixing based on the ideal molality solution approximation

$\Delta G_{mix,\vartriangle}$	Gibbs free energy of mixing based on the difference between the Gibbs free energy and the sum of the standard state Gibbs free energies on the molality scale.
ΔG_r^o	Standard state Gibbs free energy of reaction. This is used regardless of whether the species standard states are on the molality scale.
$\tilde{H}$	Total Enthalpy of the solution (J kmol^{-1}), presented on a per kmol basis. $n\tilde{H}$ or H denotes the extensive quantity.
$\tilde{H}_k^{\vartriangle}$	Molar enthalpy of the molality-based standard state for species k. (J kmol^{-1}).
$\bar{H}_k$	Partial molar Enthalpy of species k (J kmol^{-1}).
$\tilde{H}_k^{o}\left(T_r, P_r\right)$	Absolute standard state Enthalpy under the NIST conditions for species k.
$\Delta\bar{H}_{f,k}^{o}\left(298\,\mathrm{K}, 1\,\mathrm{bar}\right)$	Standard heat of formation of species k at 298.15 K and 1 bar
I	Total ionic strength
J	Total relative heat capacity of the solution (J kmol^{-1} K^{-1})
L	Mixture excess enthalpy or relative enthalpy (J kmol^{-1}).
${}^{\phi}L$	Apparent relative molal enthalpy of mixing, Eqn. (169).
m_k	Molality of the solute k, (gmol (kg solvent)$^{-1}$
$m^{\vartriangle}$	constant equal to 1 gmol (kg solvent)$^{-1}$
$\tilde{M}_o$	Conversion between number of gmol of solvent and the number of kg of solvent (kg solvent gmol^{-1})
n	Total number of electrons transferred in a chemical reaction
n_o	Total number of moles of the solvent
n_k	Total number of moles of the solute k
R	Gas Constant
T	Temperature (Kelvin)
$\tilde{V}_k^{o}$	Standard state molar volume of species k
$V_{ex,\vartriangle}$	Excess volume of mixing for the solution, based on the deviation from the ideal molality solution basis on a per kmol basis (m^3 kmol^{-1}).
${}^{\phi}\tilde{V}$	Apparent excess molal volume of mixing for the solution (m^3 (kmol salt)$^{-1}$)

X_k	Mole fraction of species k
z_i	Charge of species i

9 References

1. M. E. Coltrin, “Benchmark calculations of activity coefficients and chemical potentials for concentrated electrolyte solutions,” Sandia Memo, Albuquerque, NM, May 13, 2005

2. J. M. Smith, H. C. Van Ness, *Introduction to Chemical Engineering Thermodynamics,* McGraw-Hill Book Co., New York, N. Y. 1975, p. 216.

3. H. K. Moffat and M. E. Coltrin, “Using NIST / JANAF / Chemkin Thermodynamic Databases in Aqueous Chemistry Applications,” Sandia Memo, Sandia National Labs, Albuquerque, NM, June 1, 2005

4. H. K. Moffat, “Implementation of Debye-Hückel Model in Cantera,“ Sandia Memo, Sandia National Labs, Alb., NM Aug. 1 (2005).

5. H. K. Moffat, “Notes on a Pitzer Model Implementation within Cantera,” Sandia Memo, Sandia National Labs, Albuquerque, NM (2006).

6. D. G. Archer, Thermodynamic Properties of the KCl + H_2O System,” *J. Phys. Chem. Ref. Data,* **28**, 1 – 17 (1999); D. G. Archer, “Thermodynamic Properties of the NaBr + H_2O System,” *J. Phys. Chem. Ref. Data,* **20**, 509 – 555 (1991); D. G. Archer, “Thermodynamic Properties of the NaCl + H_2O System. II. Thermodynamic Properties of NaCl (aq), $NaCl{\cdot}2H_2O$(cr), and Phase Equilibria,” *J. Phys. Chem. Ref. Data*, **21**, 793 – 829 (1992).

7. T. J. Wolery and Jarek, EQ3/6 (2003). T. J. Wolery, “EQ3NR: A computer program for the aqueous speciation-solubility calculations: User’s Guide and Documentation”, UCRL-53414, Lawrence Livermore Laboratory, Livermore, CA, April 18, 1983.

8. H. K. Moffat, “CADS: Cantera Aerosol Dynamics Simulator,” SAND2007-4216, Sandia National Laboratories, Albuquerque, NM (2007).

9. Ball, Jenne, and Nordstrom, WATEQ, 1979.

10. C. M. Bethke, “The Geochemist’s Workbench, Release 4.0, A User’s Guide to Rxn, Act2, Tact, React, and GtPlot,” July 16, 2002.

11. C. M. Bethke, “Geochemical Reaction Modeling”, Oxford University Press, New York (1996).

12. K. S. Pitzer, “Thermodynamics of Electrolytes I. Theoretical Basis and General Equations,” *J. Phys. Chem.*, **77**, 268 – 277 (1973).

13. D. L., Parkhurst, “*User's guide to PHREEQC--A computer program for speciation, reaction-path, advective-transport, and inverse geochemical calculations,”* U.S. Geological Survey Water-Resources Investigations Report 95–4227, p. 143 (1995); D. L. Parkhurst, C. A. Appelo,

"User's Guide to PHREEQCJ," http://wwwbrr.cr.usgs.gov/projects/GWC_coupled/phreeqc/html/final.html, 1999.

14. C. E. Harvie and J. H. Weare, "The prediction of mineral solubilities in natural waters: the Na-K-Mg-Ca-Cl-SO_4-H_2O system from zero to high concentration at 25 °C," *Geochimica et Cosmochimica Acta*, 44, 981 – 997 (1980).

15. C. E. Harvie, N. Møller, J. H. Weare, "The prediction of mineral solubilities in natural waters: The Na-K-Mg-Ca-H-Cl-SO_4-OH-HCO_3-CO_3-CO_2-H_2O System to high ionic strengths at 25°C," *Geochimica et Cosmochimica Acta*, 48, 723 – 51 (1984).

16. Z.-C. Wang, M. He, L.D. Gong, "Thermodynamics of Aqueous Complex Solutions Containing 3/1 Rare Earth Electrolyte Pairs and Salting-Out Agents to Very High Concentration," *J. Phys. Chem. B*, **111**, 3704 – 3715 (2007). Z.-C. Wang, M. He, J. Wang, J.-L. Li, *J. Solution Chem.*, **35,** 1137 (2006); M. He, Z.-C. Wang, *J. Solution Chem.*, **35,** 1607 (2006).

17. M. Azaroual, Ch. Kervevan, M.-V. Durance, P. Durst, "SCALE2000: reaction-transport software dedicated to thermokinetic prediction and quantification of scales. Applicability to desalination problems," *Desalination*, **165**, 409 – 419 (2004).

18. K. S. Pitzer, "Ion Interaction Approach: Theory and Data Correlation,", in *Activity Coefficients in Electrolyte Solutions*, 2nd Edition, Ed. K. S. Pitzer, CRC Press, Boca Raton, Fl (1991).

19. J. A. Rard, A. M. Wijesinghe, "Conversion of parameters between different variants of Pitzer's ion-interaction model, both with and without ionic strength dependent higher-order terms", *J. of Chemical Thermodynamics*, **35**, 439 – 473 (2003).

20. J. D. Dale, E. L. Shock, G. MacLeod, A. C. Aplin, S. R. Larter, "Standard partial molal properties of aqueous alkylphenols at high pressures and temperatures," *Geochimica et Cosmochimica Acta*, **61**, 4017 – 4024 (1997).

21. H. C. Helgeson, D. H. Kirkham, G. C. Flowers, "Theoretical prediction of the thermodynamic behavior of aqueous electrolytes at high pressures and temperatures: IV: Calculation of activity coefficients, osmotic coefficients, and apparent molal standard and relative partial molal properties to 600°C and 5kb," *Amer. J. Sci*., **281**, 1249 – 1516. (1981).

22. H. C. Helgeson, "Prediction of the thermodynamic properties of electrolytes at high pressure and temperatures," *Physics and Chemistry of the Earth*, v. **13-4**, 133 – 177 (1981).

23. J. C. Newman, K. E. Thomas-Alyea, *Electrochemical Systems*, Third Ed., J. Wiley, New York, 2004.

24. http://webbook.nist.gov

25. D. G. Goodwin, “Defining Phases and Interfaces, Cantera 1.5,” http://sourceforge.net/projects/cantera, Aug. 14 2003.

26. D. G. Goodwin, “Creating Phase and Interface Models,” Cantera Workshop, July 25, 2004, http://sourceforge.net/projects/cantera.

27. H. K. Moffat and M. E. Coltrin, “Using NIST / JANAF / Chemkin Thermodynamic Databases in Aqueous Chemistry Applications,” Sandia Memo, Sandia National Labs, Albuquerque, NM, June 1, 2005

28. H. K. Moffat, “A General Equilibrium Solver based on an Optimized Stoichiometric Formulation, Sandia Memo in prep, 2009.

29. Cox, J. D., Wagman, D. D., Medvedev, V. A., *CODATA Key Values for Thermodynamics*, Hemisphere Publishing Corp., New York, 1989. (http://www.codata.org/codata/databases/key1.html)

30. H. C. Helgeson, “Thermodynamics of Hydrothermal Systems at Elevated Temperatures and Pressures,” *American J. of Science*, **267**, 729 – 804 (1969).

31. L. F. Silvester and K. S. Pitzer, “Thermodynamics of Electrolytes 8. High-Temperature Properties, including enthalpy and heat capacity, with application to sodium chloride,” *J. Phys. Chem.*, **81**, 1822 – 1828 (1977).

32. W. Wagner and A. Pruβ, “The IAPWS Formulation 1995 for the Thermodynamic Properties of Ordinary Water Substance for General and Scientific Use,” *J. Phys. Chem. Ref. Data*, **31,** 387 – 442 (2002).

33. J. C. Tanger and H. C. Helgeson, “Calculation of the Thermodynamic and Transport Properties of Aqueous Species at High Pressure and Temperatures; Revised Equations of State for the Standard Partial Molal Properties of Ions and Electrolytes,” *Amer. J. of Science,* **288**, 19 – 98 (1988).

34. E. L. Shock and H. C. Helgeson, “Calculation of the thermodynamic and transport properties of aqueous species at high pressures and temperatures: Correlation algorithms for ionic species and equation of state predictions to 5 kb and 1000C.” *Geochimica et Cosmochimica Acta*, **52,** 2009 – 2036 (1988).

35. A. N. Anderko, Sridhar, et al. "A general model for the repassivation potential as a function of multiple aqueous solution species." *Corrosion Science,* **46**, 1583 – 1612 (2004).

36. E. H. Oelkers, H. C. Helgeson, et al., “Summary of the Apparent Standard Partial Molal Gibbs Free Energies of Formation of Aqueous Species, Mineral, and Gases at Pressures 1 to 5000 Bars and Temperatures 25 to 1000 °C,” *J. Phys. Chem. Ref. Data*, **24**, 1401 (1995).

37. *CRC Handbook of Chemistry and Physics*, 73rd Edition, Ed. D. R. Lide, CRC Press, Boca Raton, 1992, pp. 15 – 20.

38. D. J. Bradley, K. S. Pitzer, "Thermodynamics of Electrolytes. XII Dielectric properties of water and Debye-Hückel parameters to 350 C and 1 kbar," *J. Phys. Chem.*, **83**, 1599 (1979): **87**, 3798 (1983).

39. M. Uematsu and E. U. Franck, "Static dielectric constant of water and steam", *Journal of Physical and Chemical Reference Data*, **9**(4), p. 1291 – 1304, (1980)

40. P. S. Z. Rogers, K. S. Pitzer, "Volumetric Properties of Aqueous Sodium Chloride Solutions," *J. Phys. Chem. Ref. Data*, **11**, 15, (1982).

41. K. S. Pitzer, J. C. Peiper, R. H. Busey, "Thermodynamic Properties of Aqueous Sodium Chloride Solutions," *J. Phys. Chem. Ref. Data*, **13**, 1, (1984).

42. R. A. Robinson, R. H. Stokes, *Electrolyte Solutions*, Dover Publ., Mineola, NY (1959).

43. Sandia National Laboratories, In-Drift Precipitates/Salts Model, Analysis Model Report ANL-EBS-MD-000045 (Rev.03), U.S. Department of Energy, Office of Civilian Radioactive Waste Management, Las Vegas, Nevada (2007).

44. D. G. Goodwin, "An Open-Source, Extensible Software Suite for CVD Process Simulation," in *Chemical Vapor Deposition XVI and EUROCVD 14*, M. Allendorf, F. Maury, F. Teyssandier, Editors, PV 2003-08, p. 155 – 161, The Electrochemical Society Proceedings Series, Pennington, NJ (2003); see also (http://www.cantera.org).

45. Huayang Zhu, Robert J. Kee, Vinod M. Janardhanan, Olaf Deutschmann, and David G. Goodwin, "Modeling Elementary Heterogeneous Chemistry and Electrochemistry in Solid-Oxide Fuel Cells," *Journal of The Electrochemical Society*, **152**, A2427 – A2440 (2005)

46. G. Milazzo, S. Caroli, V. K. Sharma, *Tables of Standard Electrode Potentials*, J. Wiley, New York, 1978.

47. J. W. Johnson, E. H. Oelkers, H. C. Helgeson, "SUPCRT92: A software package for calculating the Standard Molal Thermodynamic Properties of Minerals, Gases, Aqueous Species, and Reactions from 1 to 5000 bar and 0 to 1000 °C," *Computers and Geosciencies*, **18**, 899 – 947 (1992).

48. H. K. Moffat, "Implementation of a Pitzer Model for Strong Electrolyte Thermochemistry within Cantera", Sandia Memo, Sandia National Labs, Albuquerque, NM, June 12 (2006).

49. J. W. Johnson, D. Norton, "Critical phenomena in hydrothermal systems: State, thermodynamic, electrostatic, and transport properties of H_2O in the critical region," *Am. Jour. Science*, **291**, 541 – 648 (1991).

50. H. K. Moffat, “Electrode Reactions within Cantera - An Example using the Standard Hydrogen Electrode,” Sandia Memo, Sandia National Laboratories, Albuquerque, NM, June 8 2007.

51. E. L. Shock and H. C. Helgeson, “Calculation of the thermodynamic and transport properties of aqueous species at high pressures and temperature: Standard partial molal properties of organic species,” *Geochimica et Cosmochimica Acta*, **54**, 915 – 945 (1990).

52. E. L. Shock, H. C. Helgeson, D. A. Sverjensky, “Calculation of the thermodynamic and transport properties of aqueous species at high pressures and temperatures: Standard partial molal properties of inorganic neutral species” *Geochimica et Cosmochimica Acta*, **53**, 2157 –2183 (1989).

53. Y. Huo, D. G. Goodwin, “Numerical Modeling of Single-Chamber SOFCs with Hydrocarbon Fuels,” *J. Electrochem. Soc.*, **154**, B207 – B217 (2007).

54. H. Zhu, R. J. Kee, V. M. Janardhanan, O. Deutschmann, D. G. Goodwin, “Modeling Elementary Heterogeneous Chemistry and Electrochemistry in Solid-Oxide Fuel Cells,” *J. Electrochem. Soc.*, **152**, A2427 – A2440 (2005).

55. W. G. Bessler, J. Warnatz, D. G. Goodwin, “The Influence of equilibrium potential on the hydrogen oxidation kinetics of SOFC Anodes,” *Solid State Ionics*, **177**, 3371 – 3383 (2007).

56. J. A. Miller, F. M. Ruplee, R. J. Kee, “Chemkin Thermodynamic Data Base,” Sandia Report, SAND87-8215B, Sandia Labs, Livermore, CA 1987.

57. M. W. Chase, C. A. Davies, J. R. Downey, D. J. Furip, R. A. McDonald, A. N. Syverud, JANAF Thermochemical Tables,” *J. Phys. Chem. Ref. Data.*, **14**, 1 (1985).

58. G. Milazzo, S. Caroli, V. K. Sharma, *Tables of Standard Electrode Potentials*, J. Wiley, New York, 1978.

59. A. J. Bard, R. Parsons, J. Jordan, *Standard Potentials in Aqueous Solutions*, Marcel Dekker, New York, 1985.

60. S. G. Bratsch, “Standard electrode potentials and temperature coefficients in water at 298.15 K”, *J. Phys. Chem. Ref. Data*, **18**, 1 – 21 (1989).

61. D. A. Jones, *Principles and Prevention of Corrosion, 2nd Ed.*, Prentice Hall, Upper Saddle River, NJ (1996).

62. J. O’M Bockris, S. U. M. Khan, *Surface Electrochemistry*, Plenum, New York, N.Y. (1993).

63. A. J. Bard, L. R. Faulkner, *Electrochemical Methods: Fundamentals and Applications*, J. Wiley, New York, 2001.

64. J. O’M Bockris, A. K. N. Reddy, M. Gamboa-Aldeco, *Modern Electrochemistry*, Kluwer Academic/Plenum Publishing, New York, 2000.

65. R. Parsons, J. O-M. Bockris, “Calculation of the Energy of Activation of Discharge of Hydrogen Ions at Metal Electrodes,” *Trans. Faraday Soc.*, **47**, 914 – 928 (1951).

66. S. M. Sterner, A. R. Felmy, C. S. Oakes, K. S. Pitzer, “Correlation of thermodynamic data for aqueous electrolyte solutions to very high ionic strength using INSIGHT: Vapor saturated water activity in the system $CaCl_2$-H_2O to 250 degrees C and solid saturation,” *Int. J. of Thermophysics,* **19**, 761 – 770 (1998).

67. E. L. Shock, E. H. Oelkers, J. W. Johnson, D. A. Sverjensky, and H. C. Helgeson, “Calculation of the thermodynamic properties of aqueous species at high pressures and temperatures – Effective electrostatic radii, dissociation constants, and standard partial molal properties to 1000°C and 5 kbar”, *J. Chemical Society, Faraday Trans.*, **88**(6), p. 803 – 826 (1992).

68. A. M. Wijesinghe J. A. Rard, “Conversion and optimization of the parameters from an extended form of the ion-interaction model for $Ca(NO_3)(_2)$(aq) and $NaNO_3$(aq) to those of the standard Pitzer model, and an assessment of the accuracy of the parameter temperature representations,” *J. Chemical Thermodynamics*, **37**, 1196 – 1218 (2005).

69. E. C. W. Clarke and D. N. Glew, “Evaluation of thermodynamic functions for aqueous sodium chloride from equilibrium and calorimetric measurements”, *J. Phys. Chem. Ref. Data,* **14**(2), p. 489 – 610 (1985).

70. R. G. Bates, *Determination of pH: Theory and Practice,* 2nd Ed. Wiley & Sons, NY, NY (1973).

71. M. Conceição P. de Lima, K. S. Pitzer, “Thermodynamics of Saturated Aqueous Solutions Including Mixtures of NaCl KCl, and CsCl,” *J. of Solution Chemistry*, **12**, 171 – 185 (1983).

72. J. Greenberg and N. Møller, “The prediction of mineral solubilities in natural waters: A chemical equilibrium model for the Na-K-Ca-Cl-SO_4-H_2O system to high concentration from 0 to 250 °C,” *Geochimica et Cosmochimica Acta*, **53**, 2503 – 2518 (1989).

73. J. A. Rard and D. G. Miller, “Isopiestic determination of the Osmotic coefficientsof aqueous sodium sulfate, magnesium sulfate, and sodium sulfate-magnesium sulfate at 25°C”, *J. Phys. Chem. Eng. Data,* **26**(1), 33 – 38 (1981).

74. H. F. Holmes and R.E. Mesmer, “Isopiestic studies of aqueous solutions at elevated temperatures VII. $MgSO_4$, and $NiSO_4$”, *J. Chem. Thermodynamics,* **43**, 709 – 719 (1983).

75. D. G. Archer and J. A. Rard, “Isopiestic Investigation of the Osmotic and Activity Coefficients of Aqueous $MgSO_4$ and the Solubility of $MgSO_4 \cdot 7H_2O$(cr) at 298 K: Thermodynamic Properties of the $MgSO_4$ + H_2O System to 440 K”, *J. Phys. Chem. Eng. Data,* **43**(5), 791 – 806 (1998).

76. J. A. Rard, S. L. Clegg, and D. A. Palmer, “Isopiestic Determination of the Osmotic Coefficients of Na_2SO_4(aq) at 25 and 50 °C, and Representation with Ion-Interaction (Pitzer) and Mole Fraction Thermodynamic Models”, *J. of Solution Chemistry*, **29**(1), p. 1 – 49 (2000).

77. R. T. Pabalan and K. Pitzer, “Thermodynamics of Concentrated Electrolyte Mixtures and the Prediction of Mineral Solubilities to High Temperatures for Mixtures in the System Na-K-Mg-Cl-SO_4-OH-H_2O”, *Geochimica et Cosmochimica Acta*, **51**(9), 2429 – 2443 (1987).

78. D. G. Archer, “Thermodynamic Properties of the NaBr + H_2O System”, *J. Phys. Chem. Ref. Data,* **20**(3), 509 – 555 (1991).

79. H. F. Holmes, C. F. Baes Jr., R. E. Mesmer, “Isopiestic studies of aqueous solutions at elevated temperatures. II NaCl + KCl mixtures,” *J. Chem. Thermodynamics*, **11**, 1035–1050 (1979).

80. F. Farelo, G. Von Brachel, H. Offermann, “Solid-Liquid Equilibria in the Ternary System NaCl–KCl– H2O,” *Canadian J. of Chemical Eng.*, **71,** 141 – 146 (1993).

81. D. G. Archer, “Thermodynamic Properties of the KCl + H_2O System,” *J. Phys. Chem. Ref. Data,* **28,** 1 – 15 (1999).

82. R. T. Pabalan, K .S. Pitzer, “Apparent Molar Heat Capacity and Other Thermodynamic Properties of Aqueous KCl Solutions to High Temperatures and Pressures,” *J. Chem. Eng. Data,* **33**, 354 – 362 (1988).

83. G. N. Lewis and M. Randall, “Thermodynamics”, revised by K. S. Pitzer and L. Brewer, *McGraw-Hill Series in Advanced Chemistry*, (1961), p. 723.

84. W. R. Smith and R. W. Missen, “Chemical Reaction Equilibrium Analysis: Theory and Algorithms”, *J. Wiley & Sons*, New York (1982).

85. N. Møller, J. P. Greenberg, and J. H. Weare, “Computer Modeling for Geothermal Systems: Predicting Carbonate and Silica Scale Formation, CO_2 Breakout and H_2S Exchange”, *Tranport in Porous Media*, 33, p. 173 – 204 (1998).

86. C. Kervevan, M. Azaroual, and P. Durst, “Improvement of the Calculation Accuraccy of Acid Gas Solubility in Deep Reservoir Brines: Applications to the Geological Storage of CO_2”, *Oil & Gas Science and Technology*, **60**(2), p. 357 – 379 (2005).

87. M. Wolf, O. Breitkopf, and R. Puk, “Solubility of Calcite in Different Electrolytes at Temperatures Between 10° and 60° C and at CO2 Partial Pressures of About 1 kPa”, *Chemical Geology*, 76, p. 291 – 301 (1989).

88. C. Monnin, “An ion interaction model for the volumetric properties of natural waters: density of the solution and partial molal volumes of electrolytes to high concentration at 25°C”, *Geochim. Cosmochim. Acta,* **53,** p. 1177 – 1188 (1989).

89. C. Monnin, “The influence of pressure on the activity coefficients of the solutes and on the solubility of minerals in the system Na-Ca-Cl-SO_4-$H_2$0 to 200°C and 1 kbar, and to high NaCl concentration”, *Geochimica et Cosmochimica Acta,* **54**, pp. 3265 – 3282 (1990).

90. Distribution

1	MS0382	S. F. Domino	1541
1	MS0382	D. J. Glaze	1541
1	MS0754	P. V. Brady	6310
1	MS0735	J. A. Merson	6310
1	MS0706	D. J. Borns	6312
1	MS0751	T. Dewers	6315
1	MS0754	L. J. Criscenti	6316
1	MS0754	R. T. Cygan	6316
1	MS0754	J. L. Krumhansl	6316
1	MS0754	J. A. Greathouse	6316
1	MS0779	M. D. Siegel	6772
1	MS0776	Y. Wang	6782
5	MS0778	Carlos F. Jové Colón	6786
1	MS0778	C. R. Bryan	6786
1	MS1399	D. Sassani	6786
1	MS1399	P. Vaughn	6786
1	MS0776	M. K. Knowles	2552
1	MS0825	J. S. Lash	1510
1	MS0836	Terry Aselage	1514
5	MS0836	H. K. Moffat	1516
1	MS0836	K. S. Chen	1516
1	MS0836	I. Khalil	1516
1	MS0836	R. Rao	1514
1	MS0888	S. J. Glass	1825
1	MS0888	K. R. Zavadil	1825
1	MS0889	N. R. Sorensen	1825
1	MS0889	D. G. Enos	1825
1	MS0889	L. M. Serna	1825
1	MS0836	M. J. Martinez	1514
1	MS1086	M. E. Coltrin	1126
1	MS1135	J. C. Hewson	1532
1	MS1415	K. Leung	1114
1	MS1304	J. P. Sullivan	1132
1	MS1411	R. A. Roach	1814
1	MS1411	C. C. Battaile	1814
1	MS9291	M. A. Allendorf	8624
1	MS9409	R. S. Larson	8365
1	MS0899	Technical Library	9536 (electronic copy)

1 Prof. D. G. Goodwin, California Institute of Technology, dgoodwin@caltech.edu

1 Prof. R. J. Kee, Colorado School of Mines, rjkee@mines.edu

Sandia National Laboratories